FACULTEIT FARMACEUTISCHE WETENSCHAPPEN

Evaluation of dual color fluorescence fluctuation spectroscopy for the characterization of antisense oligonucleotide/carrier complexes for intracellular delivery

Evaluatie van fluorescentie fluctuatie spectroscopie voor de karakterisatie van antisense oligonucleotide/drager complexen voor intracellulaire vrijstelling

ir. Bart Lucas

Thesis submitted in fullfillment of the requirements for the degree of
Doctor in Pharmaceutical Sciences
Proefschrift voorgedragen tot het bekomen van de graad van
Doctor in de Farmaceutische Wetenschappen

2005

Decaan:
Prof. Dr. Apr. Jean-Paul Remon

Promotoren:
Prof. Dr. Apr. Joseph Demeester
Prof. Dr. Apr. Stefaan De Smedt

The author and the promotors give the athorization to consult and to copy parts of this thesis for personal use only.
Any other use is limited by the Laws of Copywright, especially concerning the obligation to refer to the source whenever results from this thesis are cited.

De auteur en de promotors geven de toelating dit proefschrift voor consultatie beschikbaar te stellen en delen ervan te kopiëren voor persoonlijk gebruik. Elk ander gebruik valt onder de beperkingen van het auteursrecht, in het bijzonder met betrekking tot de verplichting uitdrukkelijk de bron te vermelden bij het aanhalen van resultaten uit dit proefschrift.

Gent, 24 januari 2005

De promotoren

Prof. Dr. Apr J. Demeester

Prof. Dr. Apr. S. De Smedt

de auteur

ir. Bart Lucas

Oud Perzisch citaat

‘De nacht verbergt een wereld maar onthult een heelal.’

Dankwoord

Eindelijk is het zover: de tijd is aangebroken om een heleboel mensen te bedanken die gezorgd hebben voor een belangrijke bijdrage aan dit werk.

Vooreerst wil ik graag Prof. Jo Demeester en Prof. Stefaan De Smedt bedanken voor het vertrouwen en de enthousiaste begeleiding. Het is immers een voorrecht om als doctoraatsstudent te genieten van de bijstand van 2 promotoren.
Toen mijn ingenieursdiploma nog in het verschiet lag, boden jullie mij reeds de kans om mijn tanden te zetten in een interessant project. Het was een hele uitdaging om vanuit een totaal verschillende achtergrond mij zo snel mogelijk in te burgeren in de wereld van macromoleculaire geneesmiddelen en fluorescentiemicroscopie.
Het is een boeiende ervaring te mogen meehelpen bij het opstarten van een nieuw onderzoeksveld in het labo. In combinatie met een aangename werkomgeving en experimentele vrijheid heeft dit inderdaad geleid tot een zeer bevredigend eindresultaat.

Tijdens mijn initiatie in de FFS-wereld was de praktische ingesteldheid van dr. Els Van Rompaey een grote stimulans. Els, dankzij jouw pionierswerk met de oligo'tjes kon mijn project reeds met een aantal belangrijke inzichten van start gaan. Je had immers al uitgevist waarom FCS en PCH niet bruikbaar zijn en waarom een alternatieve piekanalyse wel werkt. Door je nuchtere kijk op de dingen was het trouwens zeer aangenaam om in jouw gezelschap te werken. In een later stadium van je eigen onderzoek introduceerde je de anti-ICAM-1 test in ons labo en wist je de kinderziekten ervan op te lossen.
Voor deze biologische test hadden we echter een celcultuur nodig, en dit had ongetwijfeld heel wat meer voeten in de aarde gehad zonder de tussenkomst van Koen Deryckere die de omgang met dergelijke levende materie in ons labo introduceerde.

Mijn eerste experimentele FFS-stapjes gebeurden op het labo van Prof Engelborghs van de Katholieke Universiteit Leuven. Yves en Jo, dankjewel voor de praktische hulp en leerrijke discussies, want mede dankzij jullie kregen die eerste stapjes al vlug vaart.

Dr. Mark Hink en Prof. Ton Visser van Universiteit Wageningen hebben eveneens een erg cruciale rol gespeeld in de beginfase. Jullie maakten het mogelijk om tweekleurige FFS metingen te doen nog voor ons labo over de techniek beschikte.
A special word of thanks also to Dr. Norbert Opitz who actually implemented a copy of his home-made dual color FFS module on our confocal microscope.
Dr. Roland Brock (Institute for Cell Biology Tübingen) is gratefully acknowledged for having me at his lab. The assistance and guidance of Dr. Rainer Pepperkok during my stay at his lab (Cell Biology/Cell Biophysics Programm, EMBL Heidelberg) is also gratefully acknowledged.

Vervolgens wil ik graag de andere mensen van het labo bedanken met wie ik altijd prettig samengewerkt heb: Jurgen, Farzaneh, Katrien (al geruime tijd een trouwe FFS-partner-in-crime), Tinneke, Kevin, Lies, Roos, Ine, Bruno, Koen, Stefaan, Niek, Hanne, Barbara, Jie… Dankzij jullie kon wetenschap gepaard gaan met een flinke dosis humor en collegialiteit!

Een speciaal dankwoordje gaat naar onze administratie-Tarzan en –Jane, alias Bruno & Katharine, zonder jullie inzicht in de papieren jungle zouden vele witte jassen af en toe serieus verloren lopen. Merci om steeds paraat te staan! En dit geldt uiteraard ook voor de spreekwoordelijke Jerome van het lab: Bertrand die altijd klaar staat om volle dossierkasten te verslepen, vast te draaien wat los zit en los te krijgen wat vast zit.

En dan mag ik natuurlijk ook onze labo-duizendpoot Jurgen niet vergeten, met wie ik meer dan 2 jaar hetzelfde bureau gedeeld heb, een leerrijke en aangename periode.
A special word of thanks also to Farzaneh, my loyal companion on our journey (together with Stefaan D.) on the second floor from office 1 to office 2, to office 3,…

Omdat een gemotiveerde en zelfredzame stagiair goud waard is in onderzoekstermen, dank ik graag Evelyn, Roselien, Annelies, Ine en Eva voor hun bijdrage aan dit werk.

IWT-Vlaanderen (het Instituut voor de aanmoediging van Innovatie door Wetenschap en Technologie in Vlaanderen) en Universiteit Gent hebben dit doctoraatswerk mogelijk gemaakt, want naast onderzoek dient er ook brood op de plank.

Natuurlijk heeft ook het thuisfront een grote rol gespeeld, ook degene die het einde (en sommige zelfs het begin) van deze doctoraatsperiode niet meer hebben kunnen meemaken. Ook de uitgebreide vriendenkliek heeft voor heel wat leuk tegengewicht gezorgd. En dan nog een extra mercike voor een paar mensen die mij al heel lang kennen en aan wie ik veel te danken heb: de zus, Lies & Jo.

Gent, januari 2005

Bart

List of abbreviations and symbols

BSA	bovine serum albumine
CSLM	confocal scanning laser microscopy
DLS	dynamic light scattering
DMEM	Dulbecco's modified eagle medium
DNA	desoxyribonucleic acid
DOPE	dioleylphosphatidylethanolamine
DOTAP	1,2-dioleoyl-3-trimethylammoniumpropane
DOTMA	1, 2-dioleoylpropyl-3-N,N,N-trimethylammonium chloride
DS	dextran sulfate
EDTA	ethylenediaminetetraacetic acid
ELISA	Enzyme-Linked Immuno-Sorbent Assay
FBS	fetal bovine serum
FCS	fluorescence correlation spectroscopy
FDA	food and drug administration
FFS	fluorescence fluctuation spectroscopy
FIDA	fluorescence intensity distribution histogram
FIMDA	fluorescence intensity multiple distributions analysis
FITC	fluorescein-isothiocyanate
FLIM	fluorescence life time imaging
FRET	fluorescence resonance energy transfer
GPC	gel permeation chromatography
Hepes	4-(2-hydroxyethyl)-1-piperazineethanesulfonic acid
HRP	horseradish peroxidase
ICAM-1	intracellular adhesion molecule-1
ICS	image correlation spectroscopy
kDa	kilodalton
mRNA	messenger ribonucleic acid
M_n	number average molecular mass
M_w	weight average molecular mass
ONs	oligonucleotides

OPD	o-phenylenediamine dihydrochloride
NGS	normal goat serum
PBS	phosphate buffered saline
PCH	photon count histogram
pDMAEMA	poly(2-dimethylamino)ethyl methacrylate
pEG	polyethylene glycol
pEG-pEI	poly(ethylene glycol)-poly-ethylene-imine
pEI	poly-ethylene-imine
pLL	poly-L-lysine
PNA	peptide nucleic acids
PO-ONs	phosphodiester ONs
PS-ONs	phosphorothioate ONs
Rh	rhodamine
Rh-ONs	rhodamine labeled ONs
RISC	RNA induced silencing complex
RNase H	ribonuclease H
RNA	ribonucleic acid
SDS	sodium dodecyl sulfate
TBE	buffer based on Tris, Boric Acid and EDTA
TNF-α	tumor necrosis factor-α
Tris	tris(hydroxymethyl)methylamine
w/w ratio	weight/weight ratio
ζ	zeta potential

Chapter 1

Oligonucleotide delivery – Aims of this thesis

1. Introduction

Antisense technology reflects a naturally occurring physiological event since endogenously expressed antisense molecules exist which are able to regulate endogenous gene expression and to defend both prokaryotes and eukaryotes against viral invasion [1;2]. Antisense technology has a wide perspective of potential applications. At present, most of these applications are in fundamental research where inhibition of gene expression provides insight into the function and regulation of the genes studied. Despite the recent withdrawal of a first generation antisense candidate in a phase 3 clinical trial [3], a growing interest remains in developing drugs based upon the antisense mechanism, mainly aimed at interfering with viral infections and cancer. In August 1998, the first antisense molecule (Fomivirsen®, Vitravene) to treat cytomegalovirus infection was approved by the FDA [4]. Over 20 (first generation) antisense candidates are currently in various stages of clinical development, whereas oligonucleotides (ONs) of the second and third generation promise lower toxicity and increased stability against enzymatic degradation [5]. Replacing the sugar-phosphate backbone by a synthetic peptide backbone has resulted in a nucleic acid analogue called PNA (peptide nucleic acids), combining the sequence specific action of antisense and chemical/hydrolytic (enzymatic) stability [6].

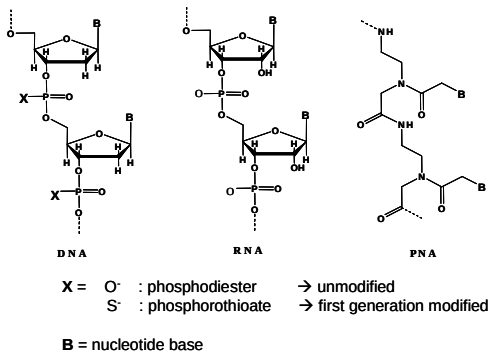

Figure 1. Structure of single stranded DNA, RNA and PNA

The ability of antisense molecules to bind to complementary mRNA through Watson-Crick base pairing may sound simple. However, where and how antisense reaches its target(s) is still largely obscure. It is generally believed that antisense either sterically blocks mRNA's function (Figure 2B) or promotes enzyme-mediated mRNA degradation (Figure 2C). RNase H is an endonuclease that recognizes RNA-DNA duplexes and selectively cleaves the mRNA strand. The mechanism is catalytic: once a mRNA molecule is cleaved, the antisense dissociates from the mRNA chain and is able to bind to a second mRNA. However, chemical modifications and/or changes in the backbone can reduce or eliminate RNase H recognition of the ONs/RNA duplex [7;8]: phosphodiester and phosphorothioate ONs can activate RNase H, whereas PNA's are unable to activate RNase H. Further, any RNase which recognizes double stranded RNA's or RNA/DNA duplexes could play a role in the action of antisense ONs. Regardless of the mechanism of action, the expression level of the targeted protein will only become noticeably reduced after significant turnover of the pre-existing endogenous protein pool.

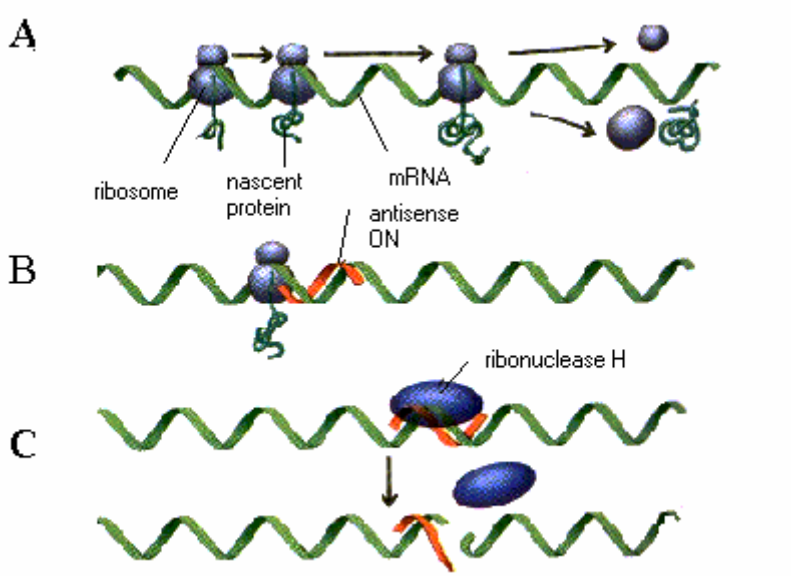

Figure 2. Schematic representation of the biochemical working mechanism of ONs. The translation of mRNA (green) into proteins is accomplished by ribosomes, which travel along the mRNA transcripts (A). Binding of an antisense oligonucleotide (orange) can inhibit the translation (B): it can prevent the ribosomes from beginning or completing their journey. Also RNase H can be activated. RNase H cuts the mRNA at the site where the ON has bound (C).

With respect to antisense delivery, it is important to take into account that the antisense molecules can be active in both cytoplasm and nucleus. In the cytoplasm, the antisense can sterically block polypeptide elongation (translational arrest) and/or induce

RNase H mediated mRNA degradation. In the nucleus, the antisense can sterically inhibit splicing of pre-mRNA and/or induce enzymatic pre-mRNA destabilization [9].

More recently, double stranded RNA (siRNA) was found to initiate sequence-specific gene silencing also in mammalian cells [10]. Consequently, there is growing interest in its therapeutic possibilities. siRNA consists of about 22 nucleotides in length and is homologous to the gene that is being suppressed. The 22-nucleotide sequences serve as a guide sequence that instructs a multicomponent nuclease, RNA-induced silencing complex (RISC) to destroy specific mRNA's [11].

2. Biological barriers for the delivery of antisense oligonucleotides

The biological efficacy of administered antisense ONs is restrained as they must overcome several obstacles before they reach their intracellular target (in the cytoplasm and/or the nucleus). The cellular uptake of antisense oligonucleotides is poor due to their large size, hydrophilicity, and negatively charged backbone. In addition, they are very susceptible to degradation by nucleases in the extracellular matrix and inside the cell. Consequently, therapeutic ONs as well as RNA are strongly dependent on carriers to cross cellular membranes, to escape from endosomes and to maintain their physicochemical properties in extra- and intracellular matrices. Several laboratories have been encouraged to look for appropriate pharmaceutical carrier systems for ONs. Different types of cationic lipids and cationic polymers are under investigation as non-viral carriers for antisense ONs [12;13]. Cationic lipids as well as cationic polymers spontaneously form interpolyelectrolyte complexes with negatively charged nucleic acids, called respectively lipoplexes and polyplexes [14]. The physicochemical features that govern the biological activity of lipo- and polyplexes are however not well understood, partly due to the complexity of the association and dissociation behavior of such complexes. Indeed, a critical step in the delivery of ONs is the dissociation of the ONs from the complexes at the right place; i.e. in the cytoplasm of the target cell [15]. If the affinity between the ONs and the cationic carriers is too low, the complex will dissociate prematurely, e.g. when it is still in the blood stream or in the extracellular environment, while a strong affinity might prevent the release of the ONs intracellularly. A critical balance between 'being associated extracellularly' and 'being dissociated intracellularly' needs to be maintained.

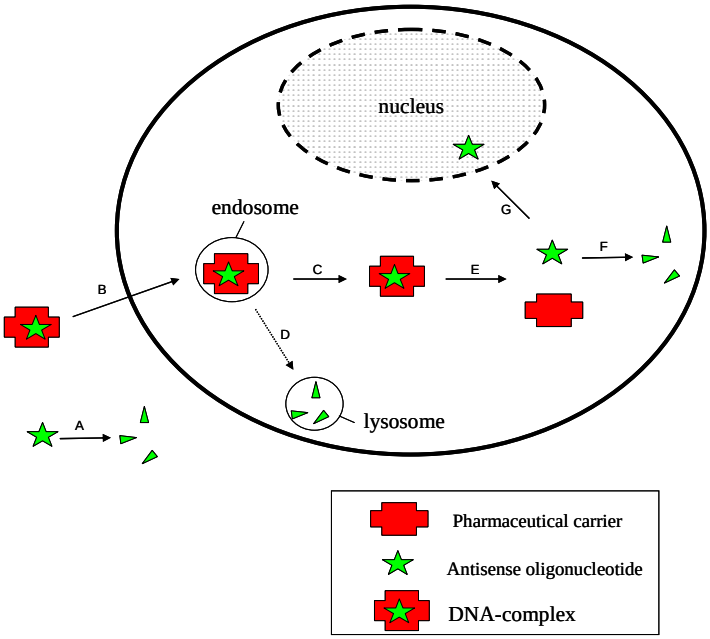

Figure 3. Schematic representation of the biological barriers for ON delivery: The carrier/ONs complex must be stable in the extracellular matrix (A). The carrier/ONs complex has to overcome the cellular membrane (B) and must escape from the endosomes (C) before the latter fuse with the lysosomes (D). Once the ONs are released from their carrier in the cytoplasm (E), the ONs must be resistant to nuclease activity (F). In case the nucleus is the biological target for the ONs, nuclear import is obligatory (G).

To obtain real breakthroughs in understanding the complex matter of intracellular dissociation of DNA/carrier complexes there is an urgent need for tools which allow studying the dissociation of DNA/carrier complexes in cells. As overviewed below, several advanced light microscopy techniques show potential for this purpose.

3. Fluorescence imaging and FRET to study DNA release in cells

In many studies DNA complexes inside cells are visualized using fluorescently labeled DNA. In other reports both the DNA and its carrier are labeled with spectrally different fluorophores and dual color microscopy is used to observe simultaneously the DNA and its carrier in the cell [16-18]. The colocalization of the fluorescent markers may indicate that the DNA and its carrier are associated, a lack of colocalization may indicate that the DNA is released from its carrier. However, due to the resolution limit of a microscope it remains possible that the fluorescent-labeled molecules are observed colocalized without being associated. Fluorescence resonance energy transfer (FRET) between a donor fluorophore on the DNA and an acceptor fluorophore on the carrier (or vice versa) could be a better alternative to study the complexation. Indeed, FRET only occurs when the donor and acceptor

fluorophores are in close proximity, in other words when the DNA is associated to its carrier. However, FRET needs a proper positioning of the donor and acceptor molecules, which is hard to obtain in DNA/carrier complexes as they arise through (spontaneous) self assembling of the DNA and the carrier molecules. To our knowledge, FRET between fluorophores on cationic liposomes and (intercalating) dyes on pDNA have only been reported using a conventional fluorimeter [19-22]. Intracellular FRET studies by means of fluorescence microscopes on DNA/carrier-complexes did not appear in literature so far. However, rather recently the Kataoka group reported on intracellular FRET measurements on DNA/carrier complexes where both the donor and the acceptor label were attached to the plasmid DNA [23]. FRET was reported to occur when the 'double labeled' pDNA was complexed to the cationic polymers or cationic lipids: upon complexation the pDNA molecule condenses which brings the donor and acceptor fluorophore in each others proximity [24]. The intracellular release of the pDNA could be observed as the FRET signal disappeared upon dissociation of the pDNA from its carrier whereby the DNA molecule is decondensed. The FRET approach of the Kataoka group clearly offers an advantage, as one does not need to label each cationic carrier when different cationic carriers are investigated. Meanwhile, one also avoids changes in the physicochemical properties of the carrier due to the label.

4. Fluorescence fluctuation techniques

In conventional imaging, average intensities of fluorescence are directly measured as a function of space to monitor the distribution of the labeled components throughout the cells. In techniques like fluorescence recovery after photobleaching (FRAP), fluorescence polarization and fluorescence lifetime imaging (FLIM), intensities of fluorescence are monitored as a function of time. The fluctuations of the intensities are however not of direct interest.

Modern fluorescence fluctuation techniques are capable to determine the absolute fluorophore concentration as well as molecular brightness and/or diffusional characteristics of individual molecular species within one sample mixture. Therefore, fluorescence fluctuation spectroscopy (FFS) requires a confocal detection volume and low fluorophore concentrations. As illustrated in Figure 4, the detector monitors the fluorescence fluctuations caused by the diffusion of fluorescent molecules through the focal volume of a microscope. The experimental fluorescence fluctuation profile can be further processed using:

- autocorrelation analysis to distinguish between different species based on their temporal behavior: Fluorescence Correlation Spectroscopy (FCS) and Image Correlation Spectroscopy (ICS).
- fluorescence intensity analysis to distinguish between different species based on their difference in fluorescence: Photon Counting Histogram analysis (PCH), Fluorescence Intensity Distribution Analysis (FIDA), or a heuristic statistical analysis of the fluorescence fluctuation data as described by Van Craenenbroeck et al. [25;26].

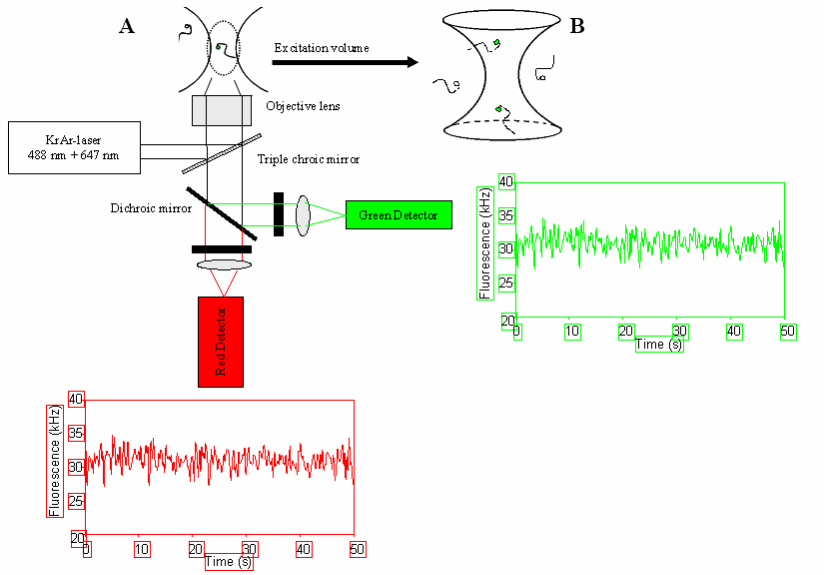

Figure 4. (A) Schematic setup of a dual color FFS instrument. The excitation light from the laser is reflected by a triple chroic mirror into the back aperture of the objective lens. The light emitted by the fluorescent molecules in the excitation volume passes through the objective lens and the triple chroic mirror, to be split by the subsequent dichroic mirror into a red and a green component. Both green and red detector monitor the fluorescence intensity as a function of time. (B) Schematic view of fluorescently labeled ONs, freely migrating through the excitation volume. Inside the excitation volume the fluorophores are excited and emit light (filled circles), outside the excitation volume the fluorophores remain in a dark ground state (open circle).

When only one of the interacting components is fluorescently labeled, changes in diffusion behavior or molecular brightness of the label are an indication for association. FCS can resolve different species on the basis of different translational diffusion coefficients [27;28]. However, a change in the molecular weight by a factor of eight is required to detect a change in the correlation time by a factor of two. [29]. FIDA/PCH discriminate different fluorescent species according to their specific molecular brightness. Hereby, size information given by the diffusion time of the molecule is no longer needed [30-32].

Both FCS and FIDA have also been extended to variants with two detectors monitoring different polarization components or spectral emission bands of fluorescence in the same focal volume, respectively called two dimensional FIDA (2D-FIDA) and Fluorescence Cross Correlation Spectroscopy (FCCS) [33;34]. Combining FCS and FIDA into FIMDA allows simultaneous determination of diffusion coefficients and molecular brightness values from a single measurement [35]. The combination of FIDA with fluorescence lifetime analysis distinguishes fluorescence species on the basis of both their specific molecular brightness and the lifetime of the excited state [36].

For large molecules (like DNA-complexes), slow diffusion becomes a limiting factor for detection using FCS [27;37]. In contrast to conventional FCS, the size information given by the diffusion time of the molecule is no longer needed when using intensity analysis or cross correlation analysis, allowing the sample to be moved relative to the focus. Development of scanning fluorescence correlations spectroscopy wherein the intensity fluctuations are measured as a function of position rather than time provides a means to study aggregation in systems like biological cell membranes but provides no information about the dynamics. Using the scanning FCS technique a study of the distribution of antibodies specific for the epidermal growth factor was carried out on A431 cells [38]. Because the latter measurements are slow and usually require fixed preparations, image correlation spectroscopy was introduced [39;40]. Image correlation spectroscopy relies on the spatial intensity fluctuations in images collected with a confocal laser scanning microscope. To obtain dynamic information, analysis of many temporally spaced images is needed. Spatial autocorrelation analysis of the images yielded information on the molecular concentration and aggregation state. Collecting a time series of images from a sample followed by correlation analysis between different images in the time series as well as spatial autocorrelation in the individual images provides information on molecular dynamics. Additionally, a two color image cross correlation spectroscopy variant has been used to demonstrate colocalization of two different molecules on the surface of cells. The introduction of video rate system enabled to measure diffusion coefficients that are three orders of magnitude larger than those measurable with ICS on slower CLSM systems [41].

FFS is sensitive in changes in the aggregation state of the fluorophore, as the autocorrelation function is influenced by the square of the specific brightness of each component. However, whenever highly intense fluorescence peaks appear in the fluctuations profiles, auto- and cross-correlation analysis are no longer feasible. In both single and dual

color FFS, these highly intense fluorescence peaks have been reported for several polymer/oligonucleotide complexes [42-44] as well as for liposome/oligonucleotide complexes [45]. As a consequence one cannot study the complexation of oligonucleotides based upon a change in their mobility (as correlation analysis is necessary to obtain the diffusion coefficient from the fluctuations) [42;44]. As an alternative approach, the fluorescence fluctuations could be analysed by photon histogram analysis (PCH) as this allows to distinguish between free and complexed molecules based on their difference in molecular brightness. However, previous work in our group has shown that the highly intense fluorescence peaks also did not allow to apply PCH analysis on the fluorescence fluctuations of DNA/carrier complexes mainly due to the 'heterogenity' of the highly intense fluorescence peaks appearing in the fluorescence fluctuation profiles [43]. In conclusion, searching for the presence or absence of highly intense fluorescence peaks in the fluorescence fluctuation profiles seems to be the only way of analysis one can use to know whether oligonucleotides are complexed to/or dissociated from their carriers. However, highly intense fluorescence peaks may also be due to aggregation of free ONs with cellular components, which could be misinterpreted as being original carrier/ONs-complexes. Therefore, the fluorescent labeling of both the carrier and the ONs should improve the signal specificity. In dual color FFS, both interacting components are labeled with spectrally different fluorophores (e.g. red and green) and their emission light is detected separately by two detectors monitoring the same focal volume. When dissociated, the components are only detected in one detector, as they carry a red or a green fluorophore. However, when associated, the complex is detected in both detectors simultaneously as it bears both red and green fluorophores.

5. Some critical remarks

Since both single- and dual color FFS detect fluorescent molecules at the single molecule level, also fluorescent contaminants present at low concentration will be detected. As a result, the used fluorescent molecules should be extensively purified to remove any free dye. It should be noted that a certain degree of contamination can be tolerated if properly corrected for in the data analysis. Also the type of fluorescent dyes has to be carefully selected. In general they should be highly fluorescent (i.e. they should generate high counts per molecule), preferentially at low laser excitation power, and show little photobleaching. Fluorescence enhancement or quenching of the fluorophores may occur in the reaction under investigation. However, changes in molecular brightness can only be corrected for to a limited

extend in autocorrelation analysis [25] and fluorescence intensity distribution analysis might be more suitable.

When dual color FFS is considered, the experimental setup is also critical since two laser beams have to be focused in the same spot, and the detection volumes have to be brought to a perfect overlap. Autofluorescence of the cells and photobleaching can further complicate the data analysis. Autofluorescence excited at 532 nm was reported to depend on the incubation conditions of the cells. FFS revealed that the changes in autofluorescence were due to changes in molecular brightness of the autofluorescent particles as the average number of particles detected in the focal volume did not change [46]. Also, at high laser excitation power, cell photodamaging can be observed. Some of these problems which arise intracellularly can be addressed by using two photon excitation (2PE) [47-49]. In 2PE, the simultaneous absorption of two photons of approximately half the energy is required for transition to the excited state. Only the focal plane receives sufficient photon flux for this simultaneous absorption to occur. In one photon excitation, the out-of-focus fluorescence is rejected due to the insertion of pinholes, but illumination still occurs all along the cone-like profile of the focused laser beam. Therefore out of focus photobleaching and photodamaging effects will be more severe when 1PE is used. Using 2PE, photobleaching and photodamaging only occur in the focal plane.

6. Aims and outline of this thesis

To overcome the problems in antisense delivery, many groups are currently screening a high number of pharmaceutical carriers for ONs delivery. However, while much effort is oriented towards the synthesis of new carriers, the optimization of the physicochemical and pharmaceutical features of the complexes is frequently neglected. We believe that rational design of improved vectors requires a better knowledge of the multistage process by which pharmaceutical vectors deliver ONs into cells. In this optimization process we should pay attention to all the critical steps involved in the delivery of ONs by pharmaceutical carriers: (1) the preparation of the carrier/ONs-complexes, (2) the stability of the complexes in biological fluids, (3) the transport of the complexes from the extracellular space to the intracellular environment and (4) the cellular behavior of the complexes. An important step, which has to occur once the complexes arrive in the cells, is the release of the ONs from their carrier.

Although the association and dissociation of pharmaceutical carrier/ONs complexes have been studied extensively in vitro (i.e. in buffer), information on the complexation in biological media, and especially in the cellular environment is limited. Therefore, very challenging is the development of innovative methods to study the behavior of pharmaceutical carrier/ONs complexes in the cytoplasm and nucleus of cells. With this scope in mind, this thesis deals with dual color fluorescence fluctuation spectroscopy. The main aim of this thesis is to evaluate the potential of this method to study the complexation between ONs and their carriers in buffer and in the living cells.

In this chapter **(Chapter 1)** the basic principles of antisense therapy and the obstacles in non viral antisense delivery were briefly summarized. A literature overview on advanced fluorescence microscopy techniques that allow studying intracellular processes was made. Advanced microscopy techniques clearly show potential to help to a better understanding of the mechanisms which process macromolecular therapeutics or nanoscopic drug vectors in biological environments. The experimental results in **Chapter 2** will illustrate the need for advanced microscopy techniques to understand why some carrier/ONs combinations show biological activity, whereas other combinations fail. Therefore, we wish to evaluate the use of dual color FFS to study the dissociation/association of ONs from/to their carrier in buffer and in living cells. In **Chapter 3** we will elucidate the complexation behavior between oligonucleotides and the cationic polymer poly-L-Lysine (pLL) by single and dual color FFS. Poly-L-Lysine is a well-studied cationic polymer and is used in this study as a model for cationic homopolymers used as pharmaceutical carrier. In **Chapter 4** we will evaluate to what extent dual color FFS is able to study the model pLL/ONs complexes in living cells. In the following chapters, two alternative types of carrier/ONs-complexes will be studied by dual color FFS in buffer: pegylated polymer/ONs complexes in **Chapter 5** and liposome/ONs complexes in **Chapter 6**. Using liposome/ONs complexes as a model, we will also prove that dual color FFS is an excellent technique to study the stability of carrier/ONs-complexes in cell lysate and in living cells.

Reference List

1. Shi,F. and Hoekstra,D., Effective intracellular delivery of oligonucleotides in order to make sense of antisense, Journal of Controlled Release, 97 (2004) 189-209.

2. Vanhee-Brossollet,C. and Vaquero,C., Do natural antisense transcripts make sense in eukaryotes?, Gene, 211 (1998) 1-9.

3. Filmore,D., Assessing antisense. An FDA withdrawal signals another setback, but hope remains for next-generation drugs., Modern Drug Discovery, (June 2004) 49-50.

4. Potera,C., First antisense NDA filed - Fomivirsen goes before the agency for product review, Genetic Engineering News, 18 (1998) 1.

5. Filmore,D., Assessing antisense. An FDA withdrawal signals another setback, but hope remains for next-generation drugs., Modern Drug Discovery, (2004) 49-50.

6. Ray,A. and Norden,B., Peptide nucleic acid (PNA): its medical and biotechnical applications and promise for the future, Faseb Journal, 14 (2000) 1041-1060.

7. Crooke,S.T., Lemonidis,K.M., Neilson,L., Griffey,R., Lesnik,E.A., and Monia,B.P., Kinetic Characteristics of Escherichia-Coli Rnase H1 - Cleavage of Various Antisense Oligonucleotide-Rna Duplexes, Biochemical Journal, 312 (1995) 599-608.

8. Veal,G.J., Agrawal,S., and Byrn,R.A., Sequence-specific RNase H cleavage of gag mRNA from HIV-1 infected cells by an antisense oligonucleotide in vitro, Nucleic Acids Research, 26 (1998) 5670-5675.

9. Shi,F. and Hoekstra,D., Effective intracellular delivery of oligonucleotides in order to make sense of antisense, Journal of Controlled Release, 97 (2004) 189-209.

10. Elbashir,S.M., Harborth,J., Lendeckel,W., Yalcin,A., Weber,K., and Tuschl,T., Duplexes of 21-nucleotide RNAs mediate RNA interference in cultured mammalian cells, Nature, 411 (2001) 494-498.

11. Zamore,P.D., Ancient pathways programmed by small RNAs, Science, 296 (2002) 1265-1269.

12. De Smedt,S.C., Demeester,J., and Hennink,W.E., Cationic polymer based gene delivery systems, Pharmaceutical Research, 17 (2000) 113-126.

13. Gao,X. and Huang,L., Cationic liposome-mediated gene transfer, Gene Ther., 2 (1995) 710-722.

14. Felgner,P.L., Barenholz,Y., Behr,J.P., Cheng,S.H., Cullis,P., Huang,L., Jessee,J.A., Seymour,L., Szoka,F., Thierry,A.R., Wagner,E., and Wu,G., Nomenclature for synthetic gene delivery systems, Human Gene Therapy, 8 (1997) 511-512.

15. Zabner,J., Fasbender,A.J., Moninger,T., Poellinger,K.A., and Welsh,M.J., Cellular and molecular barriers to gene transfer by a cationic lipid, J. Biol. Chem., 270 (1995) 18997-19007.

16. Godbey,W.T., Wu,K.K., and Mikos,A.G., Tracking the intracellular path of poly(ethylenimine)/DNA complexes for gene delivery, Proceedings of the National Academy of Sciences of the United States of America, 96 (1999) 5177-5181.

17. Marcusson,E.G., Bhat,B., Manoharan,M., Bennett,C.F., and Dean,N.M., Phosphorothioate oligodeoxyribonucleotides dissociate from cationic lipids before entering the nucleus, Nucleic Acids Research, 26 (1998) 2016-2023.

18. Zelphati,O. and Szoka,F.C., Mechanism of oligonucleotide release from cationic liposomes, Proc. Natl. Acad. Sci. U. S A, 93 (1996) 11493-11498.

19. Clamme,J.P., Bernacchi,S., Vuilleumier,C., Duportail,G., and Mely,Y., Gene transfer by cationic surfactants is essentially limited by the trapping of the surfactant/DNA complexes onto the cell membrane: a fluorescence investigation, Biochimica et Biophysica Acta-Biomembranes, 1467 (2000) 347-361.

20. Lleres,D., Dauty,E., Behr,J.P., Mely,Y., and Duportail,G., DNA condensation by an oxidizable cationic detergent. Interactions with lipid vesicles, Chemistry and Physics of Lipids, 111 (2001) 59-71.

21. Madeira,C., Loura,L.M.S., ires-Barros,M.R., Fedorov,A., and Prieto,M., Characterization of DNA/lipid complexes by fluorescence resonance energy transfer, Biophysical Journal, 85 (2003) 3106-3119.

22. Madeira,C., Loura,L.M.S., Fedorov,A., Prieto,M., and ires-Barros,M.R., Characterization of DNA/lipid complexes by fluorescence resonance energy transfer, Journal of Liposome Research, 13 (2003) 75.

23. Itaka,K., Harada,A., Yamasaki,Y., Nakamura,K., Kawaguchi,H., and Kataoka,K., In situ single cell observation by fluorescence resonance energy transfer reveals fast intra-cytoplasmic delivery and easy release of plasmid DNA complexed with linear polyethylenimine, Journal of Gene Medicine, 6 (2004) 76-84.

24. Itaka,K., Harada,A., Nakamura,K., Kawaguchi,H., and Kataoka,K., Evaluation by fluorescence resonance energy transfer of the stability of nonviral gene delivery vectors under physiological conditions, Biomacromolecules, 3 (2002) 841-845.

25. Van Craenenbroeck,E., Matthys,G., Beirlant,J., and Engelborghs,Y., A statistical analysis of fluorescence correlation data, Journal of Fluorescence, 9 (1999) 325-331.

26. Van Craenenbroeck,E., Vercammen,J., Matthys,G., Beirlent,J., Marot,C., Hoebeke,J., Strobbe,R., and Engelborghs,Y., Heuristic statistical analysis of fluorescence fluctuation data with bright spikes: Application to ligand binding to the human serotonin receptor expressed in Escherichia coli cells, Biological Chemistry, 382 (2001) 355-361.

27. Giese,A., Bieschke,J., Eigen,M., and Kretzschmar,H.A., Putting prions into focus: application of single molecule detection to the diagnosis of prion diseases, Archives of Virology, 16 (2000) 161-171.

28. Schwille,P., Fluorescence Correlation Spectroscopy and Its Potential for Intracellular Applications, Cell Biochemistry and Biophysics, 34 (2001) 383-408.

29. Meseth,U., Wohland,T., Rigler,R., and Vogel,H., Resolution of fluorescence correlation measurements, Biophysical Journal, 76 (1999) 1619-1631.

30. Chen,Y., Muller,J.D., Berland,K.M., and Gratton,E., Fluorescence fluctuation spectroscopy, Methods, 19 (1999) 234-252.

31. Chen,Y., Muller,J.D., So,P.T., and Gratton,E., The photon counting histogram in fluorescence fluctuation spectroscopy, Biophys. J, 77 (1999) 553-567.

32. Kask,P., Palo,K., Ullmann,D., and Gall,K., Fluorescence-intensity distribution analysis and its application in biomolecular detection technology, Proceedings of the National Academy of Sciences of the United States of America, 96 (1999) 13756-13761.

33. Kask,P., Palo,K., Fay,N., Brand,L., Mets,U., Ullmann,D., Jungmann,J., Pschorr,J., and Gall,K., Two-dimensional fluorescence intensity distribution analysis: Theory and applications, Biophysical Journal, 78 (2000) 1703-1713.

34. Schwille,P., MeyerAlmes,F.J., and Rigler,R., Dual-color fluorescence cross-correlation spectroscopy for multicomponent diffusional analysis in solution, Biophysical Journal, 72 (1997) 1878-1886.

35. Palo,K., Metz,U., Jager,S., Kask,P., and Gall,K., Fluorescence intensity multiple distributions analysis: Concurrent determination of diffusion times and molecular brightness, Biophysical Journal, 79 (2000) 2858-2866.

36. Palo,K., Brand,L., Eggeling,C., Jager,S., Kask,P., and Gall,K., Fluorescence intensity and lifetime distribution analysis: Toward higher accuracy in fluorescence fluctuation spectroscopy, Biophysical Journal, 83 (2002) 605-618.

37. Bieschke,J., Giese,A., Schulz-Schaeffer,W., Zerr,I., Poser,S., Eigen,M., and Kretzschmar,H., Ultrasensitive detection of pathological prion protein aggregates by dual-color scanning for intensely fluorescent targets, Proceedings of the National Academy of Sciences of the United States of America, 97 (2000) 5468-5473.

38. Stpierre,P.R. and Petersen,N.O., Average Density and Size of Microclusters of Epidermal Growth- Factor Receptors on A431 Cells, Biochemistry, 31 (1992) 2459-2463.

39. Srivastava,M. and Petersen,N.O., Image cross-correlation spectroscopy analysis of diffusion, flow and intermolecular interactions, Biophysical Journal, 72 (1997) WP220.

40. Wiseman,P.W., Squier,J.A., Fan,G.Y., Ellisman,M.H., and Wilson,K.R., Image correlation spectroscopy (ICS) and 2-color image cross correlation spectroscopy (ICCS) using 2-photon video microscopy, Biophysical Journal, 78 (2000) 798Plat.

41. Wiseman,P.W., Squier,J.A., Ellisman,M.H., and Wilson,K.R., Two-photon image correlation spectroscopy and image cross- correlation spectroscopy, Journal of Microscopy-Oxford, 200 (2000) 14-25.

42. Van Rompaey,E., Sanders,N., De Smedt,S.C., Demeester,J., Van Craenenbroeck,E., and Engelborghs,Y., Complex formation between cationic polymethacrylates and oligonucleotides, Macromolecules, 33 (2000) 8280-8288.

43. Van Rompaey,E., Chen,Y., Muller,J.D., Gratton,E., Van Craenenbroeck,E., Engelborghs,Y., De Smedt,S., and Demeester,J., Fluorescence fluctuation analysis for the study of interactions between oligonucleotides and polycationic polymers, Biological Chemistry, 382 (2001) 379-386.

44. Van Rompaey,E., Engelborghs,Y., Sanders,N., De Smedt,S.C., and Demeester,J., Interactions between oligonucleotides and cationic polymers investigated by fluorescence correlation spectroscopy, Pharmaceutical Research, 18 (2001) 928-936.

45. Jurkiewicz,P., Okruszek,A., Hof,M., and Langner,M., Associating oligonucleotides with positively charged liposomes, Cellular & Molecular Biology Letters, 8 (2003) 77-84.

46. Brock,R., Hink,M.A., and Jovin,T.M., Fluorescence correlation microscopy of cells in the presence of autofluorescence, Biophysical Journal, 75 (1998) 2547-2557.

47. Berland,K.M., So,P.T.C., Chen,Y., Mantulin,W.W., and Gratton,E., Scanning two-photon fluctuation correlation spectroscopy: Particle counting measurements for detection of molecular aggregation, Biophysical Journal, 71 (1996) 410-420.

48. Eid,J.S., Muller,J.D., Chen,Y., and Gratton,E., Dual channel two photon FCS study in a cell, Biophysical Journal, 78 (2000) 2597Pos.

49. McClendon,S., Yu,W.M., and Gratton,E., Two-photon FCS using a dual channel single photon counting system, Biophysical Journal, 72 (1997) TU465.

Chapter 2

On the biological activity of anti-ICAM-1 oligonucleotides complexed to non-viral carriers.

Parts of this chapter have been published in Journal of Controlled Release 96: 207-219 (2004).

1. Introduction

Today, most studies on the cellular behavior of DNA carriers deal with the delivery of plasmid DNA. The cellular behavior of ONs packed in pharmaceutical carriers has been investigated less systematically [1]. This may be partially explained by the fact that the cellular delivery of plasmids can be evaluated rather easily by measuring the cellular expression of the corresponding protein. However, the biological evaluation of antisense ONs effects is more difficult because of the "high background": antisense ONs have to decrease a pre-existing high level of target RNA or translated protein. Modified assays are recently developed to counter this problem [2;3].

In the first part of this chapter, we studied the biological efficiency of anti-ICAM-1 ONs packed in several types of pharmaceutical carriers. We used a well-studied antisense assay in which the ability of the ONs to downregulate the expression of the intercellular adhesion molecule-1 (ICAM-1, a 90-110 kDa membrane glycoprotein) is evaluated. The ICAM-1 gene plays an important role in inflammatory diseases like rheumatoid arthritis, ulcerative colitis, Crohn's disease, … [4;5]. Published data describe antisense-specific and effective inhibition of ICAM-1 by antisense oligonucleotides in tissue culture [6;7], in rodents [8;9] and in humans [10].

As related projects of our group are focusing on pulmonary gene delivery through inhalation [11], the human lung epithelial cell line A549 was used to determine the biological efficiency of the ONs. ICAM-1 is normally expressed at low levels on the surface of these cells. In response to tumor necrosis factor-alfa (TNF-alfa), an increased expression ("upregulation") of ICAM-1 has been demonstrated [12]. When targeted to human ICAM-1 mRNA, antisense ONs can inhibit the upregulated expression in A549 cells by different

mechanisms. The oligonucleotide “ISIS 1939”, which targets specific sequences in the 3’-untranslated region of the mRNA, is biologically active by RNase H mediated degradation of the targeted mRNA. The oligonucleotide “ISIS 1570” targets the AUG translation initiation codon. In the latter case, the protein level is reduced but not the ICAM-1-mRNA level [6].

Antisense ONs can bind to mRNA both in the cytoplasm and in the nucleus, therefore reaching the nucleus should not be a requisite for biological activity. However, as RNase H is more abundant in the nucleus [13], the nuclear accumulation of the ONs might result in higher efficiency in case of “ISIS 1939” ONs. In general, it is observed that microinjection of free ONs in the cytoplasm leads to an accumulation of the ONs in the nucleus within minutes. This is attributed to simple diffusion, with subsequent trapping of the oligonucleotides [14-16]. Recently, PS-ONs are reported to continuously shuttle between the nucleus and the cytoplasm, in an active transport, carrier-mediated and nuclear pore complex mediated way [17]. In contrast to previous reports, phosphodiester oligodeoxynucleotides have been found to be actively imported into the nucleus [18].

A biological assay answers the question whether a certain pharmaceutical carrier successfully delivers ONs or not. However, it does not give an answer on the important question why one carrier is successful while another one fails. In the second part of this work, we tried to find out why some carrier/ONs combinations showed biological activity and why others did not. We were especially interested in knowing how cellular methods like flow cytometry and confocal laser scanning microscopy (CLSM) could provide us with additional information on the cellular delivery of the carrier/ONs combinations studied.

2. Materials and methods

2.1. Cell culture

Human lung carcinoma cells (A549 cells, ATCC number: CCL-185) (DSMZ, Braunschweig, Germany) were cultured in Dulbecco's modified Eagle's medium (DMEM; without phenol red) (Gibco, Merelbeke, Belgium) containing 2 mM glutamine, 10% heat inactivated fetal bovine serum (FBS), 1% penicilline-streptomycine. Cells were grown at 37°C in a humidified atmosphere containing 5% CO_2. Cells were prophylactically treated against mycoplasma with Plasmocin (Invivogen, Cayla, France). Hoechst 33258 (bisbenzimidazole) (ICN Biochemicals, Inc. Aurora, Ohio) was used to prove that cells were free of mycoplasma.

2.2. Oligonucleotides

The 20-mer ICAM-1 antisense ONs (5'-CCC CCA CCA CTT CCC CTC TC-3') employed in the present study target the 3' non-coding region of ICAM-1 mRNA. This 20-mer antisense ON corresponds to ISIS 1939. They were supplied by Eurogentec (Seraing, Belgium) as phosphorothioate ONs (PS-ONs) and phosphodiester ONs (PO-ONs). Also the 5' rhodamine green (RhGr) labeled ONs were supplied by Eurogentec.

2.3. Cationic carriers

Lipofectin (DOTMA:DOPE (weight ratio 1:1)) was purchased from Life Technologies (Gaithersburg, MD). Lipofectin is a combination of a cationic lipid (N-(1-(2,3-dioleoyloxy)propyl)-N,N,N-trimethylammonium chloride (DOTMA), Figure 1A) and a neutral lipid (dioleoylphosphatidylethanolamine (DOPE), Figure 1B).

Poly(ethylene glycol)-poly-ethylene-imine (pEG-pEI, Figure 1C) was a kind gift of the University of Nebraska. The weight average molecular weight (MW), as determined from static light scattering, was 12,4 kg/mol. The total content of nitrogen was 3.75 µmol/mg polymer.

PEI (25 kg/mol) was obtained by Sigma-Aldrich (Bornem, Belgium).

Pegylated poly (2-dimethylamino) ethylmethacrylate-co-aminoethylmethacrylate (pEG-pDMAEMA-co-AEMA, MW 1700000 g/mol, 8 mol % AEMA, Figure 1D; abbreviated as graft-pDMAEMA) was a generous gift of the University of Utrecht. Part of AEMA (max 25 %) was conjugated with pEG 5000, using a versatile method to synthesize pDMAEMA-conjugates as described elsewhere [19].

Alexa647-succinimidylester (Amersham Pharmacia, Piscataway, NJ) was used to label part of the non-pegylated AEMA. The non-conjugated label was removed by means of dialysis (molecular weight cutoff 12 kD, Medicell International Ltd.). It could be calculated that each polymer chain bore on the average 12 fluorescent labels.

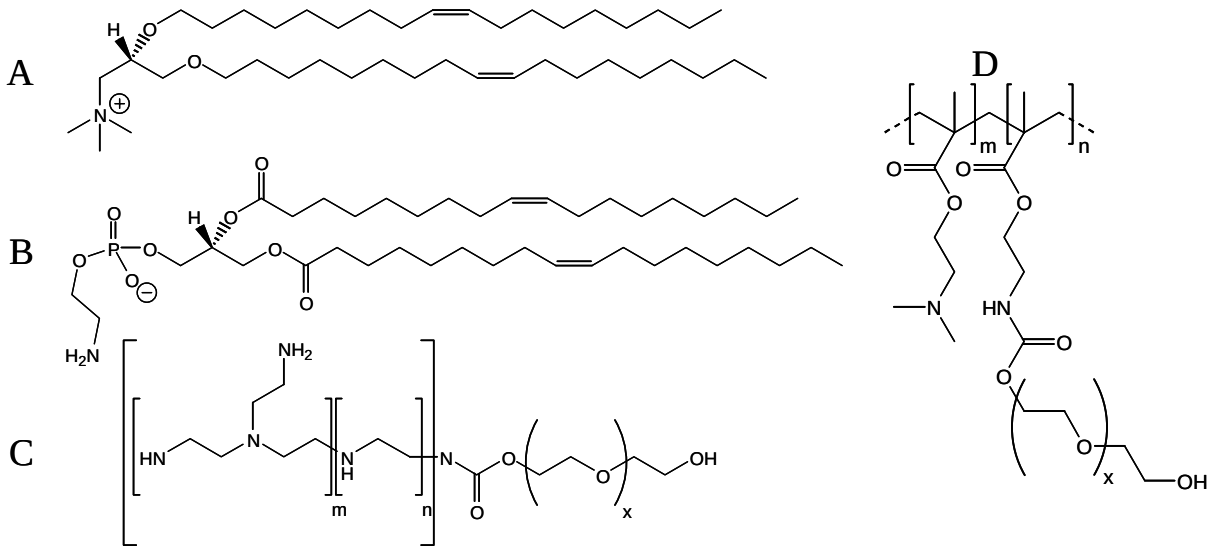

Figure 1. Structure of the cationic lipid DOTMA (A), the neutral helper lipid DOPE (B), the cationic block-copolymer pEG-pEI (C) and the cationic copolymer graft-pDMAEMA (D).

2.4. Preparation of the lipoplexes and polyplexes for cellular experiments

In case of Lipofectin, 100 µL DMEM containing 20 µg/mL Lipofectin was added to each well, followed by 50 µL of the ONs solution in DMEM.

Where graft-pDMAEMA/ONs or pEG-pEI/ONs polyplexes were used, 150 µL of the polyplex dispersion was added to each well. We emphasize that, contrary to the complexation with Lipofectin, the complexation took place before the polyplexes were applied on the cells. Polyplexes of a polymer/ONs weight ratio of 4 (w/w = 4) were prepared by mixing (in one step) polymer and ONs stock solutions (in DMEM), followed by vortexing the dispersion during 10 seconds. To obtain the desired final ONs concentration, the dispersions were further

diluted with DMEM. The polyplexes were allowed to equilibrate for 30 minutes at room temperature prior to use.

2.5. Inhibition of ICAM-1 expression in A549 cells

A549 cells were plated onto 96-well microtiter plates (10^4 cells/well). On day 3 (at 90% confluency) the cells were washed three times with phosphate buffered saline (PBS) (Gibco, Merelbeke, Belgium) and free or complexed ONs were added to the cells, followed by four hours of incubation. Subsequently, the free or complexed ONs were removed. After washing the cells three times with PBS, 100 µL culture medium supplemented with 10 ng/mL TNF-alfa was added to induce overexpression of ICAM-1. After 18 hours, the cells were washed, fixed for 15 min at room temperature in PBS containing 20 mg/mL paraformaldehyde and blocked with 2% normal goat serum (NGS) in a 1% BSA/PBS solution. The expression of ICAM-1 was measured as follows. Cells were washed and incubated for 90 min at 37°C with mouse anti-human ICAM-1 antibody (ImmunoSource, Zoersel, Belgium) (0.5 µg/mL). After removal of the mouse anti-human ICAM-1 antibody, the cells were washed and incubated for 1 h at 37°C with sheep anti-mouse antibody-horseradish peroxidase conjugate (1:1000). After 3 washes, the peroxidase activity was assessed using 100 µL of o-phenylenediamine dihydrochloride (OPD; Sigma, Bornem, Belgium). After 15 min incubation at 37°C, the reaction was stopped by adding 100 µL 2 M H_2SO_4 and the absorbance was read on an ELISA plate reader at 490 nm. A_0 is the absorption of the cells without TNF-alfa induction ("basal expression"). A_{TNF} is the absorption of the cells upon induction with TNF-alfa but in the absence of ONs. A_{ONsTNF} is the absorption of the cells upon induction with TNF-alfa and after treating the cells with (free or complexed) ONs.

2.6. Agarose gel electrophoresis experiments

The polyplex dispersions (pEI/ONs: w/w 1.6 and graft-pDMAEMA/ONs: w/w = 4) used in the gel electrophoresis experiments contained 26.7 µg/mL RhGr labeled PO-ONs or RhGr labeled PS-ONs. Thirty minutes after the preparation of the polyplex dispersions, DNase I (Roche, Belgium) or unlabeled ONs (PS or PO) were added to the dispersions. Another 30 minutes later, 30 µL of these dispersions was mixed with 5 µL of a 50% sucrose solution in distilled water and placed in the wells of a 1.1 % agarose gel. A TBE buffer was used containing 10.8 g/L Tris base, 5.5 g/L boric acid and 0.58 g/L EDTA. A potential of 100

V was applied for 60 min. The oligonucleotides in the gel were detected based upon the fluorescence of their RhGr-label.

2.7. Cellular uptake of ONs measured by flow cytometry

A549 cells were harvested using trypsin and 3 x 10^5 cells were incubated at 37 °C during 4 hours in DMEM containing RhGr-ONs (0.5 µM) either in the absence or presence of a cationic carrier (Lipofectin (13 µg/mL), graft-pDMAEMA (w/w = 4) or pEG-pEI (w/w = 4)). After incubation, the cells were centrifuged 3 times (200 g for 5 min); after each centrifugation step the pellet was washed with PBS. Consequently, the cells were resuspended in DMEM. The fluorescence intensity of the cells was recorded at 520 nm using a flow cytometer (Becton Dickinson, Erembodegem, Belgium) at an excitation wavelength of 488 nm. Cell viability was simultaneously evaluated by adding propidium iodide (detection at 700 nm, excitation at 488 nm). 5000 cells were analyzed.

2.8. Confocal laser scanning microscopy

The cells were seeded onto sterile 8-well Nunc chambers (Nalge Nunc Int., Naperville, Il) and allowed to adhere for 1 day. 150 µL of RhGr-ONs (0.5 µM in DMEM) in the absence or presence of a cationic carrier (Lipofectin (13 µg/mL), graft-pDMAEMA (w/w = 4) or pEG-pEI (w/w = 4)) were added to the cells and incubated for 3 hours at 37°C. The cells were washed three times with PBS before investigating them by confocal laser scanning microscopy (Bio-Rad MRC 1024; Hemel Hempstadt, UK). Confocal sections were taken every 0.5 µm. Cell viability was simultaneously evaluated by adding propidium iodide. We used a 60x water immersion objective and a krypton/argon laser (488 nm) for the excitation of the RhGr.

3. Results and discussion

3.1. Biological activity of ICAM-1 antisense ONs in the presence or absence of cationic carriers

To evaluate the biological activity of ONs bound to different carriers we used the ICAM-1 assay. In this assay we determined the inhibition of the ICAM-1 protein expression on the surface of A549 cells induced by TNF-alfa. ISIS 1939 PS-ONs and its phosphodiester analog (PO-ONs) were chosen because they are more active than ISIS 1570 [6].

It was important to assure that ICAM-1 experiments were done on mycoplasma-free cells. Indeed, we observed that in mycoplasma infected cells the basal ICAM-1 expression (A_0) was increased to the same level as the induced ICAM-1 expression (A_{TNF}) (data not shown). We observed that the treatment of the cells with Plasmocin successfully eliminated the mycoplasma: extranuclear Hoechst 33258 fluorescence was absent while the basal ICAM-1 expression returned to a normal level. These observations agreed with the study of Fabisiak et al. who reported that cytokine levels (as measured by ELISA) in mycoplasma infected cells were 50-fold higher than in the non-infected lines. They also observed that treatment of these cells with mycoplasma removal agents eliminated extranuclear Hoechst fluorescence and significantly reduced the cytokine levels [20].

Maus et al. reported that cationic liposomes themselves inhibit the TNF-alfa induced ICAM-1 expression in human endothelial cells [21]. To verify whether the cationic carriers used in this study influence the ICAM-1 expression, we determined the ICAM-1 expression of the A549 cells in the presence and absence of the (free) carriers. As Figure 2 shows, Lipofectin did not influence the ICAM-1 expression, in the concentrations used in this study. Also graft-pDMAEMA, and pEG-pEI did not influence the ICAM-1 expression (data not shown).

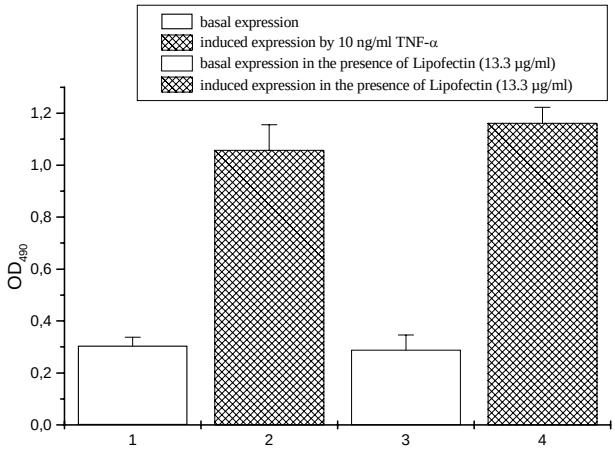

Figure 2. Basal (empty bar) and TNF-α induced (shaded bar) ICAM-1 expression of A549 cells in the presence (bar 3 and 4) and absence (bar 1 and 2) of Lipofectin (n = 6).

In the absence of a carrier, the PS-ONs and PO-ONs failed to inhibit TNF-alfa induced ICAM-1 expression even at concentrations of up to 1 µM (data not shown). Probably, this can be explained by the inability of naked ONs to diffuse passively through the cellular membrane as they are large (5-10 kDa), negatively charged, hydrophilic molecules.

Figure 3A shows that after treatment with Lipofectin/PO-ONs no significant decrease in the level of induced ICAM-1 protein expression was observed for different concentrations of PO-ONs (0.25-1.2 µM). Other groups already showed that cationic lipids were not able to confer antisense activity on PO-ONs [6;22]. Although, as shown in Figure 3B, Lipofectin/PS-ONs complexes were able to significantly decrease the ICAM-1 expression.

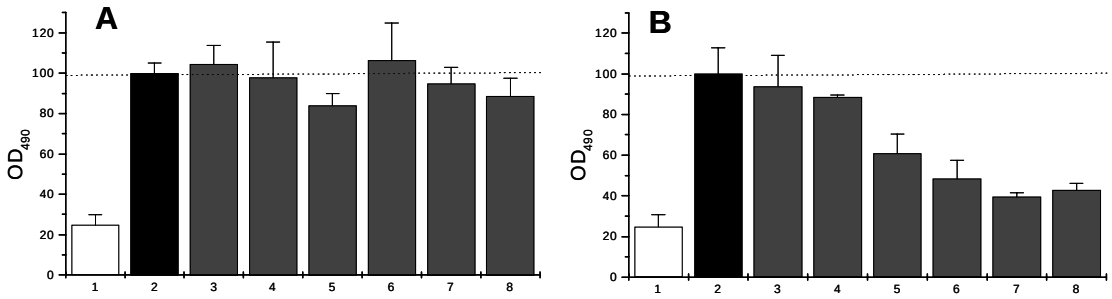

Figure 3. Inhibition of ICAM-1 expression in A549 cells by PO-ONs (A) and PS-ONs (B) in the presence of Lipofectin. A549 cells were treated with serum-free medium containing Lipofectin (13.3 µg/mL) and the indicated concentration of ONs (3: 100 nM, 4: 250 nM, 5: 500 nM, 6: 750 nM, 7: 1 µM, 8: 1,2 µM). Bar 1 and 2 show respectively the basal and the induced ICAM-1 expression. The ICAM-1 expression of TNF-alfa-treated cells was set to 100 %. All the data are expressed as mean values of 4 measurements (n = 4).

Figure 4 shows that, in contrast to Lipofectin, graft-pDMAEMA efficiently delivered both PO-ONs as well as PS-ONs to ICAM-1 mRNA. Especially, a very efficient inhibition of the ICAM-1 expression was obtained when graft-pDMAEMA/PS-ONs complexes were used, even at very low PS-ONs concentrations.

We further observed that the ICAM-1 expression was not inhibited using pEG-pEI as a carrier for the PS-ONs and the PO-ONs (data not shown).

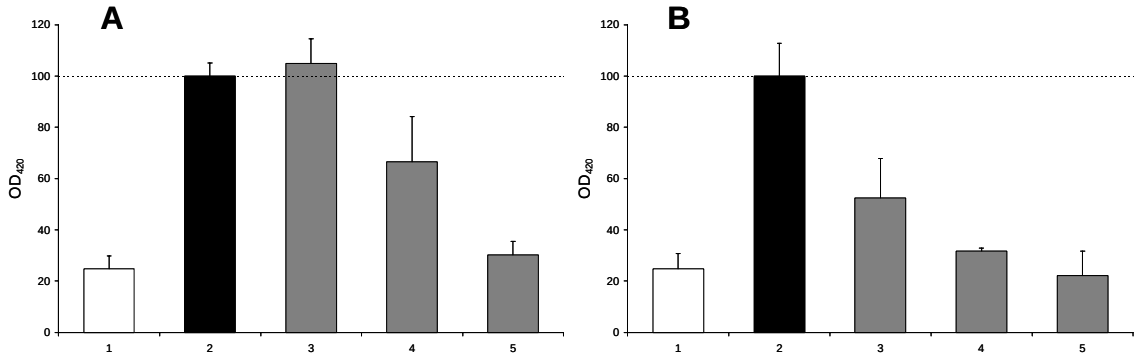

Figure 4. Inhibition of ICAM-1 expression in A549 cells by PO-ONs (A) and PS-ONs (B) in the presence of graft-pDMAEMA. A549 cells were treated with graft-pDMAEMA/ONs complexes (w/w = 4) in serum-free medium at the indicated concentration of ONs (3: 100 nM, 4: 500 nM, 5: 1 µM). Bar 1 and 2 show respectively the basal and the induced ICAM-1 expression. The ICAM-1 expression of TNF-alfa-treated cells was set to 100 %. All the data are expressed as mean values of 4 measurements (n = 4).

Three major questions were revealed from Figures 3 and 4:

(a) How to explain why PS-ONs complexed to Lipofectin were biologically active while PO-ONs complexed to Lipofectin did not show antisense activity? (Figure 3B versus Figure 3A)

(b) Why is there a discrepancy between Lipofectin and graft-pDMAEMA in the delivery of PO-ONs? (Figure 3A versus Figure 4A)

(c) Why do PS-ONs complexed to graft-pDMAEMA show a better biological effect than PO-ONs complexed to graft-pDMAEMA? (Figure 4B versus Figure 4A)

One hypothesis to explain the first question is that the oligonucleotides dissociate from the cationic lipid already during the endosomal escape. Marcusson et al. suggested from CLSM measurements that the lipid indeed stays in the endosomal compartment while the oligonucleotides travel through the cell [23]. Consequently, free PO-ONs and PS-ONs are delivered in the cytoplasm. As PS-ONs are more resistant to intracellular nucleases, this may

explain why PS-ONs complexed to Lipofectin were biologically active while PO-ONs complexed to Lipofectin did not show antisense activity.

One hypothesis to explain the second question is that graft-pDMAEMA may stay associated with the ONs in the cytoplasm for a longer time and, consequently, may protect the ONs from nuclease degradation. Though our CLSM-observations show similar distributions for ONs complexed to graft-pDMAEMA or complexed to Lipofectin (see 3.3.), gelelectrophoresis shows that Lipofectin/ONs complexes are easily destabilized in a buffer solution containing the extracellular DNase I (Figure 5A), whereas graft-pDMAEMA/ONs complexes remain very stable (Figure 5B), even over a few days.

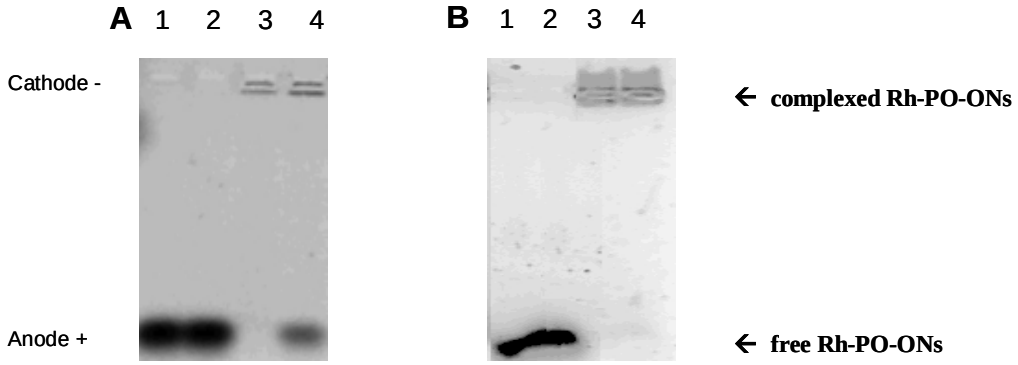

Figure 5. (A) Gel electrophoresis on free RhGr-PO-ONs (lane 1 and 2) and Lipofectin/RhGr-PO-ONs complexes (lane 3 and 4). Lane 2 and 4 show the effect of incubating the sample with DNase I for over 24 h. The RhGr-PO-ONs concentration in all the dispersions was 20 µg/mL, the DNase I concentration was 14 µg/mL. (B) Gel electrophoresis on free RhGr-PO-ONs (lane 1 and 2) and graft-pDMAEMA/RhGr-PO-ONs complexes (lane 3 and 4). Lane 2 and 4 show the effect of incubating the sample with DNase I for over 24 h. The RhGr-PO-ONs concentration in all the dispersions was 20 µg/mL, the DNase I concentration was 14 µg/mL.

Besides the protective characteristics of the polymer (see question b) and the nuclease resistance of the PS-ONs (see question a), other phenomena might explain why graft-pDMAEMA/PS-ONs showed a better activity than graft-pDMAEMA/PO-ONs (question c). We wondered whether the chemical modification of PO-ONs into PS-ONs influences the interaction of the oligonucleotides with their carriers, which may, on its turn, influence their biological effect. Therefore, RhGr-PO-ONs/carrier and RhGr-PS-ONs/carrier complexes were exposed to increasing concentrations of respectively (unlabeled) PS-ONs and PO-ONs followed by gel electrophoresis analysis. Figure 6A shows the results of graft-pDMAEMA/RhGr-PO-ONs complexes exposed to unlabeled PS-ONs; Figure 6B shows the results of graft-pDMAEMA/RhGr-PS-ONs complexes exposed to unlabeled PO-ONs. The

"competition experiment" in Figure 6 shows that graft-pDMAEMA formed more stable complexes with RhGr-PS-ONs (Figure 6B) than with RhGr-PO-ONs (Figure 6A): while PS-ONs were able to displace RhGr-PO-ONs from graft-pDMAEMA, PO-ONs could not displace the RhGr-PS-ONs from their carrier.

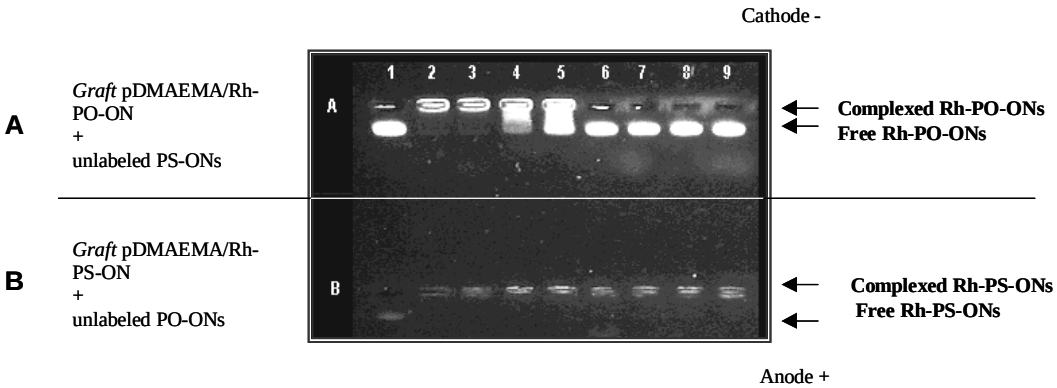

Figure 6. (A) Gel electrophoresis on graft-pDMAEMA/RhGr-PO-ONs complexes (w/w = 4) exposed to increasing concentration of unlabeled PS-ONs. The RhGr-PO-ONs concentration in all the dispersions is 26.7 µg/mL. Lane 1 contains RhGr-PO-ONs alone. Lane 2 contains graft-pDMAEMA/RhGr-PO-ONs complexes. In lanes 3-9 unlabeled PS-ONs were added to the graft-pDMAEMA/RhGr-PO-ONs complexes in 0.5; 1; 1.5; 3; 4; 5 and 6-fold to the RhGr-PO-ONs concentration. (B) Gel electrophoresis on graft-pDMAEMA/RhGr-PS-ONs complexes (w/w = 4) exposed to increasing concentrations of unlabeled PO-ONs. The RhGr-PS-ONs concentration in all the dispersions is 26.7 µg/mL. Lane 1 contains RhGr-PS-ONs alone. Lane 2 contains graft-pDMAEMA/RhGr-PS-ONs complex. In lanes 3-9 unlabeled PO-ONs were added to the pDMAEMA/RhGr-PS-ONs in 0.5; 1; 1.5; 3; 4; 5 and 10-fold to the RhGr-PS-ONs concentration.

Similar results were obtained when using the polymer pEI (Figure 7): PS-ONs were able to displace RhGr-PO-ONs from pEI while PO-ONs could not displace RhGr-PS-ONs from pEI. Dheur et al. used this result to explain why in their experiment the pEI/PO-ONs complexes exerted antisense activity while the pEI/PS-ONs complexes did not. They argued that the pEI/PS-ONs complexes were too stable to release the PS-ONs from the carrier [24]. However, following this argumentation and considering our results in Figure 6, one would expect no antisense activity for the graft-pDMAEMA/PS-ONs complexes, while Figure 4B clearly shows a biological effect. It illustrates that it is hard to correlate the outcome of measurements like e.g. gel electrophoresis with the cellular behavior of DNA complexes. Therefore, techniques which could measure the intracellular dissociation behavior of DNA-complexes are highly recommended as they would yield more biologically relevant information.

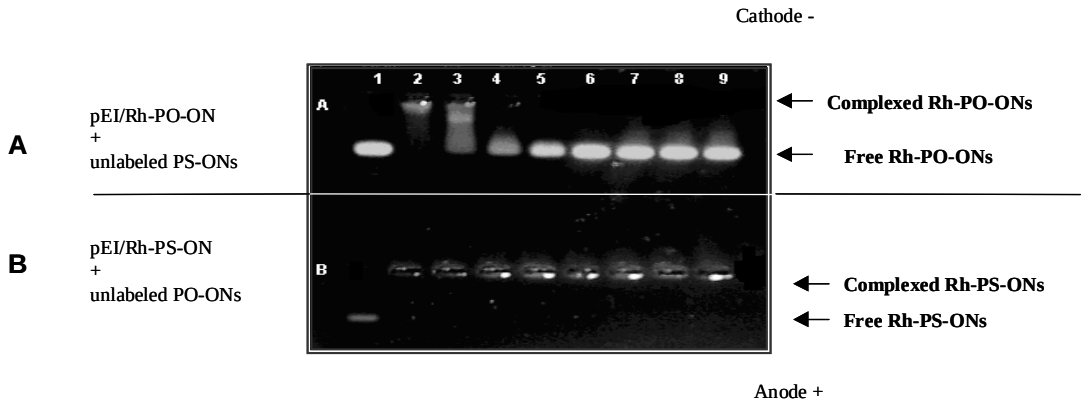

Figure 7. (A) Gel electrophoresis on pEI/RhGr-PO-ONs complexes (w/w = 1.6). The RhGr-PO-ONs concentration in all the dispersions is 26.7 µg/mL. Lane 1 contains RhGr-PO-ONs alone. Lane 2 contains pEI/RhGr-PO-ONs complexes. For lanes 3-9 unlabeled PS-ONs were added to the pEI/RhGr-PO-ONs complexes in 0.5; 1; 1.5; 3; 4; 5 and 6-fold to the RhGr-PO-ONs concentration. (B) Gel electrophoresis on pEI/RhGr-PS-ONs complexes (w/w = 1.6). The RhGr-PS-ONs concentration in all the dispersions is 26.7 µg/mL. Lane 1 contains RhGr-PS-ONs alone. Lane 2 contains pEI/RhGr-PS-ONs complexes. For lanes 3-9 unlabeled PO-ONs were added to the pEI/RhGr-PS-ONs complexes in 0.5; 1; 1.5; 3; 4; 5 and 6-fold to the RhGr-PS-ONs concentration.

3.2. Cellular uptake experiments by flow cytometry

The cellular uptake of the rhodamine green labeled ONs (both PO-ONs and PS-ONs) was evaluated by flow cytometry. A major advantage of flow cytometry is that in a short time a huge population of cells can be evaluated for the absence or presence of fluorescent ONs. A disadvantage of the method is that we cannot obtain information on the intracellular localization and the integrity of the ONs. However, some groups did distinguish between endosomal or cytoplasmatic localization of ONs from flow cytometric studies. Therefore, they labeled the ONs with the pH sensitive dye fluorescein isothiocyanate (FITC) [25].

Upon exposure of the A549 cells to RhGr-labeled PO-ONs, no enhancement of cell-associated fluorescence compared to the blanco cells could be observed. Figure 8A shows that all data were located in the upper left side of the graph. It indicates that the cells did not take up free RhGr labeled PO-ONs. This explains why free PO-ONs did not show any biological effect in the ICAM-1 assay (see 3.1). In case of RhGr-labeled PS-ONs, all cells showed a higher fluorescence as compared to the blanco cells, also after a washing step with acid glycine buffer (pH 2.0) (data not shown). However, we suggest that the increase in fluorescence of the cells was attributed to surface bound RhGr-PS-ONs and not to internalized RhGr-PS-ONs, as could be confirmed by CLSM measurements (see 3.3.).

Figure 8B shows that the complexation of RhGr-PO-ONs with Lipofectin resulted in an increased fluorescence in 90% of the cells. Figure 3A showed that the Lipofectin/PO-ONs complexes did not suppress the ICAM-1 expression. Combining the results from the flow cytometric measurements and the ICAM-1 assay indicates that the absence of antisense activity of Lipofectin/PO-ONs complexes was not attributed to an inefficient entrance of the complexes in the cells.

As Lipofectin/PS-ONs complexes were biologically active, it was expected that flow cytometry would reveal the cellular uptake of ONs. Indeed, Figure 8C shows that in case of complexation of RhGr-PS-ONs with Lipofectin almost all the cells showed increased fluorescence compared to the blanco cells. Even very bright cells could be detected.

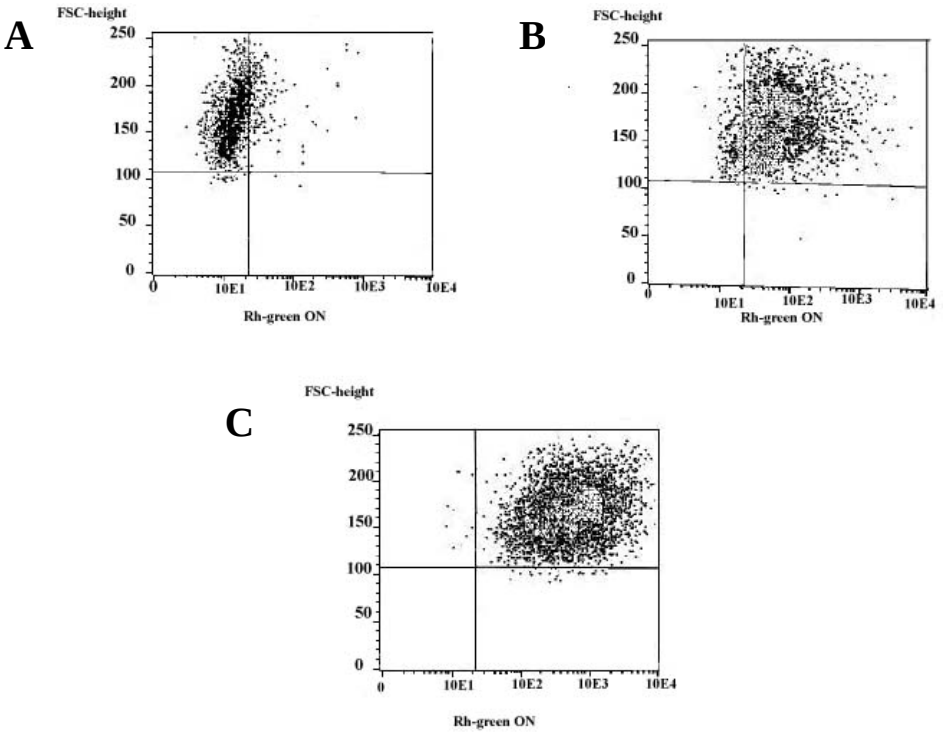

Figure 8. Cellular uptake of RhGr-ONs as studied by flow cytometry. A549 cells were treated for 4 hours with 0.5 µM free PO-ONs (A) and ONs in combination with Lipofectin (13 µg/mL): 0.5 µM PO-ONs (B) and 0.5 µM PS-ONs (C). The threshold of the upper left part is calculated after measuring the fluorescence of blanco cells. The x-axis is a measure of the fluorescence intensity of the cells. The y-axis shows the forward scattering (FSC) and is a measure of cell size.

Complexation of RhGr-PO-ONs with graft-pDMAEMA resulted in an enhanced cell-associated fluorescence for 73% of the cells (data not shown). Also, graft-pDMAEMA/RhGr-PS-ONs complexes were efficiently taken up by the cells (data not shown).

When labeled ONs were complexed with pEG-pEI no enhancement of cell-associated fluorescence could be observed (data not shown), even with RhGr-ONs concentrations of 1 µM. Probably the absence of antisense activity in the ICAM-1 assay by the pEG-pEI based complexes (see 3.1.) can be explained by the inability of these complexes to enter the cells or by extracellular dissociation of the complexes.

3.3. Intracellular localization experiments by CLSM

In contrast to flow cytometry, CLSM can be used to study the intracellular distribution of the labeled ONs. In this study, the intracellular localization experiments were done on unfixed cells as non-viable cells have the property of internalizing significantly more ONs than viable ones (data not shown). CLSM experiments showed that A549 cells did not take up free RhGr-PO-ONs and RhGr-PS-ONs (data not shown). In case of RhGr-PS-ONs a faint staining of the cell surface could be detected, whereas in case of RhGr-PO-ONs no fluorescence at all was observed. These results agreed with those of the flow cytometric experiments and confirmed that the absence of biological activity in the ICAM-1 assay was due to the inability of free ONs to enter the cell.

Figure 9 shows that, in the case of complexation with Lipofectin, a part of the RhGr-PO-ONs was in the nuclei, as they stained green, while another part of the RhGr-PO-ONs was in the endosomes as revealed from the punctate regions in the cytoplasm. Similar CLSM results were observed for Lipofectin/RhGr-PS-ONs. The CLSM experiments showed that Lipofectin was able to deliver both types of ONs in the cellular environment, which agreed with the flow cytometric observations. However, only the Lipofectin/PS-ONs complexes showed antisense activity.

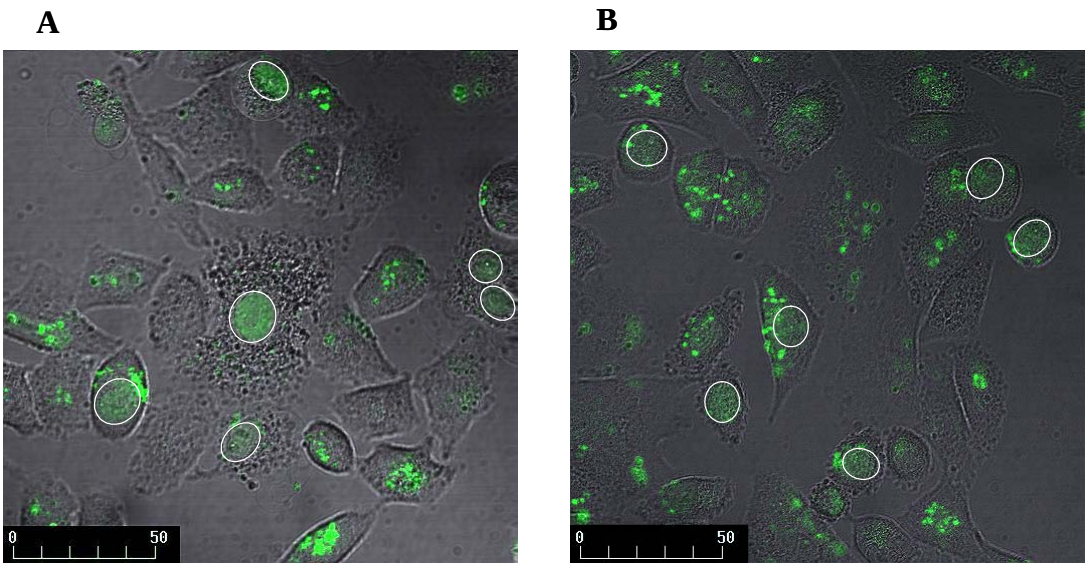

Figure 9. Transmission picture (gray), merged with a CLSM picture (green) of A549 cells transfected with RhGr-PS-ONs (A) and RhGr-PO-ONs (B) complexed with Lipofectin. A circle is drawn around the nuclei with green fluorescence, indicating nuclear accumulation of the RhGr-ONs. A scale bar is indicated in µm.

Where graft-pDMAEMA is concerned, for both types of ONs, again similar CLSM images were obtained as with Lipofectin. Punctate green regions could be observed in the cytoplasm, indicating that part of the RhGr-ONs were undissociated from their carrier and/or still in the endosomes. Part of the cells showed green stained nuclei, corresponding with nuclear accumulation of the RhGr-ONs and therefore an indication for the successful dissociation of the ONs from their carrier. These observations were expected as both graft-pDMAEMA/PS-ONs as graft-pDMAEMA/PO-ONs showed biological activity (see 3.1.). The intracellular dissociation of ONs from graft-pDMAEMA was confirmed by dual color experiments. Cells transfected with Alexa647-graft-pDMAEMA/RhGr-ONs complexes (Figure 10) showed that the polymer is unable to enter the nucleus (as expected for a polymer of very large molecular weight), whereas part of the oligonucleotides accumulated in the nucleus, proving they have been able to dissociate from their carrier in the cytoplasm.

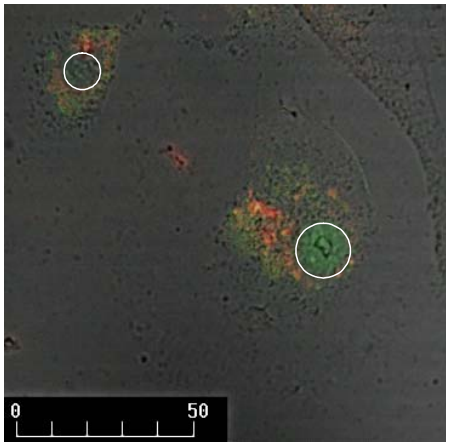

Figure 10. Transmission image (gray), merged with both red and green CLSM images of A549 cells transfected with RhGr-PO-ONs complexed with Alexa647-graft-pDMAEMA. A circle is drawn around the nuclei with green fluorescence, indicating nuclear accumulation of the RhGr-ONs. A scale bar is indicated in µm.

Complexation of ONs with pEG-pEI did not result in a significant staining of the cytoplasm or nuclei of the A549 cells. Consequently, the absence of the antisense effect, as observed in the ICAM-1 assay, could be explained by a low cellular uptake or by the dissociation of the complex in the culture medium.

4. Summary and conclusion

In this study we showed that free PO-ONs and PS-ONs failed to decrease the ICAM-1 protein level. Using CLSM and flow cytometric measurements we showed that this is due to the inability of naked ONs to diffuse passively through the cellular membrane, as they are large, negatively charged hydrophilic molecules.

Although flow cytometric and CLSM experiments clearly showed cellular uptake for PS-ONs and PO-ONs complexed with Lipofectin, Lipofectin/PO-ONs did not show a decrease in the ICAM-1 protein level while Lipofectin/PS-ONs showed a biological effect (Figure 3). We therefore suggested that the absence of antisense activity of Lipofectin/PO-ONs complexes is not attributed to an inefficient entrance of the complexes in the cells but rather to enzymatic degradation of the PO-ONs. Due to the backbone modification, PS-ONs are more stable in cells than PO-ONs [26], which may explain why they showed biological activity.

Contrary to Lipofectin, graft-pDMAEMA efficiently increased the antisense activity of both types of ONs (Figure 4). Noticeably, graft-pDMAEMA/PS-ONs showed a very efficient inhibition of the ICAM-1 expression. As expected, flow cytometric and (dual color) CLSM experiments showed indeed cellular uptake and intracellular dissociation of both graft-pDMAEMA/PS-ONs and graft-pDMAEMA/PO-ONs complexes.

The gel electrophoresis competition experiments showed that graft-pDMAEMA forms more stable complexes with PS-ONs than with PO-ONs. However, as the graft-pDMAEMA/PS-ONs complexes were more biologically active than the graft-pDMAEMA/PO-ONs, it would be wrong to conclude from the gel electrophoresis experiments that the graft-pDMAEMA/PS-ONs complexes are too stable to dissociate intracellularly. Although in literature results from non-cellular experiments like gel electrophoresis are often used to predict the intracellular dissociation behavior of DNA complexes, our results clearly show that measuring the dissociation behavior of DNA-complexes intracellularly is highly recommended.

Although flow cytometry and CLSM are useful to understand the cellular uptake and intracellular localization of ONs, our experiments show that the outcome of CLSM and flow

cytometry measurements cannot explain why PO-ONs are active when complexed to graft-pDMAEMA while they are unactive when complexed to Lipofectin. Similarly, one cannot explain from CLSM and flow cytometry why PS-ONs complexed to graft-pDMAEMA better decrease the ICAM-1 protein expression than PO-ONs complexed to graft-pDMAEMA. As PO-ONs become susceptible to degradation by cytoplasmic DNase as soon as they are released from their carrier, one could argue that a better understanding of the time and (intracellular) place at which dissociation of the complexes occurs is crucial to explain these observations.

Compared with the spatial analysis of the DNA and the carrier (as in dual color microscopy), the temporal analysis of the movement of the DNA and the carrier could be more robust to conclude whether the fluorescently labeled species are interacting. While dual color microscopy answers the question “are the DNA and the carrier located together”, dual color FFS may answer the question whether they really move together. Because FFS can be applied on a cellular scale, we were interested to explore whether it will also allow studying the dissociation of carrier/ONs complexes intracellularly. Therefore, in Chapter 3 the complexation behavior between oligonucleotides and the cationic polymer poly-L-Lysine will first be studied in buffer by both single and dual color FFS.

Reference List

1. Kang,S.H., Zirbes,E.L., and Kole,R., Delivery of antisense oligonucleotides and plasmid DNA with various carrier agents, Antisense & Nucleic Acid Drug Development, 9 (1999) 497-505.

2. Kang,S.H., Cho,M.J., and Kole,R., Up-regulation of luciferase gene expression with antisense oligonucleotides: Implications and applications in functional assay developments, Biochemistry, 37 (1998) 6235-6239.

3. Batrakova,E.V., Han,H.Y., Alakhov,V.Y., Miller,D.W., and Kabanov,A.V., Effects of pluronic block copolymers on drug absorption in Caco-2 cell monolayers, Pharmaceutical Research, 15 (1998) 850-855.

4. Rothlein,R., Dustin,M.L., Marlin,S.D., and Springer,T.A., A Human Intercellular-Adhesion Molecule (Icam-1) Distinct from Lfa-1, Journal of Immunology, 137 (1986) 1270-1274.

5. Bernstein,C.N., Sargent,P., and Gallatin,W.M., beta 2 integrin ICAM expression in Crohn's disease, Clinical Immunology and Immunopathology, 86 (1998) 147-160.

6. Chiang,M.Y., Chan,H., Zounes,M.A., Freier,S.M., Lima,W.F., and Bennett,C.F., Antisense Oligonucleotides Inhibit Intercellular-Adhesion Molecule-1 Expression by 2 Distinct Mechanisms, Journal of Biological Chemistry, 266 (1991) 18162-18171.

7. Bennett,C.F., Condon,T.P., Grimm,S., Chan,H., and Chiang,M.Y., Inhibition of Endothelial-Cell Adhesion Molecule Expression with Antisense Oligonucleotides, Journal of Immunology, 152 (1994) 3530-3540.

8. Stepkowski,S.M., Wang,M.E., Amante,A., Kalinin,D., Qu,X., Blasdel,T., Condon,T., Kahan,B.D., and Bennett,F.C., Antisense ICAM-1 oligonucleotides block allograft rejection in rats, Transplantation Proceedings, 29 (1997) 1285.

9. Bennett,C.F., Kornbrust,D., Henry,S., Stecker,K., Howard,R., Cooper,S., Dutson,S., Hall,W., and Jacoby,H.I., An ICAM-1 antisense oligonucleotide prevents and reverses dextran sulfate sodium-induced colitis in mice, Journal of Pharmacology and Experimental Therapeutics, 280 (1997) 988-1000.

10. Yacyshyn,B.R., Bowen-Yacyshyn,M.B., Jewell,L., Tami,J.A., Bennett,C.F., Kisner,D.L., and Shanahan,W.R., A placebo-controlled trial of ICAM-1 antisense oligonucleotide in the treatment of Crohn's disease, Gastroenterology, 114 (1998) 1133-1142.

11. Sanders,N.N., Van Rompaey,E., De Smedt,S.C., and Demeester,J., On the transport of lipoplexes through cystic fibrosis sputum, Pharmaceutical Research, 19 (2002) 451-456.

12. Vandermeeren,M., Preveral,S., Janssens,S., Geysen,J., Saison-Behmoaras,E., Van Aerschot,A., and Herdewijn,P., Biological activity of hexitol nucleic acids targeted at Ha-ras and intracellular adhesion molecule-1 mRNA, Biochemical Pharmacology, 59 (2000) 655-663.

13. Wu,H.J., MacLeod,A.R., Lima,W.F., and Crooke,S.T., Identification and partial purification of human double strand RNase activity - A novel terminating mechanism for oligoribonucleotide antisense drugs, Journal of Biological Chemistry, 273 (1998) 2532-2542.

14. Clarenc,J.P., Lebleu,B., and Leonetti,J.P., Characterization of the Nuclear-Binding Sites of Oligodeoxyribonucleotides and Their Analogs, Journal of Biological Chemistry, 268 (1993) 5600-5604.

15. Tsuji,A., Koshimoto,H., Sato,Y., Hirano,M., Sei-Iida,Y., Kondo,S., and Ishibashi,K., Direct observation of specific messenger RNA in a single living cell under a fluorescence microscope, Biophysical Journal, 78 (2000) 3260-3274.

16. Lorenz,P., Baker,B.F., Bennett,C.F., and Spector,D.L., Phosphorothioate antisense oligonucleotides induce the formation of nuclear bodies, Molecular Biology of the Cell, 9 (1998) 1007-1023.

17. Lorenz,P., Misteli,T., Baker,B.F., Bennett,C.F., and Spector,D.L., Nucleocytoplasmic shuttling: a novel in vivo property of antisense phosphorothioate oligodeoxynucleotides, Nucleic Acids Research, 28 (2000) 582-592.

18. Hartig,R., Shoeman,R.L., Janetzko,A., Grub,S., and Traub,P., Active nuclear import of single-stranded oligonucleotides and their complexes with non-karyophilic macromolecules, Biology of the Cell, 90 (1998) 407-426.

19. Dijk-Wolthuis,W.N.E., van de Wetering,P., Hinrichs,W.L.J., Hofmeyer,L.J.F., Liskamp,R.M.J., Crommelin,D.J.A., and Hennink,W.E., A versatile method for the conjugation of proteins and peptides to poly[2-(dimethylamino)ethyl methacrylate], Bioconjugate Chemistry, 10 (1999) 687-692.

20. Fabisiak,J.P., Weiss,R.D., Powell,G.A., and Dauber,J.H., Enhanced Secretion of Immune-Modulating Cytokines by Human Lung Fibroblasts During Invitro Infection with Mycoplasma-Fermentans, American Journal of Respiratory Cell and Molecular Biology, 8 (1993) 358-364.

21. Maus,U., Rosseau,S., Mandrakas,N., Schlingensiepen,R., Maus,R., Muth,H., Grimminger,F., Seeger,W., and Lohmeyer,J., Cationic lipids employed for antisense oligodeoxynucleotide transport may inhibit vascular cell adhesion molecule-1 expression in human endothelial cells: A word of caution, Antisense & Nucleic Acid Drug Development, 9 (1999) 71-80.

22. Monia,B.P., Johnston,J.F., Sasmor,H., and Cummins,L.L., Nuclease resistance and antisense activity of modified oligonucleotides targeted to Ha-ras, Journal of Biological Chemistry, 271 (1996) 14533-14540.

23. Marcusson,E.G., Bhat,B., Manoharan,M., Bennett,C.F., and Dean,N.M., Phosphorothioate oligodeoxyribonucleotides dissociate from cationic lipids before entering the nucleus, Nucleic Acids Research, 26 (1998) 2016-2023.

24. Dheur,S., Dias,N., Van Aerschot,A., Herdewijn,P., Bettinger,T., Remy,J.S., Helene,C., and Saison-Behmoaras,E.T., Polyethylenimine but not cationic lipid improves antisense activity of 3'-capped phosphodiester oligonucleolides, Antisense & Nucleic Acid Drug Development, 9 (1999) 515-525.

25. Pichon,C., Roufai,M.B., Monsigny,M., and Midoux,P., Histidylated oligolysines increase the transmembrane passage and the biological activity of antisense oligonucleotides, Nucleic Acids Research, 28 (2000) 504-512.

26. Tonkinson,J.L. and Stein,C.A., Patterns of Intracellular Compartmentalization, Trafficking and Acidification of 5'-Fluorescein Labeled Phosphodiester and Phosphorothioate Oligodeoxynucleotides in Hl-60 Cells, Nucleic Acids Research, 22 (1994) 4268-4275.

Chapter 3

Dual Color FFS to study the complexation between poly-L-Lysine and oligonucleotides

Parts of this chapter have been published in Macromolecules 35: 8152-8160 (2002).

1. Introduction

Currently, the stability of DNA complexes is usually assessed using polyanion-disruption assays [1;2]. Katayose and Kataoka have studied the dissociation of poly(ethylene glycol)-poly-L-Lysine/DNA complexes through the addition of poly(L-aspartic acid) [3]. However, to obtain real breakthroughs in the design and the understanding of the dissociation of DNA complexes in cells, there is an urgent need for advanced physicochemical methods, which allow characterizing this critical step in cells. Fluorescence fluctuation spectroscopy (FFS), which can be applied on a cellular scale [4], shows potential for that purpose. FFS monitors the fluorescence fluctuations caused by the diffusion of fluorescent molecules through the excitation volume of a microscope. From the fluctuation profile (Figure 1A) an autocorrelation curve can be derived (Figure 1B) which allows calculating the diffusion coefficient of the fluorescent molecules. Expecting that the diffusion of the DNA will change upon release from its cationic carrier, one could extract information on the association and dissociation of interpolyelectrolyte complexes based upon their diffusion coefficient. With this idea in mind, our group has recently introduced single color FFS in studying interactions between fluorescently labeled DNA and (non-labeled) cationic polymers like poly(2-dimethylamino)ethyl methacrylate (pDMAEMA), poly(ethylenimine) (pEI), poly(ethylene glycol)-poly(ethylenimine) (pEG-pEI) and diaminobutane-dendrimer-(NH2)64 (DAB64) [5-7]. We have shown, however, that autocorrelation analysis of the fluorescence fluctuation profiles of DNA/cationic polymer complexes is not feasible due to the presence of 'highly intense fluorescence peaks' in the fluctuation profile (Figure 1C). The highly intense fluorescence peaks are explained by the migration through the excitation volume of

'multimolecular' DNA/cationic polymer complexes, which are highly fluorescent as they carry a large number of fluorescently labeled ONs. We have concluded in this work that, in contrast to autocorrelation analysis, analyzing the fluorescence fluctuations by a method that distinguishes between species based upon their difference in fluorescence may allow the detection of associated and dissociated DNA.

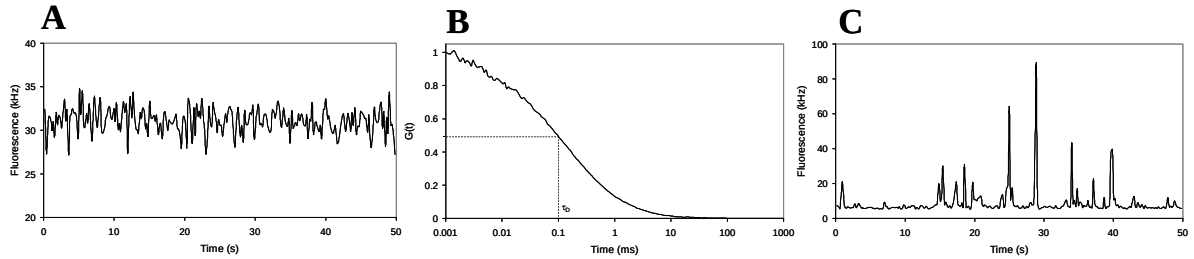

Figure 1. Fluorescence intensity profile (A) and corresponding autocorrelation function (B) of a solution of free fluorescent molecules, together with the fluorescence intensity profile of a mixture of free fluorescent molecules and bright complexes (C).

However, as mentioned in Chapter 1, the highly intense fluorescence peaks also do not allow to apply PCH analysis on the fluorescence fluctuations of DNA complexes mainly due to the 'heterogenity' of the highly intense fluorescence peaks appearing in the fluorescence fluctuation profiles [6]. In conclusion, searching for the presence or absence of highly intense fluorescence peaks in the fluorescence fluctuation profiles seems to be the only way of analysis one can use to know whether oligonucleotides are complexed to or dissociated from their carriers.

In the more complex cellular environment, highly intense fluorescence peaks may also be due to aggregation of free ONs with cellular components, which would be misinterpreted as being original ONs-complexes. Therefore, the fluorescent labeling of both the carrier and the ONs should improve the signal specificity. In dual color FFS, both interacting components are labeled with spectrally different fluorophores (e.g. red and green) and their emission light is detected separately by two detectors monitoring the same focal volume. When dissociated, the components are only detected in one detector, as they carry a red or a green fluorophore. However, when associated, the complex is detected in both detectors simultaneously as it bears both red and green fluorophores.

This chapter aims to evaluate (1) whether the complexation between cationic polymers and ONs can be investigated by dual color FFS, (2) whether the results revealed by dual color FFS are consistent with the results obtained from single color FFS. As a model, the in vitro

complexation between a 20-mer ON and the polycation poly-L-Lysine, which is intensively investigated as a pharmaceutical carrier for ONs [8], is considered.

2. Materials and methods

2.1. Oligonucleotides

The 20-mer phosphodiester ONs (5'-CCC-CCA-CCA-CTT-CCC-CTC-TC-3') (molar mass 5830 g/mol) and labeled analogues (using respectively rhodamine green and Cy5 as fluorescent marker) were synthesized by Eurogentec (Seraing, Belgium). The fluorescent labeling occurred at the 5' end of the ONs; each oligonucleotide contained one label (RhGr or Cy5). The concentration of the ONs stock solutions (in Tris-buffer at pH 8) was determined by absorption measurements at 260 nm (1 OD260 = 33 μg ONs/mL). The contribution to the absorption at 260 nm by the label was taken into account in the determination of the concentration of the labeled ONs. The ONs stock solutions were further diluted with Hepes buffer (20 mM Hepes at pH 7.4).

2.2. Cationic polymers

Poly-L-Lysine was purchased from Sigma (St. Louis, USA). The molar mass, as determined from viscosimetric measurements, equaled 30 300 g/mol and was provided by the supplier. pLL stock solutions were prepared in Hepes buffer.

To prepare rhodamine green poly-L-Lysine (RhGr-pLL), rhodamine green X-succinimidyl ester (RhGr-SE) was purchased from Molecular Probes (Eugene, OR). Poly-L-Lysine was dissolved in "labeling buffer" (0.1 M $NaHCO_3$ at pH 8.8) at 1 mg/mL. To 1 mL of this pLL solution, 50 μL of DMSO containing 0.13 mg RhGr-SE was added drop by drop. After incubation for 1 hour in the dark at ambient temperature, RhGr-pLL was purified on a G25-Sephadex column (10 x 100 mm), which was previously equilibrated with Hepes buffer. The fractions containing fluorescent pLL were collected. Finding the amine concentration using the method of Snyder and Sobocinski [9] and measurement of the absorbance of the label allowed the determination of the average number of labels attached to the pLL. It could be calculated that, on the average, the pLL chains bore one RhGr-label.

Cy5-poly-L-Lysine (Cy5-pLL) was prepared adding 1 ml of pLL solution (1mg/mL in 0.1 M $NaHCO_3$ at pH 9.3) to a vial of FluoroLink^{TM}Cy5 monofunctional dye (Amersham

Pharmacia, Piscataway, NJ). After incubation for 1 hour in the dark at ambient temperature, Cy5-pLL was purified as described above. The degree of labeling was determined to be, on the average, one Cy5-label per pLL strand.

Dextran sulfate (DS) was purchased from Sigma (St Louis, USA). The molar mass and sulfur content, provided by the supplier, equalled respectively 500 kDa and 2.3 sulfate groups per glucosyl residue. Stock solutions were prepared in Hepes buffer.

2.3. Preparation of polyplexes

The pLL/ONs complexes (varying in +/- charge ratio, see below) were prepared by adding (in one step) different volumes of the pLL stock solution to a fixed volume of the ONs stock solution. After addition of the polymer solution, the sample was vortexed for 10 seconds. To obtain the final ONs concentration of 10 µg/mL (1.7µM), the samples were further diluted with Hepes buffer. The polyplexes were allowed to equilibrate for 30 min at room temperature prior to use.

For FFS measurements on the pLL/ONs complexes, 500 µL of the sample was prepared as described above, however, the final ONs concentration equalled 0.2 µg/mL (34 nM). The +/- charge ratio of the pLL/ONs complexes investigated by FFS equalled 20. After preparation, 200 µL of the sample was immediately transferred into the Nunc cuvettes (see below) to begin the FFS measurement.

The +/- charge ratio, i.e. the ratio of the number of positive charges on the pLL chains to the number of negative charges on the ONs, was calculated assuming that 1 µg of 20-mer ONs contained 3.43 nmol negative charges and that 1 µg of pLL contained 7.81 nmol positive charges, as calculated from the molecular weight of Lysine monomer, the pKa of Lysine and the pH of the solutions.

2.4. Particle size measurements

Dynamic light scattering measurements (DLS) on the pLL/ONs polyplexes were carried out on a Malvern 4700 instrument (Malvern, Worcestershire, UK) at 25 °C and at an angle of 90 degrees. The incident beam was a HeNe laser beam (633 nm). The polyplexes were prepared as described above. To avoid dust particles, the polymer solutions were filtered before being added to the nucleotide solutions. Average pore size of the filter was 0.45 µm (Schleicher & Schuell, Dassel, Germany). The particle size was measured 30 min after the preparation of the complexes. For calculating the z-average hydrodynamic diameter from the

DLS data, the viscosity and refractive index of water at 25 °C (0.89 mPa.s and 1.333, respectively) were used. Polystyrene nanospheres (220 ± 6 nm; Duke Scientific Corp, Palo Alto, CA) were used to verify the performance of the instrument. The particle size of each sample was measured three times.

2.5. Zeta potential measurements

Zeta potential (ζ) measurements on the pLL/ONs polyplexes were performed at 25 °C on a Malvern Zetasizer 2000 (Malvern, Worcestershire, UK), which is based on electrophoretic light scattering. ζ was measured within 1 hour after the preparation of the complexes. Polystyrene nanospheres (-50 mV; Duke Scientific Corp, Palo Alto, CA) were used to verify the performance of the instrument. ζ of each sample was measured three times.

2.6. Fluorescence fluctuation spectroscopy (FFS)

As explained in the introduction, FFS basically monitors fluorescence intensity fluctuations in the excitation volume of a microscope. In dual color FFS, both interacting components are labeled with spectrally different fluorophores (e.g. red and green) and their emission light is detected separately by two detectors monitoring the same excitation volume. When dissociated, the components are only detected in one detector, as they carry a red or a green fluorophore. However, when associated, the complex is detected in both detectors simultaneously as it bears both red and green fluorophores. Autocorrelation analysis of the fluorescence fluctuations recorded in the green detector describes the diffusion behavior of all molecules emitting green light, regardless of whether they are free or associated to red-labeled components. On its turn, autocorrelation analysis of the red detector signal describes the diffusion of all red-labeled molecules. Cross-correlation analyses on the fluorescence fluctuations registered in the red and the green detector provides only information on the diffusion behavior of the dual labeled (i.e. interacting) molecules [10;11]. However, when the fluorescence quantum yield strongly increases upon binding or when several fluorescent labeled molecules associate, the fluorescence emitted by a complex becomes much higher than that of the free molecules. Highly intense fluorescence peaks appear in the fluctuation profiles (e.g. Figure 1C) and in more extreme cases auto- and cross-correlation analysis are no longer feasible. Therefore a statistical approach is considered to analyze the fluorescence fluctuation profiles when bursts of high fluorescence intensity occur. Here, a threshold level is calculated, above which all fluorescence values are identified as “highly intense fluorescence

peaks" [5;12]. In the absence of highly intense fluorescence peaks (i.e., when no threshold level could be calculated), the fluorescence fluctuations were analyzed by autocorrelation analysis and a diffusion coefficient could be calculated. In dual color FFS, the simultaneous appearance of a highly intense fluorescence peak in the red and green detector would indicate that a complex bearing both many red as well as many green labels is passing through the excitation volume. If the size of the migrating particle exceeds the dimensions of the detection volume, a peak of high fluorescence intensity is still observed on condition that the fluorescent dye is distributed throughout the particle (which is the case for homogeneously colored polystyrene beads and fluorescent-labeled carrier/ONs-complexes).

In this study, dual color FFS experiments were performed on a dual color FFS setup installed on a MRC1024 Bio-Rad confocal laser-scanning microscope [13]. An inverted microscope (Eclipse TE300D, Nikon, Japan) was used, which was equipped with a water immersion objective lens (Plan Apo 60X, NA 1.2, collar rim correction, Nikon, Japan). The 488 nm and 647 nm lines of the same krypton-argon laser (Biorad, Cheshire, UK) were used. The intensities of both excitation wavelengths were controlled independently from each other, using an acousto optic tunable filter. (Opto-Electronique, St. Rémy Les Chevreuse, France). To check whether the detectors adequately detected the fluorescence fluctuations in the excitation volumes (i.e. to verify whether the excitation volumes and the detection volumes optimally overlapped), the system was optimized as described by Schwille et al. [11]. The fluorescence fluctuations were processed by a hardware correlator and (if possible) the resulting autocorrelation curve was analyzed with specific software, yielding information on the concentration of the fluorescent molecules in the detection volume and the average diffusion time (τ_d) of the fluorescent molecules through the detection volume. The translational diffusion coefficient (D) is calculated using the measured diffusion time of a sample of free rhodamine dye with known diffusion coefficient (2.8×10^{-6} cm^2/s) as internal standard. To perform the FFS measurements, the laser beam was focused at about 100 μm above the bottom of the glass-bottomed cuvettes (Nalge Nunc International, Naperville, IL), which contained the samples. Prior to use, the thickness of the bottom of the cuvette was measured using a micrometer and the collar rim correction was adjusted for 150 μm. Diffusion coefficients were calculated using the average diffusion time of at least 20 measurements. Each pLL/ONs sample (both the single and the dual labeled) was independently prepared three times and each preparation was measured at least 10 times. The

fluorescence fluctuation profiles shown in Figure 3, Figure 4 and Figure 5 were representative for the measurements done on the respective pLL/ONs samples.

The measurements on the homemade FFS apparatus were confirmed by conducting the same experiments on a commercial instrument (Confocor II, Zeiss-Evotec, Jena, Germany).

3. Results & Discussion

Figure 2 shows the average size and ζ of the pLL/ONs complexes. The dependence of the size and surface properties of the pLL/ONs complexes on the +/- charge ratio shows a typical profile as often observed for complexes formed between oppositely charged polyions [14]. At +/- charge ratio values between 1 and 3, large aggregates are formed. In this region, ζ equals approximately zero. Consequently, almost no electric repulsion occurs between the particles, which leads to a clustering of individual polyplexes. Upon further increasing the concentration of pLL, ζ reaches a plateau. The excess of cations in the complexes may explain the positive net charge of the polyplexes. This results in electric repulsion between the polyplexes, which prevents them from aggregating, and which explains the smaller size of the polyplexes at higher +/- charge ratio values in Figure 2.

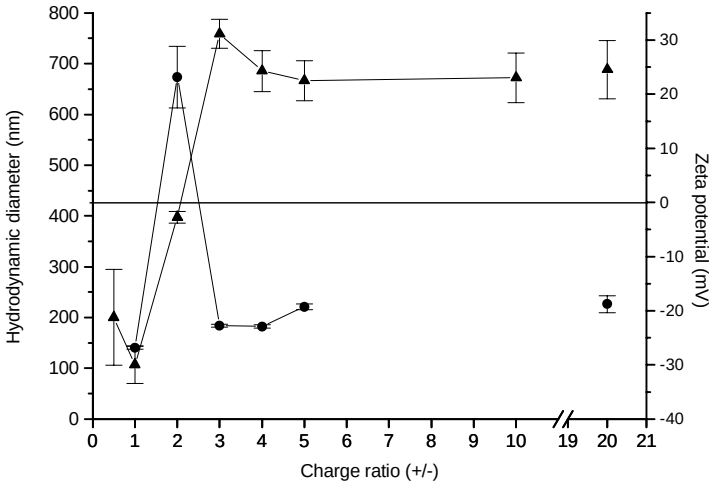

Figure 2. The z-average hydrodynamic diameter (●) and zeta potential (▲) of pLL/ONs complexes, as a function of the charge ratio. Each sample was measured three times.

Figure 3 (A-data) shows the fluorescence fluctuation profile of free (i.e. non complexed) RhGr-ONs in buffer. These data result in an autocorrelation function from which a diffusion coefficient of 0.76 ± 0.07 • 10^{-6} cm²/s is calculated. This diffusion coefficient agrees with values reported in literature [5;15].

The B-data in Figure 3 show that the association of RhGr-ONs to pLL clearly influences the fluorescence fluctuation profile. Generally, the fluorescence intensity decreases. Moreover, highly intense fluorescence peaks also appear. The fluorescence intensity of the "baseline", originating from the presence of free RhGr-ONs in the excitation volume, decreases as most of the RhGr-ONs become associated to the pLL. This lowers the average number of free RhGr-ONs in the excitation volume. It is assumed that the highly intense fluorescence peaks originate from the presence of pLL chains that bear a large number of RhGr-ONs. The distribution of the height of the peaks may be related to the polydispersity of the polyplexes with regard to the number of RhGr-ONs per polyplex. However, as the excitation profile in the confocal volume is not homogeneous and as single complexes do not necessarily always pass through the centre of the focus, the fluorescence of a complex partly depends on the place where it moves through the excitation volume. Also, differences in the degree of mutual quenching of the fluorophores depending on their spatial proximity may influence the height of the highly intense fluorescence peaks. The highly intense fluorescence peak-values disturb the calculation of an autocorrelation function from the fluorescence fluctuation profile.

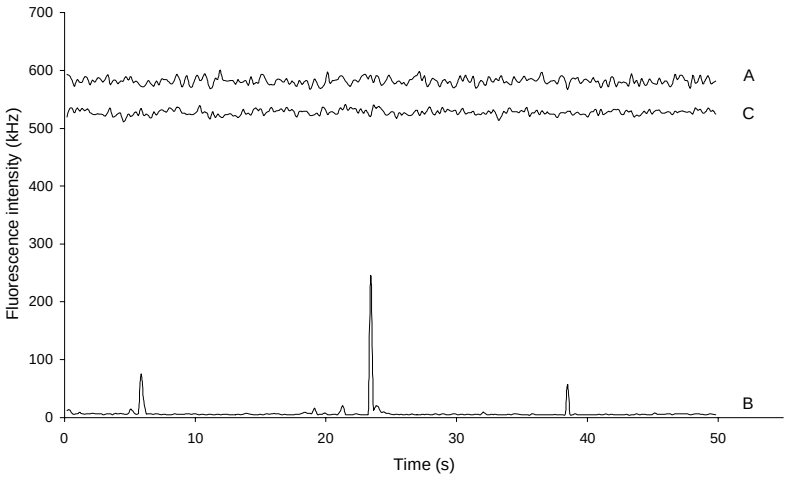

Figure 3. Fluorescence fluctuation profile, as measured by single color FFS, of respectively a RhGr-ONs solution (A), a pLL/RhGr-ONs sample (B, +/- = 20) and the same sample after addition of dextran sulfate (C, final concentration of dextran sulfate equaled 12 µg/mL).

Upon addition of dextran sulfate to the complexes (C-data in Figure 3), the fluorescence intensity of the "baseline" is almost completely restored, while the highly intense fluorescence peaks disappear. Dextran sulfate is an anionic polymer, which competes with the RhGr-ONs for binding to the pLL chains. From the fluorescence fluctuations obtained after adding dextran sulfate, an autocorrelation curve can be derived, which yields a diffusion coefficient of $0.77 \pm 0.06 \bullet 10^{-6}$ cm^2/s. This value corresponds to the diffusion coefficient as measured for free RhGr-ONs. The incomplete recovery of the fluorescence intensity of the baseline may be attributed to the adsorption of pLL/RhGr-ONs complexes to the Eppendorf tubes. Especially since we have observed that the longer the incubation time of the polyplexes prior to addition of dextran sulfate, the lower the degree of recovery of the fluorescence intensity of the baseline after adding dextran sulfate (data not shown).

In a second series of experiments, the fluorescence fluctuation profiles of RhGr-pLL/ONs complexes have been measured (Figure 4). Contrary to the measurements in Figure 3, the polymer chains, instead of the ONs, are fluorescently labeled with RhGr. The diffusion coefficient of RhGr-pLL, as calculated from the autocorrelation analysis of the A-data in Figure 4, equals $1.5 \pm 0.2 \bullet 10^{-6}$ cm^2/s. The B-data in Figure 4 show that upon complexation of RhGr-pLL to ONs, highly intense fluorescence peaks appear and that the fluorescence intensity of the baseline significantly decreases, similar to the results in Figure 3. The highly intense fluorescence peaks in the B-data of Figure 4 clearly show that a RhGr-pLL/ONs complex consists of a number of RhGr-pLL chains. Combining the results of Figure 3 and Figure 4 suggests that the pLL/ONs complexes are "multimolecular" i.e. they consist of a number of ONs associated to a number of pLL-strands. However, these data cannot prove that all pLL/ONs complexes are multimolecular.

Upon addition of dextran sulfate (C-data in Figure 4), the fluorescence intensity of the baseline is only slightly restored. Also, the highly intense fluorescence peaks do not always disappear, indicating that structures carrying many RhGr-pLL chains continue to exist. Autocorrelation analysis of the fluctuations of the baseline between highly intense fluorescence peaks yields a diffusion coefficient that is one order of magnitude lower than the value obtained for the free RhGr-pLL solution. However, a reproducible diffusion coefficient has not been obtained. These phenomena are probably attributed to the binding of the dextran sulfate polyanion to positively charged RhGr-pLL chains, resulting in complexes that are heterogeneous in size. We therefore suggest that the highly intense fluorescence peaks that

remain after adding dextran sulfate (C-data in Figure 4) are RhGr-pLL/dextran sulfate complexes. Adding dextran sulfate to a sample of free RhGr-pLL indeed has supported this hypothesis, as a diffusion coefficient of $0.10 \pm 0.01 \cdot 10^{-6}$ cm^2/s, significantly lower than the diffusion coefficient of free RhGr-pLL (i.e. $1.5 \pm 0.2 \cdot 10^{-6}$ cm^2/s), has been obtained.

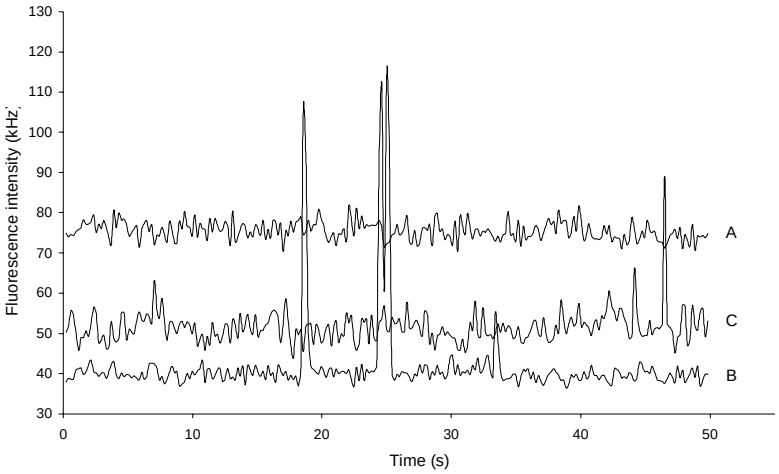

Figure 4. Fluorescence fluctuation profile, as measured by single color FFS, of respectively a RhGr-pLL solution (A), a RhGr-pLL/ONs sample (B, +/- = 20) and the same RhGr-pLL/ONs sample after addition of dextran sulfate (C, final concentration of dextran sulfate equaled 12 µg/mL).

Figure 4 shows that due to the association of the pLL to the dextran sulfate, highly intense fluorescence peaks remain in the fluorescence fluctuation profiles, although Figure 3 shows that the ONs are released from their cationic carrier. Similarly, upon dissociation of the polyplexes in the cell, the polymer and/or the ONs may unspecifically interact with different species which may result in highly intense fluorescence peaks when studied by single color FFS. Therefore, the fluorescent labeling of both the carrier and the ONs should improve the signal specificity. In this study we have evaluated whether dual color FFS allows studying the complexation between ONs and pLL. To minimize the detection of emission light from the green dye (i.e. RhGr) by the red detector, we have made use of RhGr and Cy5. It has been shown previously that the "cross-talk" between these fluorophores is limited, which makes them suitable for dual color FFS. In the dual color FFS experiments we have studied both RhGr-pLL/Cy5-ONs complexes (data not shown) as well as Cy5-pLL/RhGr-ONs complexes, which are discussed below.

Figure 5 shows the fluorescence fluctuations measured at the same time by the red (upper panel) and green (lower panel) detector. The A-data (upper panel) represent the

fluorescence fluctuation profile of free Cy5-pLL, whereas the A'-data (lower panel) are the fluorescence fluctuations of free RhGr-ONs.

As the B-data in Figure 5 show, the complexation of RhGr-ONs to Cy5-pLL decreases the fluorescence intensity of the baseline in both detectors. Moreover, highly intense fluorescence peaks also appear in both channels. It is especially clear that highly intense fluorescence peaks are registered by the two detectors at the same time. This means that at certain times a number of RhGr-ONs and a number of Cy5-pLL-strands simultaneously move through the excitation volume. This proves that the pLL/ONs complexes are indeed multimolecular as already suggested from the single color FFS results in Figure 3 and Figure 4.

Upon addition of dextran sulfate, highly intense fluorescence peaks are no longer detected by the green detector (C data in the lower panel of Figure 5). Also, the fluorescence intensity of the baseline almost completely returns to the value observed for free RhGr-ONs. The diffusion coefficient, as calculated from the autocorrelation function, equals the one obtained for free RhGr-ONs, proving that RhGr-ONs are released from the polyplexes upon addition of dextran sulfate. All these observations completely agree with the results from the single color FFS measurements on pLL/RhGr-ONs complexes (Figure 3). Moreover, upon addition of dextran sulfate, the fluorescence intensity of the baseline as registered by the red detector is only partly restored, and highly intense fluorescence peaks remain present (C data in the upper panel of Figure 5). This again agrees with the single color FFS observations on RhGr-pLL/ONs complexes in Figure 4. Also, the diffusion coefficient calculated by autocorrelating the baseline fluorescence fluctuations in between highly intense fluorescence peaks significantly differs from the diffusion coefficient of free Cy5-pLL. As suggested above, these phenomena are attributed to the binding of Cy5-pLL to dextran sulfate.

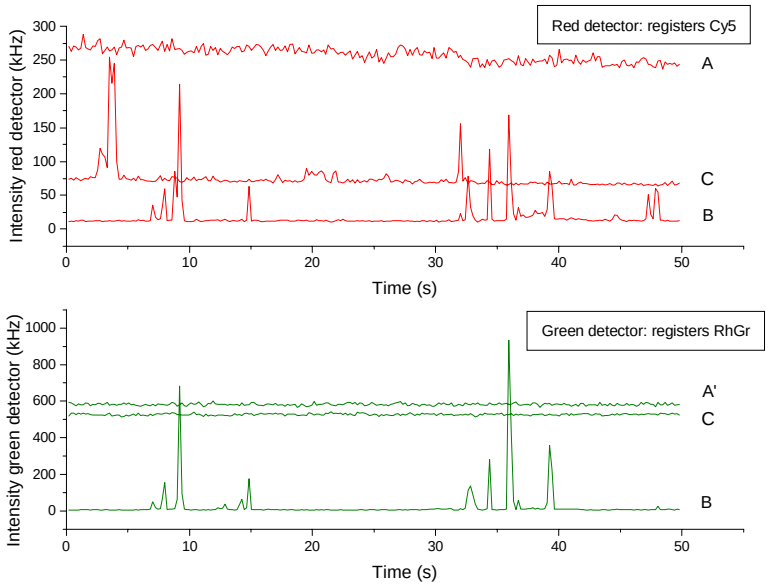

Figure 5. Fluorescence fluctuation profiles as simultaneously registered by the 'red detector' (upper panel) and 'green detector' (lower panel) of a Cy5-pLL/RhGr-ONs sample (+/- = 20) before (B) and after (C) addition of dextran sulfate. (A) and (A') are the fluorescence fluctuations of respectively a 2.0 µg/mL (free) Cy5-pLL and a 0.2 µg/mL (free) RhGr-ONs solution.

The fluorescence intensity profiles from Figure 5 are further analyzed in a two-dimensional scatter plot (Figure 6). Each data point in Figure 6 represents the green fluorescence (indicated by the x-value) and red fluorescence (indicated by the y-value) measured at a certain time in the excitation volume. First, the scatter plot shows the data obtained from the fluorescence fluctuation profiles measured in the red and green detector on free RhGr-ONs (◇) and on free Cy5-pLL (□) solutions. Second, the ●-data are derived from the fluorescence fluctuation profiles, as measured by the red and green detector, on Cy5-pLL/RhGr-ONs sample. Clearly, the ●-data at high x- and y-values originate from the highly intense fluorescence peaks in the B-data of Figure 5 and correspond to the multimolecular Cy5-pLL/RhGr-ONs complexes. The ●-data at lower x- and y-values originate from the baseline in Figure 5 (B-data) and correspond to structures bearing only one or a few Cy5-pLL strands and/or RhGr-ONs. To separate the multimolecular Cy5-pLL/RhGr-ONs complexes efficiently in the ●-data, we propose calculating a "threshold value". This threshold value, being the fluorescence intensity above which a fluorescence value is identified as a highly intense fluorescence peak, is determined for the fluorescence intensity profiles, registered by the green and red detector respectively, of the Cy5-pLL/RhGr-ONs sample (B-data in Figure 5). The horizontal dotted line in Figure 6 shows the threshold value of the fluorescence

fluctuations measurement by the red detector; the vertical dotted line shows the one for the fluorescence fluctuations measured by the green detector. These lines divide the two-dimensional scatter plot in four quadrants and allow a more detailed evaluation of the distribution of the ●-data. The ●-data in quadrant A originate from complexes that simultaneously show a high fluorescent signal both in the red and green detector; these data are attributed to complexes that consist of many Cy5-pLL and many RhGr-ONs molecules. The ●-data in quadrant B are Cy5-pLL/RhGr-ONs complexes that contain numerous RhGr-ONs but only one or a few Cy5-pLL molecules. The ●-data in quadrant D are Cy5-pLL/RhGr-ONs complexes that contain numerous Cy5-pLL chains but only one or a few RhGr-ONs. The ●-data in quadrant C do not originate at all from multimolecular complexes. They probably originate from structures carrying too little Cy5-pLL and RhGr-ONs molecules to be identified as a peak of high fluorescence intensity.

After adding dextran sulfate, the data points of the Cy5-pLL/RhGr-ONs sample (▲) approach the x-position of the data points of the original RhGr-ONs sample (♦) and only slight variations around the average x value of 530 kHz are observed. However, some of these data points have y values that differ significantly from the average y value around 70 kHz. This average y value of 70 kHz still is much lower than the 260 kHz of the original Cy5-pLL sample (□). As only slight variations around the average x value are observed, the statistical algorithm is not able to identify any outliers in the set data points; hence, no threshold value can be calculated for the green detector. This means no peaks of high green fluorescence intensity are identified. For the red detection channel, a threshold line can be calculated for the Cy5-pLL/RhGr-ONs sample after adding dextran sulfate (horizontal dotted line (red) in Figure 6). Data points located above this threshold line are identified as peaks of high red fluorescence intensity and indicate that complexes bearing many Cy5-pLL strands still exist.

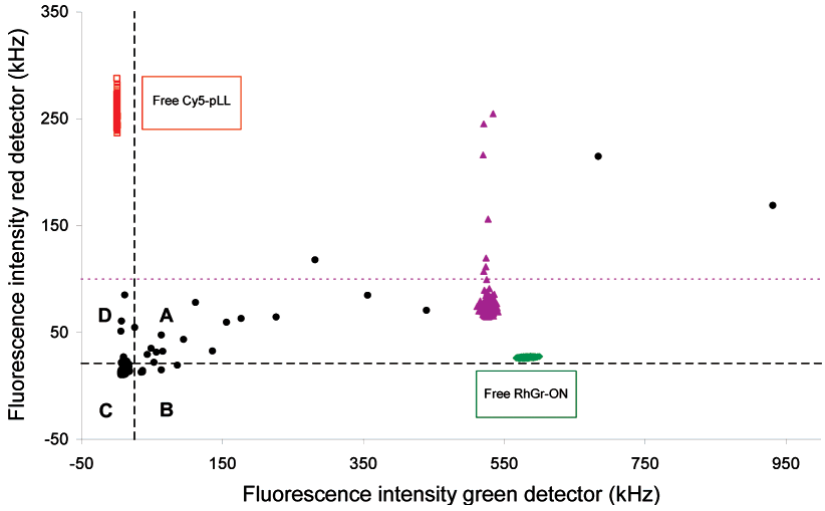

Figure 6. Scatter plot of the fluorescence fluctuations data, measured by dual color FFS as represented in Figure 5, of free RhGr-ONs (0.2 µg/mL, ♦), free Cy5-pLL (2.0 µg/mL, □) and Cy5-pLL/RhGr-ONs polyplexes before (●) and after (▲) adding dextran sulfate.

4. Summary and conclusions

This paper shows that dual color FFS is a straightforward method to detect the association and dissociation of pLL/ONs complexes. The FFS results on the dual labeled polymer/oligonucleotide complexes match the observations seen in the single color FFS measurements. Although we have not observed controversies between the single color and dual color FFS results on pLL/ONs complexes, a clear disadvantage of dual color FFS is that both interacting species have to be labeled, which enhances the risk of fluorophore induced artefacts. However, the very sensitive detectors used in FFS permit attaching only one fluorescent marker per polymer chain, which may not substantially modify the properties of the macromolecules. As explained above, a major advantage of dual color FFS over single color FFS in studying the complexation behavior of DNA complexes in cells is that it might yield a considerable improvement in signal specificity. In heterogeneous media like cells the DNA and the cationic polymers may interact not only with each other but also with many other different species. Furthermore, by two-dimensional scatter plot analysis of the dual color FFS data, we have obtained a more detailed view on the composition of the pLL/ONs complexes in the sample. Especially, dual color FFS proves that a substantial number of pLL/ONs complexes consist of numerous ONs bound to numerous pLL strands.

Reference List

1. Arigita C., Zuidam N.J., Crommelin DJA, and Hennink W.E., Association and Dissociation Characteristics of Polymer/DNA Complexes Used for Gene Delivery, Pharm. Res., 16 (1999) 1534-1541.

2. Izumrudov,V.A., Kargov,S.I., Zhiryakova,M.V., Zezin,A.B., and Kabanov,V.A., Competitive Reactions in Solutions of DNA and Water-Soluble Interpolyelectrolyte Complexes, Biopolymers, 35 (1994) 523-531.

3. Katayose,S. and Kataoka,K., Water-soluble polyion complex associates of DNA and poly(ethylene glycol)-poly(L-lysine) block copolymer, Bioconjug. Chem., 8 (1997) 702-707.

4. Schwille,P., Fluorescence Correlation Spectroscopy and Its Potential for Intracellular Applications, Cell Biochemistry and Biophysics, 34 (2001) 383-408.

5. Van Rompaey,E., Sanders,N., De Smedt,S.C., Demeester,J., Van Craenenbroeck,E., and Engelborghs,Y., Complex formation between cationic polymethacrylates and oligonucleotides, Macromolecules, 33 (2000) 8280-8288.

6. Van Rompaey,E., Chen,Y., Muller,J.D., Gratton,E., Van Craenenbroeck,E., Engelborghs,Y., De Smedt,S., and Demeester,J., Fluorescence fluctuation analysis for the study of interactions between oligonucleotides and polycationic polymers, Biological Chemistry, 382 (2001) 379-386.

7. Van Rompaey,E., Engelborghs,Y., Sanders,N., De Smedt,S.C., and Demeester,J., Interactions between oligonucleotides and cationic polymers investigated by fluorescence correlation spectroscopy, Pharmaceutical Research, 18 (2001) 928-936.

8. Zauner,W., Ogris,M., and Wagner,E., Polylysine-based transfection systems utilizing receptor- mediated delivery, Advanced Drug Delivery Reviews, 30 (1998) 97-113.

9. Snyder,S.L. and Sobocinski,P.Z., Improved 2,4,6-Trinitrobenzenesulfonic Acid Method for Determination of Amines, Analytical Biochemistry, 64 (1975) 284-288.

10. Heinze,K.G., Koltermann,A., and Schwille,P., Simultaneous two-photon excitation of distinct labels for dual-color fluorescence crosscorrelation analysis, Proc. Natl. Acad. Sci. U. S A, 97 (2000) 10377-10382.

11. Schwille,P., MeyerAlmes,F.J., and Rigler,R., Dual-color fluorescence cross-correlation spectroscopy for multicomponent diffusional analysis in solution, Biophysical Journal, 72 (1997) 1878-1886.

12. Van Craenenbroeck,E., Matthys,G., Beirlant,J., and Engelborghs,Y., A statistical analysis of fluorescence correlation data, Journal of Fluorescence, 9 (1999) 325-331.

13. Opitz,N., Photon bursts of single/few fluorescing molecules analyzed via auto- and cross-correlation techniques implemented to CLSM., Cell. Mol. Biol., 46 (2004) 170.

14. Trinh,C.K. and Schnabel,W., Polyelectrolyte complexes from poly(N-ethyl-4-vinylpyridinium bromide) and poly(sodium methacrylate). A stopped-flow light scattering investigation, Macromolecular Chemistry and Physics, 198 (1997) 1319-1329.

15. Politz,J.C., Browne,E.S., Wolf,D.E., and Pederson,T., Intranuclear diffusion and hybridization state of oligonucleotides measured by fluorescence correlation spectroscopy in living cells, Proceedings of the National Academy of Sciences of the United States of America, 95 (1998) 6043-6048.

Chapter 4

On the cellular dissociation of polymer-oligonucleotide complexes as studied by dual color FFS

Parts of this chapter are submitted to Biochemistry.

1. Introduction

Although it is out of the scope of this chapter to review the results obtained in studies on the biophysical behavior of polymer/ONs complexes in cells, a brief glance through the literature reveals examples of polyplexes that dissociate in the cytoplasm [1-3], whereas others are believed to enter the nucleus prior to dissociation [4].

Dual color microscopy has been used frequently to study the intracellular behavior of oligonucleotide/cationic carrier complexes, since it allows the simultaneous observation of the DNA and the cationic carrier in the cell. A lack of colocalization proves that the DNA is released from its carrier. Colocalization of the fluorescent markers may indicate that the DNA and its carrier are associated. In the latter case, however, it remains possible that the fluorescent labeled molecules are colocalized without being associated. Compared with the spatial analysis of fluorescent labeled molecules, the temporal analysis of the movement of these molecules could be more robust to conclude whether the fluorescent labeled species are migrating together, i.e. are still associated. Fluorescence fluctuation spectroscopy (FFS), which can be applied on a cellular scale [5], shows potential for that purpose. While dual color microscopy answers the question “are the carrier and the oligonucleotide located together”, dual color FFS may answer the question whether they really move together.

In Chapter 3, we have proved that in buffer the association and dissociation of oligonucleotides to/from cationic polymers can be monitored by dual color FFS. When associating, the amount of detected free ONs decreases and highly fluorescent “multimolecular” polymer/ONs complexes appear (existing out of many ONs bound to many

polymer strands) which are clearly detected by FFS. When dissociating, the amount of free ONs increases and the multimolecular complexes disappear. Up to our knowledge, no reports in literature deal with FFS on polymer/ONs complexes in cells. In this study, we wish to explore (1) if dual color FFS is able to detect intact and dissociated polymer/ONs complexes in the cytoplasm and in the nucleus of living cells and (2) to what extent dual color FFS provides new information on the intracellular behavior of polymer/ONs complexes.

2. Materials and methods

2.1. Oligonucleotides

RhGr-labeled 20-mer phosphodiester ONs as described in Chapter 3 were used.

2.2. Polymers and polystyrene nanoparticles

Cy5-labeled poly-L-Lysine (Cy5-pLL) as described in Chapter 3 was used.

Cy5-labeled pegylated poly (2-dimethylamino) ethyl methacrylate – co – amino ethyl methacrylate (abbreviated as Cy5-*graft*-pDMAEMA) as described in Chapter 2 was used.

Dextran sulfate (DS) as described in Chapter 3 was used.

Tetraspeck^{TM} nanobeads (Molecular Probes, Eugene, OR) of 90 nm diameter and 500 nm diameter were used. Tetraspeck^{TM} nanobeads contain four different kinds of fluorophores with excitation/emission maxima of 365/430, 505/515, 560/580 and 660/680 nm respectively. Prior to use, the bead dispersions were sonified for 10 minutes.

2.3. Preparation of polymer/ONs complexes

The polymer/ON complexes were prepared by adding (in one step) equal volumes of the cationic polymer solution and the ONs solution, followed by vortexing during 10 seconds. To obtain the final ONs concentration of 10 µg/mL (1.7µM), the samples were further diluted with Hepes buffer. The polyplexes were allowed to equilibrate for 30 minutes at room temperature prior to use.

The +/- charge ratio, i.e. the ratio of the number of positive charges on the polymer chains to the number of negative charges on the ONs, was calculated assuming that 1 µg of 20-mer ONs contained 3.43 nmol negative charges, that 1 µg of pLL contained 7.81 nmol positive charges, as calculated from the molar mass of Lysine monomer, the pKa of Lysine and the pH of the solutions, and that 1 µg of graft-pDMAEMA contains 1.99 nmol positive

charges as calculated from the pH of the solution, the molecular weight and the pKa of the DMAEMA monomer and the degree of substitution.

2.4. Cell culture

Because of their clear morphology, Vero cells (ATCC nr.: CCL-81) were used for microinjection experiments. Vero cells were cultured in Dulbecco's modified Eagle's medium (DMEM) without phenol red (Gibco, Merelbeke, Belgium) containing 2 mM glutamine, 10% heat deactivated fetal bovine serum (FBS) and 1% penicillin-streptomycin. Cells were grown to 70% confluency on glass-bottomed cover slips (Part No. PG-1.5-14-F, Glass bottom No. 1.5, MatTek Corporation) at 37 °C in a humidified atmosphere containing 5% CO_2.

2.5. Fluorescence Fluctuation Spectroscopy

In this study, FFS experiments were performed on a home made (dual color) FFS setup as described in Chapter 3. The measurements on the homemade FFS apparatus were confirmed by conducting the same experiments on a commercial instrument (Confocor II, Zeiss-Evotec, Jena, Germany).

FFS measurements in buffer:

Cy5-pLL/RhGr-ONs samples (prepared as described above) were further diluted with Hepes buffer until a final ONs concentration of 0.2 µg/mL (34 nM). After dilution, 50 µL of the sample was immediately transferred into a 96-well plate (Grainer Bio-one, Frickenhausen, Germany) to begin the FFS measurements. Diffusion coefficients were calculated using the average diffusion time of at least 20 measurements. Each Cy5-pLL/RhGr-ONs sample was independently prepared three times and each preparation was measured at least 10 times. The fluorescence fluctuation profiles shown in the figures were representative for the measurements done on the respective Cy5-pLL/RhGr-ONs samples.

FFS measurements in cells:

FFS measurements were done on Vero cells grown to 70% confluency on glass-bottomed cover slips (Part No. PG-1.5-14-F, Glass bottom No. 1.5, MatTek Corporation).

Microinjection experiments were performed on Vero cells in imaging medium (serum containing DMEM and 10 mM Hepes). A Femtojet® microinjector and an Injectman® NI 2 micromanipulator (Eppendorf) were used. Injections were performed in the cytoplasm or the

nucleus of the cells. The Vero cells were injected with respectively free RhGr-ONs (10µM) or Cy5-pLL/RhGr-ONs (10µM RhGr-ONs, +/- charge ratio of 20) prepared in Hepes buffer.

FFS measurements were done at randomly selected places in cytoplasm or nucleus. To ensure measurements in viable cells, only non-rounded cells without the appearance of cytoplasmic blebs were selected. Confocal sections in z-direction were taken every 0.5 µm to position the excitation volume in the cell. After the CLSM/FFS measurements, cell viability was evaluated using propidium iodide.

3. Results & Discussion

3.1. FFS on dual color labeled nanobeads in buffer and in cells

As control experiment, dual color FFS measurements were first performed in the cytoplasm and nucleus of 'blanc' cells (i.e. cells which were not loaded with fluorescent molecules or fluorescent nanobeads). Generally, the fluorescence registered by the two detectors was very low while from time to time (very) small peaks appeared (the intensity of these peaks being maximally 3 kHz above the background noise).

To validate the applicability of FFS for studying the association state of complicated nanosized polymer/ONs-complexes in complex media like the cytoplasm or nucleus of cells, we performed first FFS measurements on dual color nanobeads (respectively 90 nm and 500 nm in diameter) injected in living cells. FFS measurements on a dispersion of these nanobeads in buffer revealed simultaneously occurring high fluorescence peaks of green and red fluorescence (Figure 1A). This clearly proves that the red and green detector are indeed able to simultaneously detect a highly fluorescent, dual color labeled particle that migrates through the excitation volume.

We further performed FFS measurements on the nanobeads microinjected in Vero-cells. Microinjecting 90 nm nanobeads in the nucleus (Figure 1B) or in the cytoplasm (Figure 1C) resulted in the simultaneous appearance of Cy5- and RhGr-peaks in the detection volume (positioned at a different location than the site of injection). This proves that at least part of these beads is mobile in both cytoplasm and nucleus. Microinjected 500 nm nanobeads seemed quasi immobile in the cytoplasm as CLSM time-series experiments for 30 minutes did not reveal any diffusion of the beads (data not shown). Also, in FFS measurements, the microinjected 500 nm beads did not result into simultaneous RhGr-peaks and Cy5-peaks,

which we did see for these nanobeads in buffer (data not shown), confirming that they were physically entrapped in the cytoplasm.

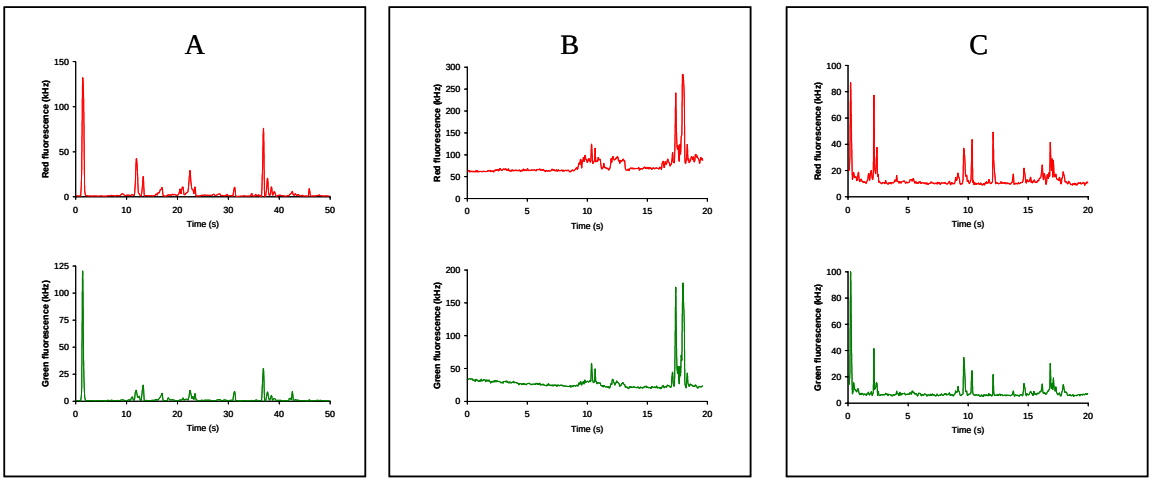

Figure 1. Fluorescence fluctuation profiles, as simultaneously registered by the 'red' and 'green' detector, of a dispersion of dual color labeled nanobeads (90 nm) in buffer (A), in the nucleus of a Vero-cell after microinjecting the nucleus (B) and in the cytoplasm of a Vero-cell after microinjecting the cytoplasm (C).

3.2. FFS on RhGr-ONs in cells

Microinjection of free RhGr-ONs in the cytoplasm resulted in nuclear accumulation of the RhGr-ONs within minutes (CLSM images not shown). This rapid nuclear accumulation of ONs has also been reported in literature [6-9]. FFS measurements confirmed these observations as the RhGr-baseline fluorescence was significantly higher in the nucleus than in the cytoplasm of the same cell: it varied between 60 kHz to 200 kHz in the cytoplasm and between 150 kHz and 600 kHz in the nucleus (dependant on the amount of RhGr-ONs injected, as according to the manufacturer no reproducible volume can be microinjected). In the fluorescence fluctuation profiles as measured in the nucleus, RhGr-peaks were absent (Figure 2A upper profile) indicating that intensive clustering of the RhGr-ONs with nuclear components (which could result in highly green-fluorescent structures) probably does not occur. Autocorrelation analysis of the fluorescence fluctuations revealed a significant slow down of the RhGr-ONs (Figure 2B), which is in agreement with the recently demonstrated interaction between antisense ONs and their target mRNA in the nucleus [10]. In the cytoplasm, however, RhGr-peaks could be observed (Figure 2A lower profile), indicating that RhGr-ONs are clustered with cytoplasmatic components. Indeed, we recently observed that upon adding diluted cell lysate to labeled ONs, part of the ONs clusters, which is observed as

the appearance of high fluorescence peaks in the green fluorescence fluctuation profile (see Chapter 6). The latter observation points out the need for a dual color FFS approach to study the dissociation of polymer/ONs complexes in cells. Single color labeled aggregates could be due to non-dissociated polymer/ONs complexes (with the polymer or the ONs being labeled) but they could also be due to dissociated polymer/ONs complexes whereby the polymer or the ONs subsequently clusters with cellular components. In opposite, when dual color labeled aggregates are observed, they are for sure due to (non-dissociated) polymer/ONs complexes.

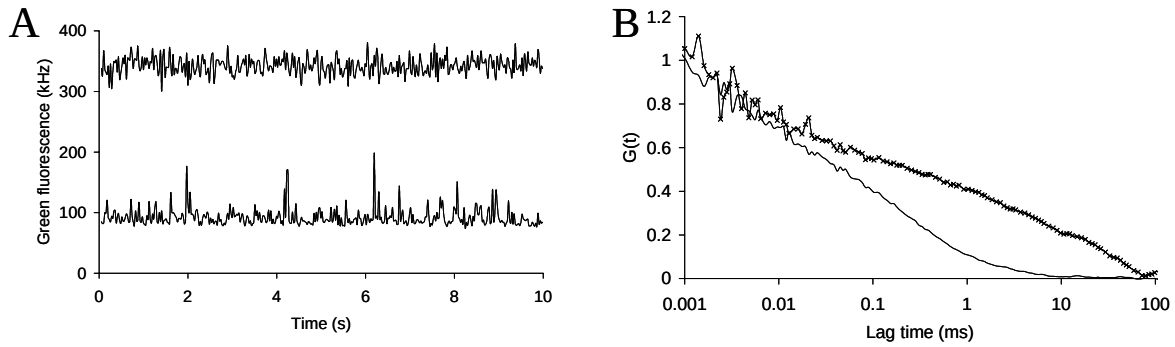

Figure 2. (A): fluorescence fluctuations in the cytoplasm (lower profile) and in the nucleus (upper profile) of a Vero-cell injected in the cytoplasm with RhGr-ONs. (B): autocorrelation curve of RhGr-ONs in buffer (___) and in the nucleus of a Vero-cell (_x_).

3.3. FFS on Cy5-polymer/RhGr-ONs complexes in cells

Microinjection of the cationic copolymer Cy5-graft-pDMAEMA in the cytoplasm resulted in a homogeneous distribution of the labeled polymer throughout the cytoplasm (data not shown). Clearly, the polymer did not reach the nucleus. It is well known that only small structures can migrate passively through the nuclear pores [11]. Therefore, it could be well expected that Cy5-graft-pDMAEMA of a molar mass of 1700 kDa would not be able to cross the nuclear membrane. After transfecting Vero-cells with Cy5-graft-pDMAEMA/RhGr-ONs complexes for 3 hours, CLSM revealed that the polymer remained located in the cytoplasm whereas part of the oligonucleotides accumulated in the nucleus (and therefore must have been released from the polymer, Figure 3). Another part of the oligonucleotides remained present in the cytoplasm, predominantly colocalized with the polymer. This proves that Cy5-graft-pDMAEMA/RhGr-ONs complexes are successfully taken up by the cells, they are subsequently released from the endosomes and they dissociate in the cytoplasm. This is in agreement with our previous results (in chapter 2) where graft-pDMAEMA proved to be an

efficient carrier for antisense ONs as biological activity could be observed when transfecting A549-cells with graft-pDMAEMA/ONs complexes [12].

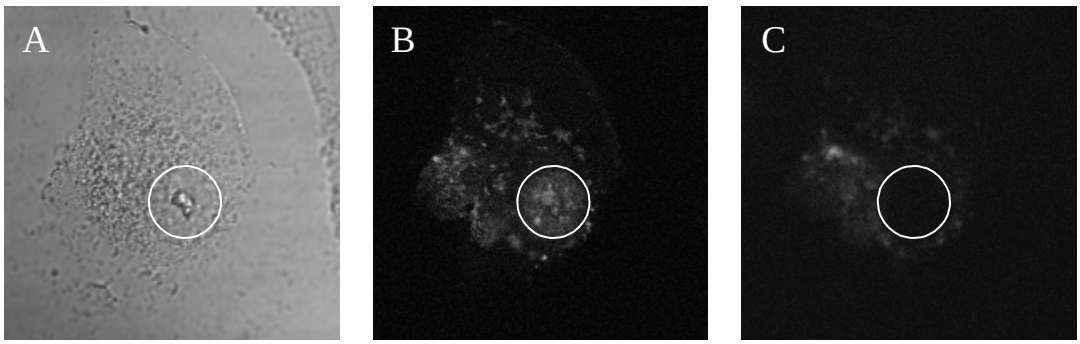

Figure 3. Transmission image (A) and confocal fluorescence images (B: green; C: red) of a Vero-cell transfected for 3 hours with Cy5-*graft*-pDMAEMA/RhGr-ONs. A circle is drawn around the nucleus.

Thus, in conclusion, CLSM experiments are sufficient to prove for certain that (part of) the Cy5-graft-pDMAEMA/RhGr-ONs complexes dissociate in the cytoplasm. When using a pharmaceutical carrier of lower molar mass, however, CLSM results may become insufficient to detect whether the complexes are associated or dissociated. Indeed, after incubating Vero-cells with Cy5-pLL/RhGr-ONs for 3 hours (the molar mass of pLL being 30 kDa), colocalized green and red spots were present in both the cytoplasm and the nucleus (Figure 4). However, this occurrence of colocalized green and red fluorescence in the cytoplasm and nuclei does not necessarily imply that all RhGr-ONs are still associated to their Cy5-pLL carrier. They may just be localized together without being associated.

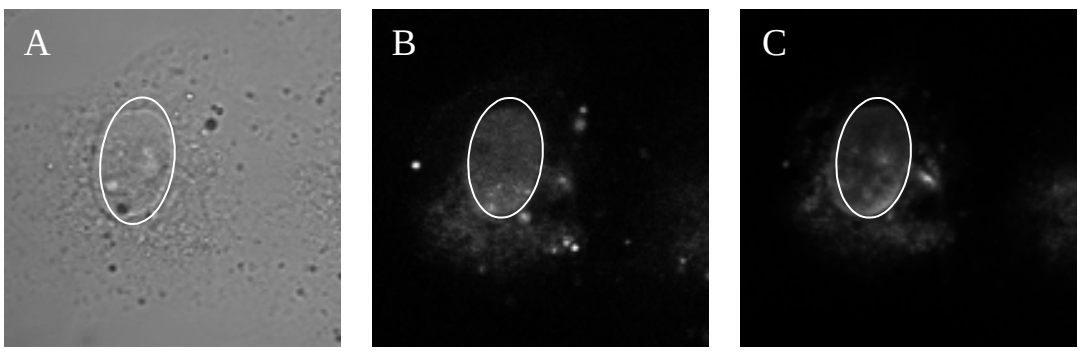

Figure 4. Transmission image (A) and confocal fluorescence images (B: green; C: red) of a Vero-cell transfected for 3 hours with Cy5-pLL/RhGr-ONs. An ellipse is drawn around the nucleus.

Via CLSM it is thus not possible to elucidate whether intact complexes were transported from the cytoplasm into the nucleus or whether dissociation occurred in the

cytoplasm followed by nuclear accumulation of the free polymer and free ONs. Therefore, we thought that the temporal analysis of the movement of these molecules via FFS, instead of the spatial analysis of the fluorescent labeled molecules via CLSM, could be more robust to conclude whether the fluorescent labeled species are associated. Figure 5D shows that FFS is able to detect simultaneously occurring RhGr-peaks and Cy5-peaks in the cytoplasm of Vero-cells already after 30 minutes of incubation of the cells with Cy5-pLL/RhGr-ONs complexes. This means that multimolecular Cy5-pLL/RhGr-ONs complexes are able to diffuse through the cytoplasm and pass through the excitation volume.

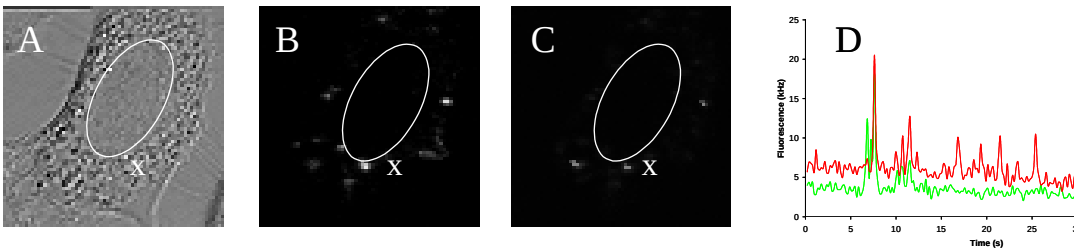

Figure 5. Transmission image (A) and confocal fluorescence images (B: green; C: red) of a Vero-cell transfected for 30 minutes with Cy5-pLL/RhGr-ONs. An ellipse is drawn around the nucleus. The fluorescence fluctuation profile as registered by the green and red FFS detector when the excitation volume is positioned in the cell at location X (D).

Upon longer incubation time, FFS was able to detect both Cy5-pLL and RhGr-ONs in the nucleus. However, simultaneously occurring Cy5- and RhGr-peaks were never observed in the nucleus (data not shown). This indicates that Cy5-pLL and RhGr-ONs migrate independently from each other in the nucleus. On the other hand, it remains possible that intact polyplexes were present in the nucleus, but that they were not detected by FFS as they did not migrate (or migrate too slowly) through the nuclear matrix and thus did not move through the excitation volume. To clear out this hypothesis, we microinjected Cy5-pLL/RhGr-ONs complexes into the nucleus of Vero-cells. The simultaneous appearance of RhGr-peaks and Cy5-peaks in Figure 6A clearly indicates that Cy5-pLL/RhGr-ONs complexes migrate through the excitation volume, proving that FFS is able to detect intact Cy5-pLL/RhGr-ONs complexes in the nucleus. Therefore, from the absence of simultaneous peaks in the nuclei of the Cy5-pLL/RhGr-ONs transfected cells, it can be concluded that intact polyplexes did not reach the nucleus. This means that the Cy5-pLL/RhGr-ONs complexes first dissociate in the cytoplasm before the RhGr-ONs and the Cy5-pLL strands enter the nucleus. Such conclusion can not be made for certain based upon CLSM experiments.

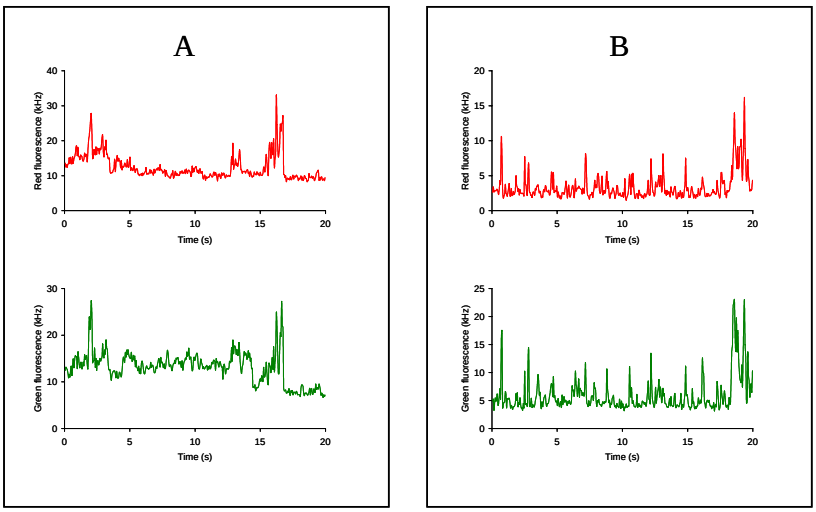

Figure 6. The fluorescence fluctuation profiles as registered by the green and red detector in the nucleus of a Vero-cell after microinjecting the nucleus with a Cy5-pLL/RhGr-ONs sample (A) and in the cytoplasm of a Vero-cell after microinjecting the cytoplasm with a Cy5-pLL/RhGr-ONs sample (B).

Also other pharmaceutical carriers of low molar mass are reported to enter the nucleus after transfection [1;13;14]. We also observed in our experiments that microinjection of free Cy5-pLL resulted into nuclear accumulation. In a next step, we dissociated Cy5-pLL/RhGr-ONs complexes with dextran sulfate prior to their microinjection in the cytoplasm of a Vero-cell. Figure 7 clearly shows that the free RhGr-ONs accumulate in the nucleus, whereas the Cy5-pLL, bound to the high molar mass dextran sulfate is now unable to access the nucleus. Also, as expected, FFS measurements in the cytoplasm of this cell revealed Cy5-peaks, attributed to the Cy5-pLL/dextran-sulfate complexes migrating through the excitation volume (data not shown).

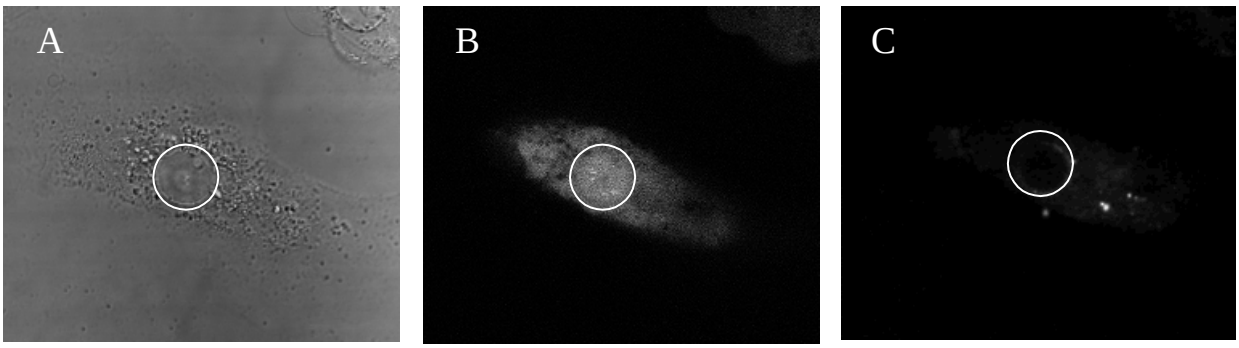

Figure 7. Transmission image (A) and confocal fluorescence images (B: green; C: red) of a Vero-cell 15 minutes after injecting the cytoplasm with a sample which consists of Cy5-pLL/dextran-sulfate complexes and released RhGr-ONs. A circle is drawn around the nucleus.

4. Conclusion

We have shown that cationic polymers of high molar mass, like graft-pDMAEMA of 1700 kDa used in this study, cannot enter the nucleus upon microinjection in the cytoplasm. When such (red-labeled) polymers are used as a carrier for (green-labeled) ONs, CLSM experiments are sufficiently suited to prove whether the polymer/oligonucleotide complexes are able to dissociate in the cytoplasm or not: upon dissociation the released green-labeled ONs enter the nucleus while the red-labeled polymer chains remain in the cytoplasm, consequently the red and green labels do not colocalize in the nucleus. However, in opposite to the high molar mass cationic polymers, cationic polymers of lower molar mass, like pLL of 30 kD used in this study, do enter the nucleus upon microinjection or transfection. Consequently, when such (red-labeled) polymers are used as carriers for (green-labeled) ONs, the nuclei might show both green and red fluorescence, regardless of whether the polyplexes are dissociated or not. Clearly, CLSM experiments cannot reveal whether the dual colored nuclei are due to intact Cy5-pLL/RhGr-ONs polyplexes or to dissociated Cy5-pLL and RhGr-ONs chains. Our results show that dual color FFS, which monitors the movement of the fluorescent molecules, can solve this question. Upon cytoplasmic microinjection or upon transfection with Cy5-pLL/RhGr-ONs complexes, FFS was able to detect simultaneously red and green fluorescence peaks in the cytoplasm. In the nucleus, however, simultaneous peaks were never observed. From these results we could conclude that the Cy5-pLL and RhGr-ONs present in the nucleus after transfection were not associated.

Reference List

1. W.T. Godbey, K.K. Wu, and A.G. Mikos, Tracking the intracellular path of poly(ethylenimine)/DNA complexes for gene delivery, Proceedings of the National Academy of Sciences of the United States of America 96 (1999) 5177-5181.

2. E.G. Marcusson, B. Bhat, M. Manoharan, C.F. Bennett, and N.M. Dean, Phosphorothioate oligodeoxyribonucleotides dissociate from cationic lipids before entering the nucleus, Nucleic Acids Research 26 (1998) 2016-2023.

3. O. Zelphati and F.C. Szoka, Mechanism of oligonucleotide release from cationic liposomes, Proc. Natl. Acad. Sci. U. S A 93 (1996) 11493-11498.

4. F. Simeoni, M.C. Morris, F. Heitz, and G. Divita, Insight into the mechanism of the peptide-based gene delivery system MPG: implications for delivery of siRNA into mammalian cells, Nucleic Acids Research 31 (2003) 2717-2724.

5. P. Schwille, Fluorescence Correlation Spectroscopy and Its Potential for Intracellular Applications, Cell Biochemistry and Biophysics 34 (2001) 383-408.

6. J.P. Clarenc, B. Lebleu, and J.P. Leonetti, Characterization of the Nuclear-Binding Sites of Oligodeoxyribonucleotides and Their Analogs, Journal of Biological Chemistry 268 (1993) 5600-5604.

7. R. Hartig, R.L. Shoeman, A. Janetzko, S. Grub, and P. Traub, Active nuclear import of single-stranded oligonucleotides and their complexes with non-karyophilic macromolecules, Biology of the Cell 90 (1998) 407-426.

8. P. Lorenz, B.F. Baker, C.F. Bennett, and D.L. Spector, Phosphorothioate antisense oligonucleotides induce the formation of nuclear bodies, Molecular Biology of the Cell 9 (1998) 1007-1023.

9. A. Tsuji, H. Koshimoto, Y. Sato, M. Hirano, Y. Sei-Iida, S. Kondo, and K. Ishibashi, Direct observation of specific messenger RNA in a single living cell under a fluorescence microscope, Biophysical Journal 78 (2000) 3260-3274.

10. F.X. Shi, W.H. Visser, N.M.J. de Jong, R.S.B. Liem, E. Ronken, and D. Hoekstra, Antisense oligonucleotides reach mRNA targets via the RNA matrix: downregulation of the 5-HT1A receptor, Experimental Cell Research 291 (2003) 313-325.

11. G. Liu, D.S. Li, M.K. Pasumarthy, T.H. Kowalczyk, C.R. Gedeon, S.L. Hyatt, J.M. Payne, T.J. Miller, P. Brunovskis, T.L. Fink, O. Muhammad, R.C. Moen, R.W. Hanson, and M.J. Cooper, Nanoparticles of compacted DNA transfect postmitotic cells, Journal of Biological Chemistry 278 (2003) 32578-32586.

12. B. Lucas, E. Van Rompaey, K. Remaut, N. Sanders, S.C. De Smedt, and J. Demeester, On the biological activity of anti-ICAM-1 oligonucleotides complexed to non-viral carriers, Journal of Controlled Release 96 (2004) 207-219.

13. J.P. Clamme, G. Krishnamoorthy, and Y. Mély, Intracellular dynamics of the gene delivery vehicle polyethylenimine during transfection: investigation by two-photon fluorescence correlation spectroscopy, Biochimica et Biophysica Acta 1617 (2003) 52-61.

14. K.D. Jensen, A. Nori, M. Tijerina, P. Kopeckova, and J. Kopecek, Cytoplasmic delivery and nuclear targeting of synthetic macromolecules, Journal of Controlled Release 87 (2003) 89-105.

Chapter 5

Studying pegylated DNA-complexes by dual color FFS

Parts of this chapter have been published in Macromolecules. 37: 3832-3840 (2004)

1. Introduction

Pharmaceutical carriers bearing hydrophilic segments (such as polyethyleneglycol, pEG) were developed to stabilize and prolong the circulation lifetime of nucleic acid containing particles, and to improve targeting strategies [1]. These 'pegylated carriers' result in DNA-complexes consisting of a more or less hydrophobic core of partially neutralized polyion strands, surrounded by a shell of hydrophilic chains. Figure 1 represents a schematic view of oligonucleotides complexed to a cationic homopolymer and a cationic block-copolymer, respectively resulting in a "non-structured" DNA-complex and a more ordered "core-shell" DNA-complex. Non-structured DNA-complexes require a substantial excess of cationic carrier over ONs to prevent spontaneous aggregation of the DNA-complexes. However, such positively charged particles are prone to nonspecific interactions with plasma proteins and negatively charged cell surfaces. This can result in aggregation or dissociation of the DNA-complexes, activation of the complement system, rapid clearance of the DNA-particles by phagocytes and aspecific binding with non-target cells. The shell of electroneutral, hydrophilic chains of core-shell DNA-particles can avoid these problems by reducing the interactions with biological macromolecules and cell surfaces.

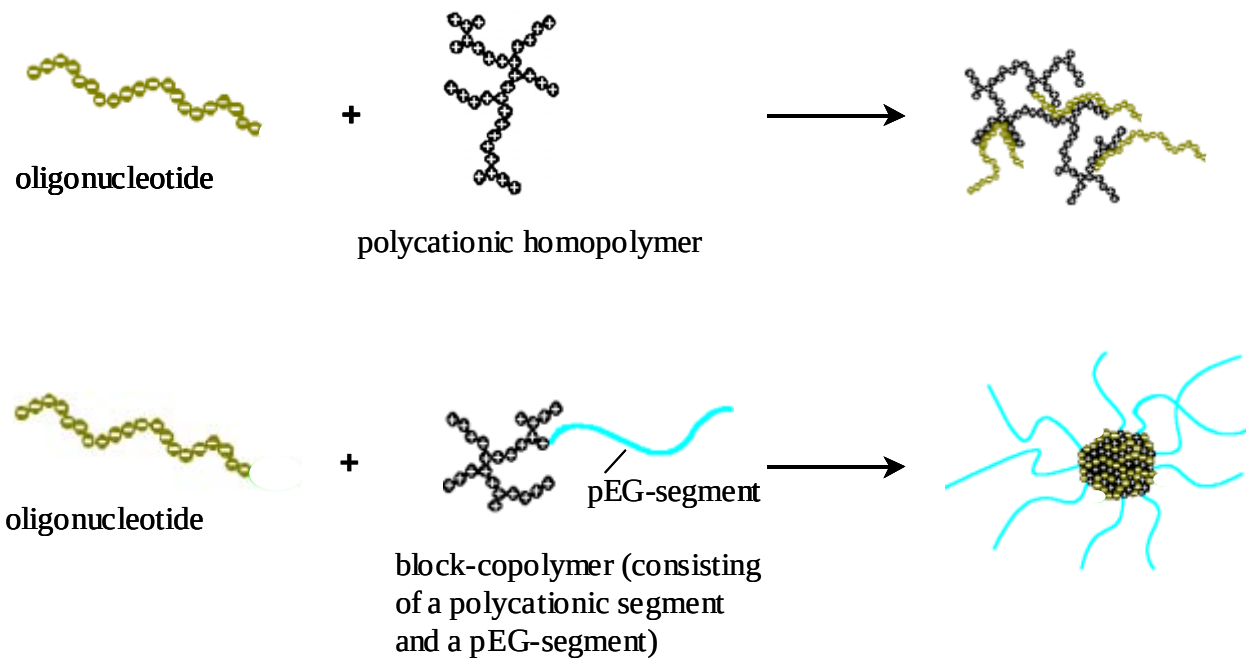

Figure 1. Schematic representation of the formation of "non-structured" DNA-complexes (A) and of DNA-complexes with a 'core-shell' architecture (B).

Our former FFS work focused on the complexation of ONs with cationic homopolymers (e.g. poly-Lysine), resulting in non-structured polyplexes [2-5]. Especially, we showed that both single and dual color FFS allow studying the association and dissociation of polymer/oligonucleotide complexes in buffer (Chapter 3) and in cells (Chapter 4). In this chapter we investigate whether dual color FFS also allows evaluating the association/dissociation behavior of pegylated DNA-complexes in buffer. Two distinct types of pegylated polycations were investigated: a diblock copolymer and a multiblock copolymer (Figure 2), equal in chemical formula but of different molecular weight and degree of pegylation. Two distinct approaches were used to fluorescent label these copolymers: the fluorophore was either attached to the cationic segment or to the distal end of the pEG-strand of the copolymer.

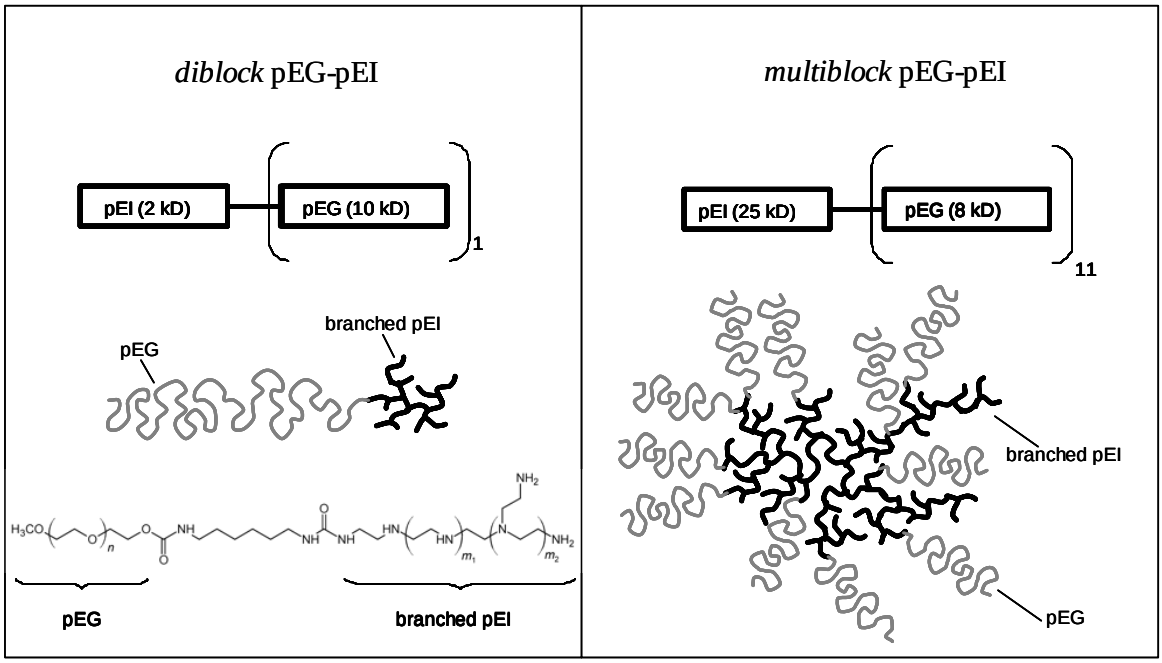

Figure 2. Schematic representation of *diblock* and *multiblock* pEG-pEI. The *diblock* pEG-pEI (batch PI20100, MW 12kD) consists of one branched pEI segment (2 kD) and one pEG-segment (10 kDa). The *multiblock* pEG-pEI (batch PI25080, MW 113 kDa) consists of one branched pEI segment (25 kD) onto which 11 pEG segments (8 kD each) are coupled.

2. Materials and Methods

2.1. Oligonucleotides

The 20-mer phosphodiester ONs (5'-CCC-CCA-CCA-CTT-CCC-CTC-TC-3') (molar mass 5830 g/mol), 25-mer phosphodiester ONs (5'-TCT-GGG-TCA-TCT-TTT-CAC-GGT-TGG-C-3') (molar mass 8183 g/mol) and labeled analogues (using rhodamine green (Rh) or Cy5 as fluorescent marker) were synthesized by Eurogentec (Seraing, Belgium). The fluorescent labeling occurred at the 5' end of the ONs: each oligonucleotide contained one label (Rh or Cy5). The ONs were used as described in Chapter 3.

2.2. Polymers

The *diblock* and *multiblock* polyethyleneglycol-polyethylenimine (pEG-pEI) copolymers (Figure 2) were synthesized by Prof. Dr. S. Vinogradov (University of Nebraska) [6]. The weight average molecular weight (MW), as determined from static light scattering, was respectively 12 kDa (for the *diblock*, batch PI20100) and 113 kDa (for the *multiblock*, batch PI25080). The total content of nitrogen was respectively 3.75 µmol/mg polymer and 4.92 µmol/mg polymer [6]. pEG-pEI stock solutions were prepared in Hepes buffer.

Branched pEI (non-pegylated) was purchased from Sigma (St Louis, USA). The molecular weight of the two batches was respectively 2 kDa and 25 kDa. Prior to use, the polymer was desalted over a Sephadex-G25 column (∅10 x 100 mm) in Hepes buffer. The polymer concentration was determined finding the amine concentration using the method of Snyder and Sobocinski [7].

FITC-pEG-N-hydroxysuccinimide (FITC-pEG-NHS, MW 5kDa) was purchased from Shearwater Corporation (Huntsville, AL, USA). Purification over a Sephadex-G25 column (∅10 x 100 mm) showed that no excess of free FITC could be detected by the absorbance detector (Waters 486, Millipore corp. Milford, MA).

2.3. Fluorescent labeling of the pEI segment in *diblock* and *multiblock* pEG-pEI

As outlined in the introduction, two types of fluorescent pEG-pEI were investigated. While in the first type the pEI-segment was fluorescent-labeled, in the second type a fluorophore was attached to the distal end of the pEG-segment (see 2.4.).

The pEI segment of both *diblock* and *multiblock* pEG-pEI was labeled using a succinimidyl-ester-activated Cy5-dye (Cy5-SE) (FluoroLink^{TM}Cy5 monofunctional dye, Amersham Pharmacia, Piscataway, NJ), following the manufacturer's procedure. The resulting fluorescent polymers were termed respectively *diblock* and *multiblock* pEG-pEI-Cy5. The *diblock* pEG-pEI-Cy5 was purified on a Sephadex-G25 column (∅10 x 100 mm), which was previously equilibrated with Hepes buffer. The fractions containing fluorescent pEG-pEI-Cy5 were collected. From the determination of both the amine concentration (using the method of Snyder and Sobocinski[17]) and the absorbance of the label, the average number of labels attached to the polymer was obtained. It could be calculated that, on the average, the pEG-pEI-Cy5 chains bore one Cy5-label. The *multiblock* pEG-pEI-Cy5 was purified via dialysis (molecular weight cut off 12-14 kDa; Medicell International Ltd.). On the average, 1 fluorophore per copolymer was detected.

2.4. Preparation of FITC-pEG-pEI

To obtain a *diblock* pEG-pEI which is fluorescent-labeled with FITC at the pEG-segment (*diblock* FITC-pEG-pEI), equal volumes of pEI (MW 2Da) and FITC-pEG-NHS

(MW 5 kDa) stock solutions (in 0.2 M $NaHCO_3$ at pH 9.3) were mixed yielding equal molar concentrations in the reaction mixture. After incubation for 1 hour, unreacted pEI was removed using a Sephadex-G50 column (∅10 x 300 mm) and 20 mM Hepes buffer (pH 7.4) as mobile phase. Non-conjugated FITC-pEG was removed by means of cation exchange chromatography using a carboxymethyl-Sephadex column (∅10 x 40 mm, loading buffer: 20 mM Hepes pH 7.4, elution buffer: 20 mM Tris pH 9 with 0.7 M NaCl), followed by desalting over a Sephadex-G50 column (∅10 x 100 mm) in Hepes buffer. Finding the amine concentration using the method of Snyder and Sobocinski[17] and measurement of the absorbance of the label allowed the determination of the average number of FITC-pEG chains conjugated to one pEI chain. It could be calculated that one pEI-chain was complexed to one FITC-pEG strand. The resulting *diblock* FITC-pEG-pEI copolymer (7 kDa) served as a labeled model for the *diblock* pEG-pEI copolymer (12 kDa, batch PI20100).

To create a labeled equivalent of the *multiblock* pEG-pEI (113 kDa, batch PI25080), a solution of the *multiblock* pEG-pEI was mixed with an equal molar amount of FITC-pEG-NHS (as described above for the fluorescent labeling of the *diblock* pEG-pEI) and further purified via dialysis (molecular weight cut off 12-14 kDa; Medicell International Ltd.).

2.5. Preparation of polyplexes

The N/P ratio of the polyplexes is defined as the molar ratio of the total number of nitrogen atoms of the polymer to the number of DNA phosphates. The polymer/ONs complexes (varying in N/P ratio) were prepared by adding (in one step) different volumes of the polymer stock solution to a fixed volume of the ONs stock solution, followed by vortexing for 10 seconds. To obtain the final ONs concentration of 10 µg/mL, the samples were further diluted with Hepes buffer. The polyplexes were allowed to equilibrate for 30 min at room temperature prior to use.

For FFS measurements on the polymer/ONs complexes, 100 µL of the sample was prepared as described above, however, the final ONs concentration equaled 0.2 µg/mL. After preparation, 50 µL of the sample was immediately transferred into a 96-well plate (Grainer Bio-one, Frickenhausen, Germany) to begin the FFS measurements.

2.6. Agarose Gel Electrophoresis

Thirty minutes after the preparation of the polyplex samples, 30 µL of these samples (containing 20 µg/mL Rh-labeled ONs) was mixed with 5 µL of a 50% sucrose solution in distilled water and placed in the wells of a 1.1 % agarose gel. A TBE buffer was used containing 10.8 g/L Tris base, 5.5 g/L boric acid and 0.58 g/L EDTA. A potential of 100V was applied for 60 min. The oligonucleotides in the gel were detected based upon the fluorescence of their Rh-label.

2.7. Spectrofluorimetry

The fluorescence of polymer/Rh-ONs complexes was measured on an SLM-Aminco Bowman spectrofluorimeter (SLM-Aminco Bowman; λ_{ex} = 488 nm, λ_{em} = 510 nm), 30 minutes after their preparation. The fluorescence of each sample was measured three times.

2.8. Particle Size and Zeta-Potential Measurements

Dynamic light scattering (DLS) and zeta-potential (ζ) measurements on the polyplexes were performed as described in Chapter 3.

2.9. Fluorescence Fluctuation Spectroscopy (FFS)

Dual color FFS experiments were performed on a home made dual color FFS setup as described in Chapter 3.

3. Results & Discussion

The electrostatic interactions between the anionic ONs and the cationic pEI-segment in pEG-pEI are responsible for the complex formation. The hydrophilic pEG-strands are neutrally charged and indifferent to these interactions. The spontaneously formed complexes consist of a more or less hydrophobic core of partially neutralized polyion strands, surrounded by a shell of neutral, hydrophilic pEG-chains. Indeed, because of this pEG-shell, the zeta-potential of the complexes equaled zero (data not shown). Even at higher N/P ratios (N/P >> 8) the zeta-potential remained zero, both when the *diblock* and the *multiblock* pEG-pEI were used. Dynamic light scattering showed that the hydrodynamic size of the complexes was

around 200 nm (data not shown) [4]. Even at N/P ratios approaching electroneutrality, the size did not change, indicating that the pEG-shell prevents aggregation of the neutral DNA-complexes.

Figure 3A shows that upon complexation of Rh-ONs with pEG-pEI the fluorescence decreases, presumably because of (self-)quenching of the fluorophores since the local concentration of labeled ONs in the complex is much larger than for Rh-ONs free in solution. However, although both *diblock* and *multiblock* pEG-pEI form core-shell type polyplexes, the quenching of the Rh-ONs is different. At higher N/P ratios, the fluorescence remains quenched for Rh-ONs complexed to the *diblock* pEG-pEI whereas there is a partial recovery of the fluorescence in cases concerning the *multiblock* pEG-pEI. Gel electrophoresis shows that for both types of polyplexes no free 25-mer Rh-ONs are present in the sample at N/P ratio higher than 8, which would also increase the fluorescence (data not shown). Therefore, the recovery of the fluorescence intensity for *multiblock* pEG-pEI at higher N/P ratio has to be related to less (self-)quenching between the Rh-labels, due to an altered distribution of the Rh-ONs in the complexes [3;4]. The discrepancy between both types of pEG-pEI is not due to their different degree of pegylation, but to the differences in their cationic segments since the same discrepancy is observed for Rh-ONs complexed to the (non-pegylated) pEI homopolymer of respectively 2 kDa and 25 kDa (Figure 3B).

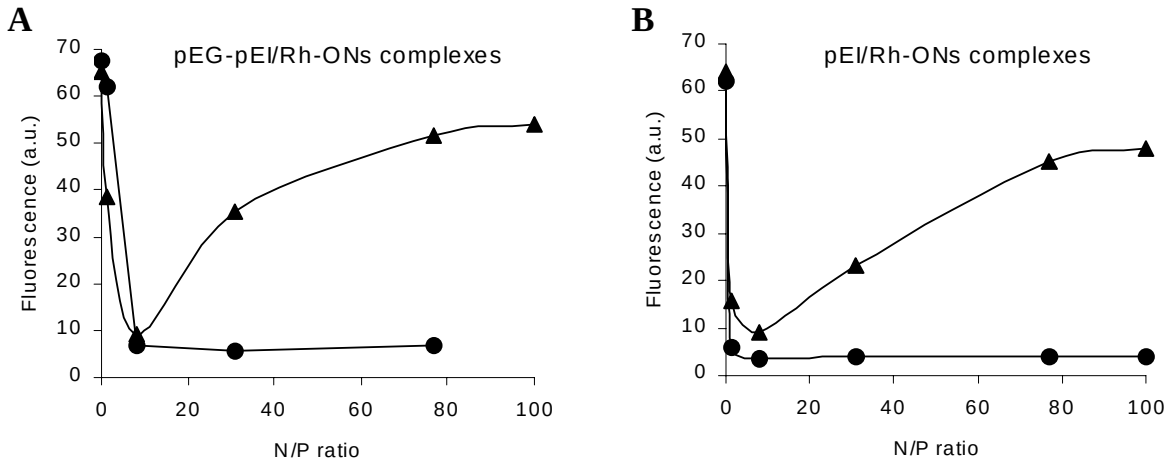

Figure 3. Fluorescence of polymer/ONs complexes (differing in N/P ratios) as measured with a conventional fluorimeter. (A) Rh-ONs (25-mer) complexed to pEG-pEI (*diblock* ● and *multiblock* ◆) and (B) Rh-ONs (25-mer) complexed to (non-pegylated) pEI (2 kDa ● and 25 kda ◆). Each sample was measured three times.

Gel electrophoresis experiments revealed another difference in complexation behavior of *diblock* and *multiblock* pEG-pEI. Figure 4 shows that *diblock* pEG-pEI is not able to fully complex *20-mer* Rh-ONs as a smear can be observed in lanes 2 to 4. It indicates that a major part of the Rh-ONs are still free which enables them to migrate towards the anode. However, *multiblock* pEG-pEI is able to complex the *20-mer* Rh-ONs completely (lanes 5 to 7). On the other hand, both *diblock* and *multiblock* pEG-pEI are able to fully complex *25*-mer Rh-ONs (lanes 9 to 11 and lanes 12 to 14). As for (non-pegylated) pEI carriers, both 2 kDa pEI and 25 kDa pEI are able to fully complex both the 25-mer and the 20-mer Rh-ONs (data not shown). Gel electrophoresis experiments on *diblock* and *multiblock* FITC-pEG-pEI analogues (data not shown) revealed a complexation behavior identical to the unlabeled pEG-pEI shown in Figure 4.

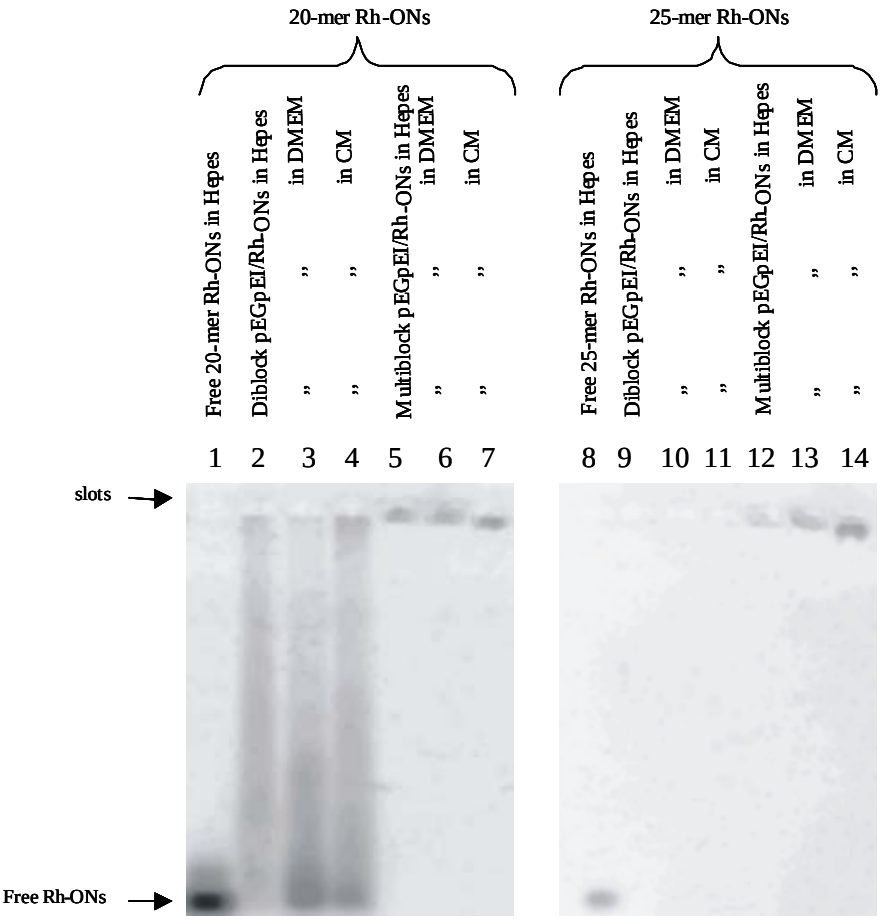

Figure 4. Gel electrophoresis on free Rh-ONs (lane 1 and 8), *diblock*-pEG-pEI/Rh-ONs complexes (lane 2 to 4 and 9 to 11) and *multiblock*-pEG-pEI/Rh-ONs complexes (lanes 5 to 7 and 12 to 14) in various media (Hepes buffer, Dulbecco's Modified Eagle Medium without serum (DMEM) and with serum (CM)). Lane 1 to 7 show 20-mer Rh-ONs, lane 8 to 14 show 25-mer Rh-ONs. The Rh-ONs concentration in all the samples was 20 µg/mL, N/P equaled 15.

Figures 5C and 5D show the fluorescence fluctuations of a *diblock* FITC-pEG-pEI/Cy5-ONs sample measured *at the same time* by the red (5C) and green (5D) detector of the FFS setup. Compared with the fluorescence fluctuations of free Cy5-ONs (Figure 5A) and free *diblock* FITC-pEG-pEI copolymer (Figure 5B), three major observations are made. First, highly intense fluorescence peaks appear in the fluorescence fluctuation profile. This can be explained as follows. When a complex exists of many fluorescent-labeled molecules, its fluorescence becomes much higher than that of a free molecule. Consequently, when such a complex comes into the focal volume, a highly intense fluorescence peak appears in the fluorescence fluctuation profile. Second, the average background fluorescence intensity, representing the average number of fluorescent molecules in the focal volume, significantly decreases upon complexation (compare Figure 5C and 5D with respectively 5A and 5B). As the Cy5-ONs and *diblock* FITC-pEG-pEI molecules organize into multimolecular complexes, the number of free Cy5-ONs and free FITC-pEG-pEI strands in the focal volume is lowered, which is reflected in the FFS curves. Third, highly intense fluorescence peaks are observed in the two detectors *at the same time.* The simultaneous appearance of the red and green peaks indicates that a complex bearing many red-labeled as well as many green-labeled components is passing through the focal volume. It proves that the pEG-pEI/ONs complexes are indeed multimolecular. Others have also reported the multimolecular nature of this class of polyplexes. Vinogradov et al. determined the molecular weight (by static light scattering) of similar pEG-pEI/ONs complexes and calculated that they consist of 23 polymer strands and 24 oligonucleotides [8]. Harada et al. calculated for similar core-shell type pEG-pLL/ONs complexes, a composition of 162 (20-mer) or 248 (15-mer) ONs and hundreds of polymer chains [9]. Simultaneously appearing peaks of high fluorescence intensity could be observed for both 20-mer and 25-mer Cy5-ONs, when complexed to *diblock* FITC-pEG-pEI. Though gel electrophoresis showed that *diblock* FITC-pEG-pEI is not able to fully complex 20-mer Cy5-ONs (Figure 4, lane 2 to 4), FFS showed that at least part of the Cy5-ONs are organized in multimolecular polyplexes.

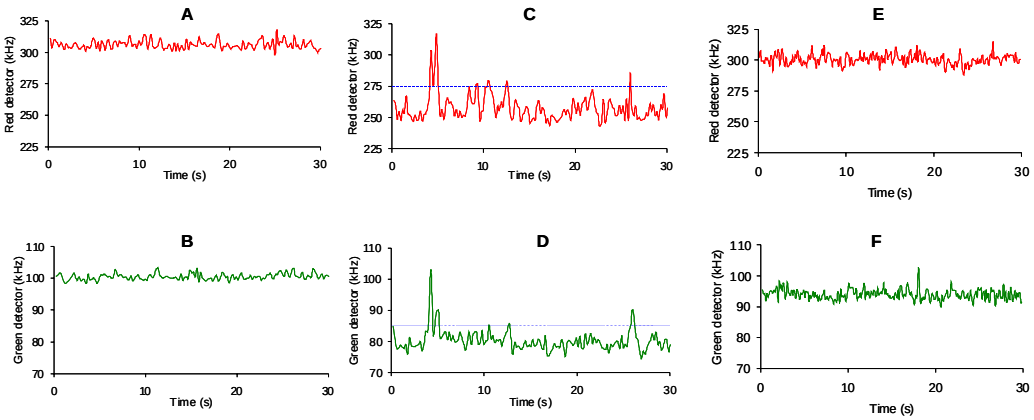

Figure 5. The fluorescence fluctuation profiles of a solution of free Cy5-ONs (A) and free *diblock* FITC-pEG-pEI (B) as registered by respectively the red and green detector. Fluorescence fluctuation profiles of a *diblock* FITC-pEG-pEI/Cy5-ONs sample (N/P = 15; 0.2 µg/mL 20-mer Cy5-ONs) as *simultaneously* registered by the FFS 'red detector' (C) and 'green detector' (D). Fluorescence fluctuation profiles of the *diblock* FITC-pEG-pEI/Cy5-ONs sample after addition of NaCl (final concentration 0.5M), as *simultaneously* registered by the FFS 'red detector' (E) and 'green detector' (F). When applicable, threshold fluorescence intensity values are indicated as dotted lines, discriminating the highly intense fluorescence peaks (which occur as a multimolecular complex diffuses through the focal volume) from the average background fluorescence intensity.

Excessive addition of NaCl clearly influences the fluorescence fluctuation profiles (Figures 5E and 5F). The average background fluorescence intensity almost completely restores to the values of free Cy5-ONs (Figure 5A) and free FITC-pEG-pEI (Figure 5B). Moreover, highly intense fluorescence peaks completely disappear. Both phenomena indicate the dissociation of the *diblock* FITC-pEG-pEI/Cy5-ONs complexes. Lane 4 in Figure 7 indeed shows that adding NaCl to the *diblock* FITC-pEG-pEI/Cy5-ONs complexes prior to loading them on gel results in the release of a significant amount of Rh-ONs, which can migrate freely through the gel. Addition of dextran sulfate to the *diblock* FITC-pEG-pEI/Cy5-ONs complexes also resulted in the complete disappearance of highly intense fluorescence peaks in the FFS curves (data not shown). No threshold value could be calculated anymore in the fluorescence fluctuation profile of the labeled ONs, while autocorrelation analysis indeed was able to determine a diffusion coefficient equal to that of the free labeled ONs. Dextran sulfate is an anionic polymer, which competes with the Cy5-ONs for binding to the pEG-pEI chains, and dissociates the *diblock* FITC-pEG-pEI/Cy5-ONs complexes as revealed from lane 5 in Figure 7.

When complexing Cy5-ONs (both 20-mer and 25-mer) with *multiblock* FITC-pEG-pEI, peaks of high fluorescence intensity were recorded simultaneously by both detectors (Figures 6C and 6D) and also the average background fluorescence intensity significantly

decreased. Upon adding NaCl, this average background fluorescence intensity only partly restored (compare Figures 8E and 8F with respectively 6A and 6B). Also a few highly intense fluorescence peaks remained. It indicates that adding NaCl only partly dissociates the *multiblock* FITC-pEG-pEI/Cy5-ONs complexes. Indeed, lane 10 in Figure 7 shows that only a minor amount of the Rh-ONs is able to migrate freely through the gel. Addition of dextran sulfate to the *multiblock* FITC-pEG-pEI/Cy5-ONs complexes resulted in the complete disappearance of highly intense fluorescence peaks in the FFS curves (data not shown). Also, gel electrophoresis shows that dextran sulfate is able to completely release the ONs from the *multiblock* pEG-pEI/ONs complexes (lane 11 in Figure 7).

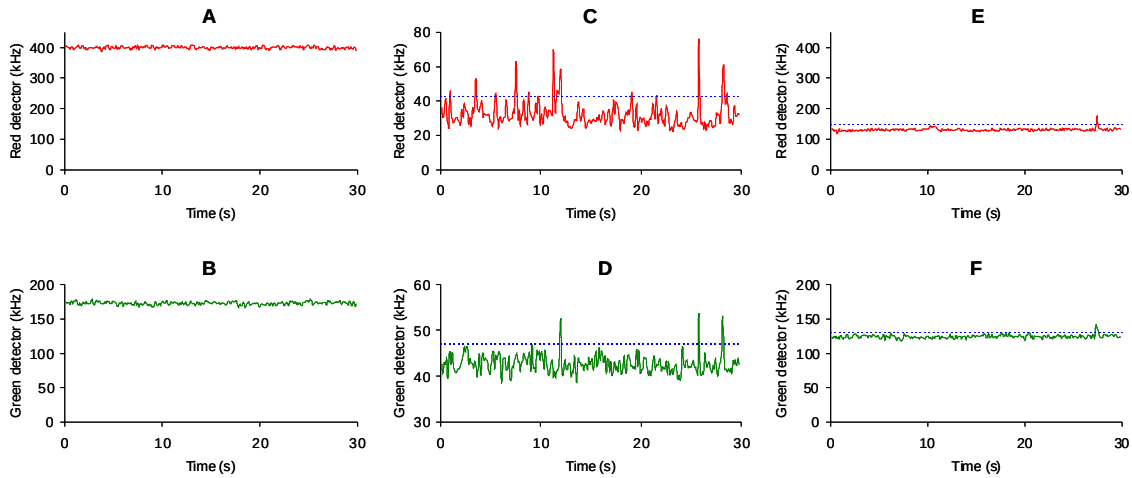

Figure 6. The fluorescence fluctuation profiles of a solution of free Cy5-ONs (A) and free *multiblock* FITC-pEG-pEI (B) as registered by respectively the red and green detector. Fluorescence fluctuation profiles of a *multiblock* FITC-pEG-pEI/Cy5-ONs sample (N/P = 15; 0.2 µg/mL 20-mer Cy5-ONs) as *simultaneously* registered by the FFS 'red detector' (C) and 'green detector' (D). Fluorescence fluctuation profiles of the *multiblock* FITC-pEG-pEI/Cy5-ONs sample after addition of NaCl (final concentration 0.5M), as *simultaneously* registered by the FFS 'red detector' (E) and 'green detector' (F). When applicable, threshold fluorescence intensity values are indicated as dotted lines.

In the FFS experiments described above, the fluorescent marker (FITC) was attached to the pEG-strand of pEG-pEI, thus residing at the surface of the core-shell polyplexes. In the following experiments, the fluorescent label (Cy5) was bound to the cationic pEI-segment of pEG-pEI, which takes part in the electrostatic interactions between the ONs and the polymer.

Dual color FFS measurements on the *diblock* pEG-pEI-Cy5/Rh-ONs samples did not reveal the simultaneous appearance of highly intense fluorescence peaks in the red and green detector or any significant changes in the average background fluorescence intensity of the FFS-curves (data not shown), indicating that multimolecular complexes did not exist. Gel electrophoresis experiments indeed confirmed these results: as revealed from lane 6 in Figure

7, the *diblock* pEG-pEI-Cy5 was not able to complex the Rh-ONs anymore, in contrast with the unlabeled polymer (compare lane 6 with lane 3 in Figure 7). The fluorophore on the cationic segment of the *diblock* pEG-pEI clearly hinders the complexation of this polymer with Rh-ONs.

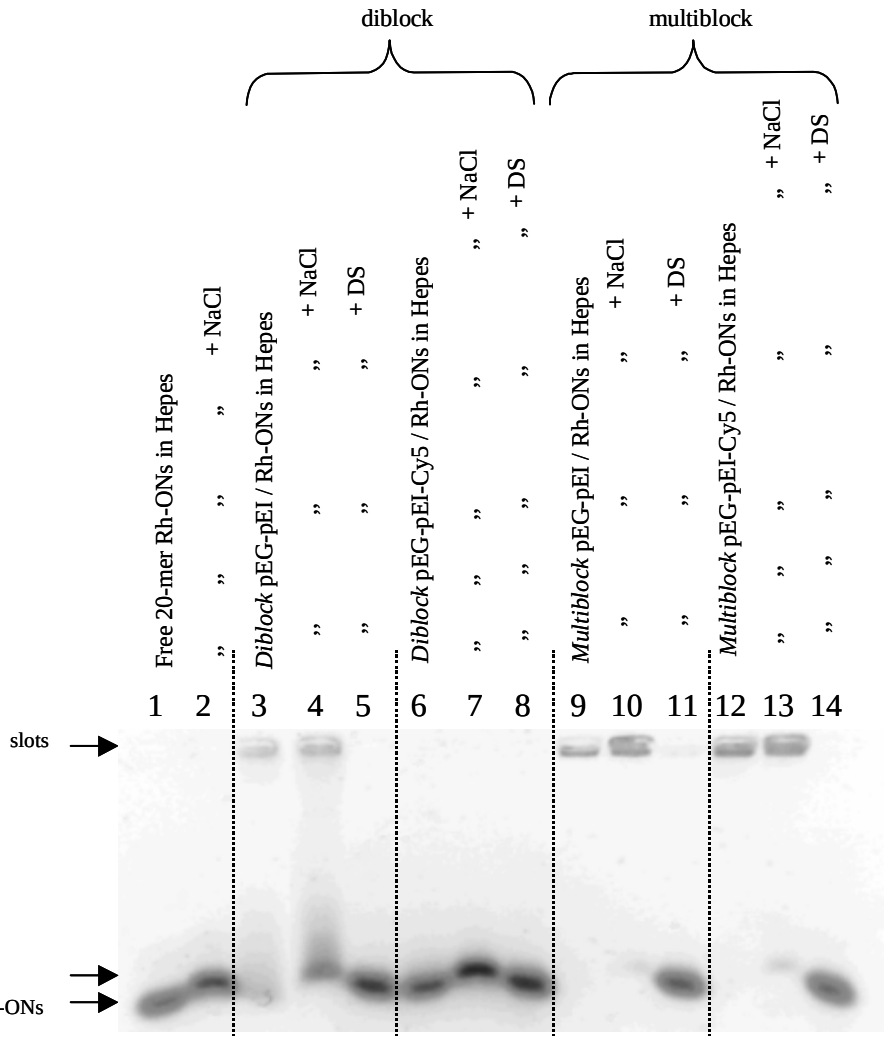

Figure 7. Gel electrophoresis on free 20-mer Rh-ONs (lane 1 and 2), *diblock* pEG-pEI/Rh-ONs complexes (lane 3 to 5), *diblock* pEG-pEI-Cy5/Rh-ONs complexes (lanes 6 to 8), *multiblock*-pEG-pEI/Rh-ONs complexes (lanes 9 to 11) and *multiblock* pEG-pEI-Cy5/Rh-ONs complexes (lanes 12 to 14). The Rh-ONs concentration in all the samples was 20 µg/mL, N/P equaled 15. Addition of salt (NaCl) or dextran sulfate (DS) to the complexes (prior to loading them on gel) clearly destabilizes (i.e. dissociates) the complexes.

The gel electrophoresis experiments show that *multiblock* pEG-pEI-Cy5, like the non-labeled copolymer, does complex with the Rh-ONs (compare lane 12 with lane 9 in Figure 7). Indeed, FFS-measurements reveal a significant decrease of the average background fluorescence intensity, indicating that the amount of non-complexed Rh-ONs and pEG-pEI-Cy5 molecules has decreased (compare Figures 8C and 8D with respectively 8A and 8B).

However, highly intense fluorescence peaks did not appear at all in the red and green fluorescence fluctuation profiles. A plausible explanation could be a strong quenching, as the Rh-labels on the ONs and the Cy5-labels on the pEI-segment of the polymer are in each other's proximity in the core of the polyplexes. On the contrary, for FITC-pEG-pEI/Cy5-ONs complexes, the FITC-label of the polymer is located at the surface of the pEG-shell, distinct from the Cy5-labeled ONs in the core of the complex. Apparently the quenching effect overrules the increase in fluorescence intensity due to the high number of fluorophores in one complex. Upon addition of NaCl, the average background fluorescence intensity only partly restored (Figure 8E and 8F), indicating that only part of the Rh-ONs is released from the polyplexes. This could also be observed from gel electrophoresis measurements: Figure 7 (lane 10 and 13) shows that both non-labeled *multiblock* pEG-pEI and *multiblock* pEG-pEI-Cy5 remain able to complex a major part of the Rh-ONs after addition of NaCl.

Upon adding dextran sulfate to *multiblock* pEG-pEI/Rh-ONs complexes prior to loading them on gel, the Rh-ONs were completely released from the complexes as they migrate freely through the gel (lanes 11 and 14 in Figure 7). In FFS-measurements, adding dextran sulfate to a sample of *multiblock* pEG-pEI-Cy5/Rh-ONs complexes indeed resulted in the recovery of the average background fluorescence intensity (data not shown).

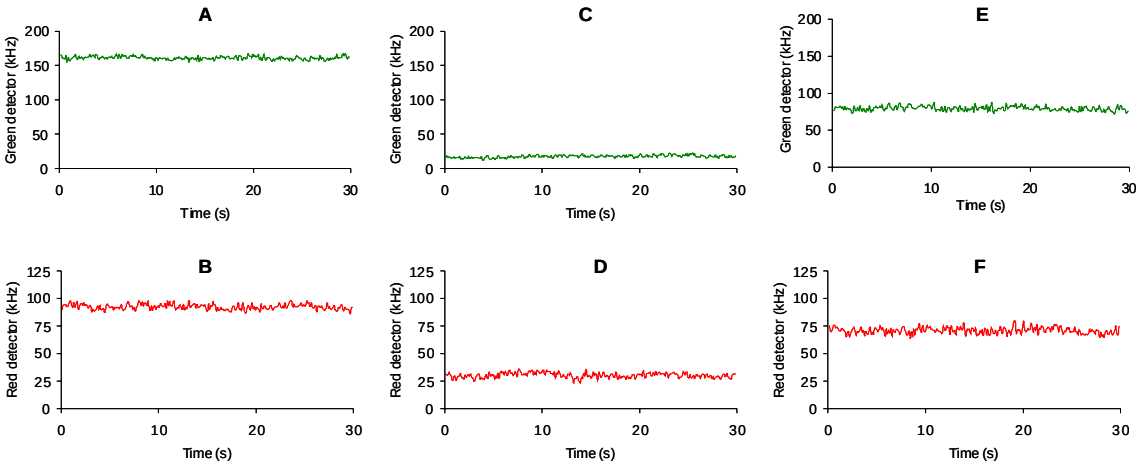

Figure 8. The fluorescence fluctuation profiles of a solution of free Rh-ONs (A) and free *multiblock* pEG-pEI-Cy5 (B) as registered by respectively the red and green detector. Fluorescence fluctuation profiles of a *multiblock* pEG-pEI-Cy5/Rh-ONs sample (N/P = 15; 0.2 µg/mL 20-mer Cy5-ONs) as *simultaneously* registered by the FFS 'green detector' (C) and 'red detector' (D). Fluorescence fluctuation profiles of the same *multiblock* pEG-pEI-Cy5/Rh-ONs sample after addition of NaCl (final concentration 0.5M), as *simultaneously* registered by the FFS 'green detector' (E) and 'red detector' (F).

4. Summary and conclusions

For both *diblock* and *multiblock* pEG-pEI, the complexation with oligonucleotides resulted in the formation of pegylated DNA-complexes with a core-shell structure, as evidenced by zeta-potential measurements. However, differences in complexation behavior between the two types of pEG-pEI were observed. Gel electrophoresis demonstrated that the *diblock* pEG-pEI showed better complexation behavior for 25-mer Rh-ONs than for 20-mer Rh-ONs, whereas *multiblock* pEG-pEI was able to fully complex both types of Rh-ONs. In addition, conventional fluorimetry revealed that the fluorescence of Rh-labeled ONs was differently quenched upon complexation with *diblock* and *multiblock* pEG-pEI.

Dual color FFS measurements were performed on pEG-pEI/ONs complexes, the ONs and pEG-pEI chains being labeled with spectrally different fluorophores. In cases where the fluorescent label (FITC) was attached to the free end of the pEG-segment of pEG-pEI, dual color FFS measurements on FITC-pEG-pEI/Cy5-ONs (for *diblock* as well as *multiblock* pEG-pEI) showed that both detectors simultaneously registered highly intense fluorescence signals. This indicates that a group of oligonucleotides and polymer-chains migrates together through the detection volume and therefore proves that complexes are formed, which are composed of many oligonucleotide and polymer strands. These observations prove the formation of multimolecular polyplexes, which is in agreement with the gel electrophoresis results and observations in literature. When the pEG-pEI polymers were fluorescent-labeled at their cationic pEI-segment, however, FFS did not detect multimolecular polyplexes. In the case of *diblock* pEG-pEI-Cy5, the absence of peaks of high fluorescence intensity was indeed due to the fact that no multimolecular polyplexes could be formed, as was shown by gel electrophoresis. However, gel electrophoresis showed that *multiblock* pEG-pEI-Cy5 did complex Rh-ONs. The absence of highly intense fluorescence peaks in FFS was due to the mutual quenching of both the Cy5- and Rh-labels that were in close proximity in the core of the core-shell complex. From these results, it could be concluded that dual color FFS allows studying the association and dissociation of pEG-pEI/ONs provided that the fluorescent label of the polymer is attached to the distal end of the pEG-chain.

FFS is a very sensitive technique. Experiments can be done on small sample volumes in the nanomolar concentration range. Compare 50 µL of 0.2 µg/mL ONs for FFS-measurements with 30 µL of 20 µg/mL ONs for gel electrophoresis and 1 mL of 10 µg/mL

ONs for dynamic light scattering, zeta-potential and conventional fluorimeter experiments. The very low concentrations used are a major advantage when studying scarce DNA- and polymer-material. The small sample volume required makes the technique suitable for measurements in rare media (e.g. cytoplasmic lysates) and in living cells. As a microscopy-based technique, FFS shows potential to study the biophysical behavior of DNA-complexes *in living cells*. Since gel electrophoresis can tell us whether Rh-ONs are free (migrating towards the anode) or complexed (remaining in the slots), so might dual color FFS be able to determine in the cytoplasm of a living cell whether the Rh-ONs are still complexed to their carrier or not. All this indicated by the presence or absence of simultaneous peaks in both the red and green detector channel. However, the sample material has to be analyzed with care: we have demonstrated the possibility of introducing artefacts as the fluorescent label may alter the physicochemical behavior of the polymer. *Diblock* pEG-pEI-Cy5 did not complex the Rh-ONs anymore, possibly due to steric hindrance of the fluorophore. Also unforeseen quenching phenomena can result in the absence of dual color peaks while the Rh-ONs are complexed to their carrier (as observed for *multiblock* pEG-pEI-Cy5/Rh-ONs complexes).

Reference List

1. Petersen,H., Fechner,P.M., Martin,A.L., Kunath,K., Stolnik,S., Roberts,C.J., Fischer,D., Davies,M.C., and Kissel,T., Polyethylenimine-graft-poly(ethylene glycol) copolymers: influence of copolymer block structure on DNA complexation and biological activities as gene delivery system, Bioconjug. Chem., 13 (2002) 845-854.

2. Lucas,B., Van Rompaey,E., De Smedt,S.C., Demeester,J., and Van Oostveldt,P., Dual-color fluorescence fluctuation spectroscopy to study the complexation between poly-l-lysine and oligonucleotides, Macromolecules, 35 (2002) 8152-8160.

3. Van Rompaey,E., Sanders,N., De Smedt,S.C., Demeester,J., Van Craenenbroeck,E., and Engelborghs,Y., Complex formation between cationic polymethacrylates and oligonucleotides, Macromolecules, 33 (2000) 8280-8288.

4. Van Rompaey,E., Engelborghs,Y., Sanders,N., De Smedt,S.C., and Demeester,J., Interactions between oligonucleotides and cationic polymers investigated by fluorescence correlation spectroscopy, Pharmaceutical Research, 18 (2001) 928-936.

5. Van Rompaey,E., Chen,Y., Muller,J.D., Gratton,E., Van Craenenbroeck,E., Engelborghs,Y., De Smedt,S., and Demeester,J., Fluorescence fluctuation analysis for the study of interactions between oligonucleotides and polycationic polymers, Biological Chemistry, 382 (2001) 379-386.

6. Nguyen,H.K., Lemieux,P., Vinogradov,S.V., Gebhart,C.L., Guerin,N., Paradis,G., Bronich,T.K., Alakhov,V.Y., and Kabanov,A.V., Evaluation of polyether-polyethyleneimine graft copolymers as gene transfer agents, Gene Ther., 7 (2000) 126-138.

7. Snyder,S.L. and Sobocinski,P.Z., Improved 2,4,6-Trinitrobenzenesulfonic Acid Method for Determination of Amines, Analytical Biochemistry, 64 (1975) 284-288.

8. Vinogradov,S.V., Bronich,T.K., and Kabanov,A.V., Self-assembly of polyamine-poly(ethylene glycol) copolymers with phosphorothioate oligonucleotides, Bioconjug. Chem., 9 (1998) 805-812.

9. Harada,A., Togawa,H., and Kataoka,K., Physicochemical properties and nuclease resistance of antisense-oligodeoxynucleotides entrapped in the core of polyion complex micelles composed of poly(ethylene glycol)-poly(L-lysine) block copolymers, Eur. J. Pharm. Sci., 13 (2001) 35-42.

Chapter 6

Towards a better understanding of the dissociation behavior of liposome-oligonucleotide complexes in the cytoplasm of cells

Parts of this chapter have been published in Journal of Controlled Release 103: 435-450 (2005).

1. Introduction

Cationic liposomes have been successfully used as non-viral carriers for ONs, both in cell cultures [1;2] and in animals [3;4]. It has been proved that the liposome/ONs complexes are taken up by cells via endocytosis and not through fusing with the plasma membrane [5]. The cellular mechanisms that govern the location and extent of intracellular dissociation of liposome/ONs complexes remain unclear. Dual color fluorescence microscopy studies have shown that cationic liposome/ONs complexes probably dissociate during endosomal escape and that the oligonucleotides accumulate in the nucleus whereas the lipids remain in the cytoplasm [6;7]. Szoka and colleagues have proposed a model in which the cationic lipids in the endocytosed liposome/ONs complexes interact with the anionic lipids in the inner leaflet of the endosomal membrane and flip-flop into the outer leaflet [8]. It is assumed that during these events the oligonucleotides dissociate from their carrier and escape from the endosome into the cytoplasm while the cationic lipids remain in the outer leaflet of the endosomal membrane. However, the endosomal pathway is maybe not the only way to obtain intracellular dissociation of the lipoplexes. Among others, Sanders et al. have shown that biological polyelectrolytes in the extracellular matrix are able to induce structural alterations of pDNA-containing lipoplexes, hereby releasing DNA [9]. Cytoplasmic soluble proteins are reported to induce DNA release from DNA/carrier complexes in buffer [10]. Additionally, it has been reported that lipoplexes that have been released from artificially ruptured endosomes are able to dissociate at the nuclear membranes [11]. Also, incubating lipoplexes with isolated

nuclei in buffer results in the nuclear accumulation of free ONs whereas the cationic lipids partly fuse with the nuclear membranes [12].

In our former work, we have proved that in buffer the complexation between oligonucleotides and cationic polymers can be monitored by FFS. When associating, the amount of detected free ONs decreases and highly fluorescent complexes appear, which are clearly detected by FFS. These self-assembling polymer/ONs complexes are 'multimolecular' (i.e. exist out of several ONs and several polymer strands). When dissociating, the amount of free ONs increases and the multimolecular complexes disappear [13-17].

To the best of our knowledge, only two reports in literature deal with FFS on lipoplexes. Jurkiewicz et al. studied by single color FFS the association of ONs to liposomes in buffer: the binding of the ONs to the (non-labeled) liposomes decreased the diffusion coefficient of the ONs and reduced the number of free ONs detected in the excitation volume [18]. Merkle et al. determined by dual color FFS the maximum number of 40 bp double-stranded DNA able to bind to a single liposome vesicle [19]. Giving that ONs have to be released from the lipoplexes in order to be biologically active, the intracellular dissociation of the lipoplexes is a crucial issue in the optimization of cationic liposomes for DNA-delivery. Therefore, the current chapter aims to investigate whether dual color FFS allows evaluating the complexation behavior (being association and dissociation) of liposome/ONs complexes in respectively buffer, cell lysate and the cytoplasm of living cells.

2. Materials and methods

2.1. Oligonucleotides

The 25-mer phosphodiester ONs (5'-TCT-GGG-TCA-TCT-TTT-CAC-GGT-TGG-C-3') and labeled analogues (using rhodamine (Rh) or Cy5 as fluorescent marker) were used as described in Chapter 5.

2.2. Polymers, lipids, detergents and polystyrene nanoparticles

Dextran sulfate (DS) was used as described in Chapter 3.

Sodium dodecyl sulfate (SDS) was purchased from Sigma (St Louis, USA). The phospholipids DOTAP (N-(1-(2,3-dioleoyloxy)propyl)-N,N,N-trimethyl-ammoniumchloride), DOPE (dioleoylfosfatidylethanolamine) and FITC-DOPE (i.e. DOPE being labeled at the

polar group with fluorescein-isothiocyanate) were purchased from Avanti® Polar Lipids (Alabaster, AL, USA).

TetraspeckTM beads, of respectively 90 nm diameter and 500 nm diameter, were used as described in Chapter 4.

2.3. Preparation of cationic liposomes

The cationic liposomes studied contained DOTAP and DOPE in a 1:1 molar ratio with or without 0.2 mol % FITC-DOPE. The lipids were dissolved in a 1:1 (volume) mixture of chloroform:methanol. Subsequently, the solution of lipids was placed in a round-bottomed flask and the solvents were evaporated under vacuum at 30°C. The resulting lipid film was further dried under a flow of nitrogen for 1h. The lipids were then resuspended in Hepes buffer (20 mM at pH 7.4) at a final concentration of 5 mM DOTAP and rehydrated overnight at 4 °C to allow liposome formation. The resulting liposomes were extruded at room temperature through a polycarbonate membrane, with a pore size of 0.1 µm, using the Avanti Polar Lipids Mini-extruder. The hydrodynamic size and zeta potential (ζ) of the resulting cationic liposomes were routinely checked by respectively dynamic light scattering (DLS, Malvern 4700, Malvern, Worcestershire, UK) and electrophoretic mobility measurements (Zetasizer 2000, Malvern, Worcestershire, UK), as previously described in Chapter 3. The hydrodynamic diameter and ζ of the liposomes equaled respectively 140 nm ± 11 and +49 mV ± 4.

2.4. Preparation of liposome/ONs complexes

Liposome/ONs complexes with varying +/- charge ratio were prepared. The +/- charge ratio of the liposome/ONs complexes (i.e. the ratio of the number of positive charges (originating from DOTAP) to the number of negative charges (originating from the ONs)) was calculated assuming that 1 µg of ONs contains 3.43 nmol negative charges.

The liposome/ONs complexes varying in +/- charge ratio were prepared by mixing equal volumes of a liposome sample (with increasing concentrations) and an ONs solution (10µM). After addition of the liposome sample to the ONs solution, the resulting sample was mixed during 10 seconds and further diluted until an ONs concentration of 10 µg/mL (1.2µM). The liposome/ONs complexes were allowed to equilibrate for 30 min at room temperature prior to use.

2.5. Dissociation of liposome/ONs complexes in NaCl solutions and cell lysate

To a liposome/ONs sample (the ONs concentration being 20 µg/mL (2.4µM)) an equal volume of NaCl (in varying concentrations) was added and mixed during 10 seconds. The mixture was allowed to equilibrate for 10 minutes prior to use. Dissociation experiments using dextran sulfate, SDS or cell lysate were performed in a similar way. For the experiments with cell lysate, the cell lysate (prepared as described below) was three times diluted with Hepes buffer (20 mM at pH 7.4).

2.6. Agarose gel electrophoresis experiments

30 µL of the FITC-liposome/Rh-ONs samples (containing 1.2 µM ONs) was mixed with 5 µL sucrose solution (50g sucrose/100mL distilled water) and placed in the wells of a 1.1 % agarose gel prepared in TBE buffer (10.8 g/L Tris base, 5.5 g/L boric acid and 0.58 g/L EDTA). Electrophoresis was performed by applying 100 V during 1h over the gel, which was submerged in TBE. After this time span the gel was illuminated with ultraviolet light. The Rh-ONs and the FITC-liposomes in the gel were detected based upon the fluorescence of their label. In the gel electrophoresis experiments Rh-ONs were used instead of Cy5-ONs as the Rh-fluorescence but not the Cy5-fluorescence could be excited by the UV-lamp.

2.7. Spectrofluorimetry

The fluorescence of respectively liposome/Cy5-ONs samples and FITC-liposome/ONs samples was measured on an SLM-Aminco Bowman spectrofluorimeter.

The +/- charge ratio of the liposome/Cy5-ONs complexes was varied by keeping the Cy5-ONs concentration constant at 10 µg/mL and varying the concentration of non-labeled liposomes. The +/- charge ratio of the FITC-liposome/ONs complexes was varied by keeping the FITC-liposome concentration constant at 50 µM DOTAP (0.1 µM FITC-DOPE) and varying the concentration of non-labeled ONs. The fluorescence of each sample was measured three times.

2.8. Cell culture and preparation of cell lysate

Vero cells (ATCC nr.: CCL-81) were cultured as described in Chapter 4.

Cell lysate was derived from Vero cells at 90% confluency following the Clontech Cytoplasmic Extraction Procedure. Briefly, cells were collected after centrifugation and suspended in a hypotonic lysis buffer containing protease inhibitors (10 mM Hepes at pH 7.9,

1.5 mM $MgCl_2$ and 10 mM KCl + 1 µM Leupeptine, 0.5 mM Pefabloc SC, 1 mM DTT and 0.5 mM EGTA). After 15 minutes swelling on ice, cells were centrifuged again and resuspended in 2 times the cell pellet volume of lysis buffer + protease inhibitors. This cell suspension was drawn into a narrow-gauge syringe and rapidly ejected. Lysis occurred by repeating the drawing and ejection procedure 10 times. The disrupted cell suspension was then centrifuged for 20 minutes at 11000 g and the supernatant was stored at -80 °C.

2.9. Fluorescence fluctuation spectroscopy

In this study FFS experiments were performed on a home-made dual color FFS setup as described in Chapter 3. The measurements on the homemade FFS apparatus were confirmed by conducting the same experiments on a commercial instrument (Confocor II, Zeiss-Evotec, Jena, Germany).

FFS measurements in buffer and cell lysate:

FITC-liposome/Cy5-ONs samples in Hepes buffer, NaCl or cell lysate (prepared as described above) were further diluted with Hepes buffer until a final ONs concentration of 0.2 µg/mL (24 nM). After dilution, 50 µL of the sample was immediately transferred into a 96-well plate (Grainer Bio-one, Frickenhausen, Germany) to begin the FFS measurements. Diffusion coefficients were calculated using the average diffusion time of at least 20 measurements. Each FITC-liposome/Cy5-ONs sample was independently prepared three times and each preparation was measured at least 10 times. The fluorescence fluctuation profiles shown in the figures were representative for the measurements done on the respective FITC-liposome/Cy5-ONs samples.

FFS measurements in cells:

Microinjection experiments were performed on Vero cells grown to 70% confluency on glass-bottomed cover slips (Part No. PG-1.5-14-F, Glass bottom No. 1.5, MatTek Corporation, Ashland, MA, USA) submerged in imaging medium (DMEM with FBS and 10 mM Hepes). A Femtojet® microinjector and an Injectman® NI 2 micromanipulator (Eppendorf) were used. All injections were performed in the cytoplasm of the cells. The Vero cells were injected with respectively free Cy5-ONs (5µM) or FITC-liposome/Cy5-ONs (5µM Cy5-ONs, 1250µM DOTAP) prepared in Hepes buffer.

FFS measurements were done at randomly selected places in cytoplasm or nucleus. To ensure measurements in viable cells, only non-rounded cells without the appearance of cytoplasmic blebs were selected. Confocal sections were taken every 0.5 µm to position the

excitation volume inside the cell. After the CLSM/FFS measurements, cell viability was evaluated using propidium iodide.

3. Results and discussion

3.1. Size and zeta-potential of the liposome/ONs complexes

The cationic liposomes were mixed with the anionic ONs at different +/- charge ratios. Complex formation occurred due to electrostatic interactions between the anionic ONs and the cationic DOTAP lipids in the liposomes. At a +/- charge ratio below 1, small negatively charged lipoplexes were obtained (Figure 1). However, when the charge ratio approached 1, ζ approximated zero and large aggregates were consequently formed due to the disappearance of electrical repulsion between individual lipoplexes. At higher +/- charge ratios ζ became positive and equaled the ζ of the cationic liposomes (without ONs). This most likely indicates, as also observed by others, that the ONs became sandwiched between two lipid (bi)layers [9;20]. The positive surface charge of the lipoplexes at these high +/- charge ratios resulted in an electrical repulsion between the individual lipoplexes. This prevents them from aggregating and explains their smaller size. Similar diameters and ζ values were obtained when mixing pDNA (instead of ONs) with the DOTAP/DOPE liposomes [9].

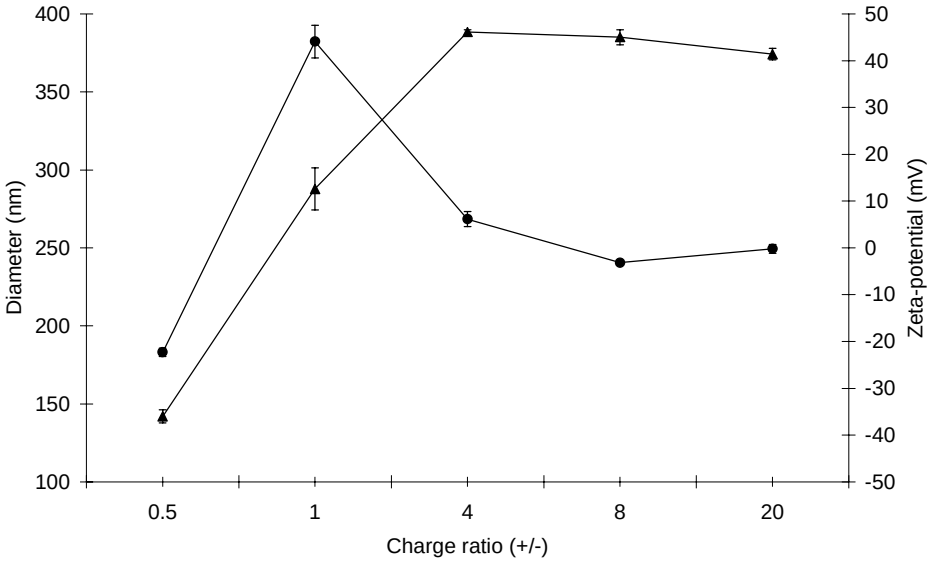

Figure 1. The z-average hydrodynamic diameter (●) and zetapotential (▲) of liposome/ONs complexes, as a function of the +/- charge ratio (n=3).

3.2. Fluorescence of liposome/ONs complexes

Figure 2 shows that the fluorescence of Cy5-ONs significantly decreases upon complexation to non-labeled DOTAP/DOPE liposomes at +/- charge ratios below 1. Their fluorescence levels off at +/- charge ratios above 1. Similar quenching behavior was observed when complexing the Cy5-ONs to FITC-labeled cationic liposomes (data not shown). The decrease in Cy5-ONs fluorescence is due to quenching of the Cy5-ONs upon association with the cationic liposomes. Alternatively, self-quenching of the Cy5-ONs in the complexes might occur. Indeed, in the liposome/Cy5-ONs complexes, the Cy5-ONs are packed together and come into such close proximity of each other that they can quench the fluorescence of their neighbours. Similarly, Rh-ONs were quenched upon complexation to cationic polymers, as was previously shown for e.g. pDMAEMA (poly-2-dimethylaminoethyl-methacrylate, Figure 2) [15]. However, in contrary to the pDMAEMA/Rh-ONs complexes, the fluorescence of the liposomes/Cy5-ONs samples did not restore at higher +/- charge ratio, which might indicate that the organization of the lipoplexes does not drastically change at higher +/- charge ratios.

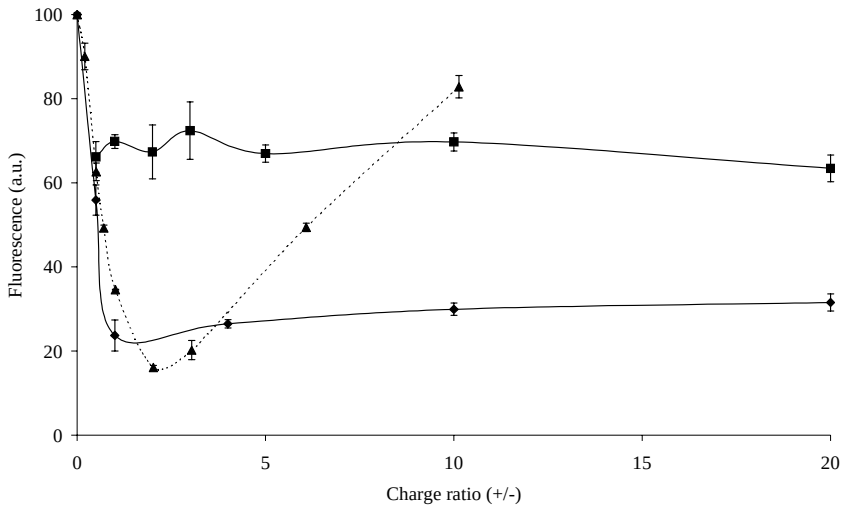

Figure 2. Fluorescence (as measured by a conventional fluorimeter) of liposome/Cy5-ONs complexes (♦), FITC-liposome/ONs complexes (■) and pDMAEMA/Rh-ONs complexes (▲) [15], as a function of the +/- charge ratio. For the liposome/Cy5-ONs and pDMAEMA/Rh-ONs samples, the ONs concentration was kept constant (10 µg/mL) and the concentration of respectively non-labeled liposome and non-labeled pDMAEMA was varied. Excitation occurred at 650 nm (Cy5) or 520 nm (Rh), while the fluorescence was measured at 670 nm (Cy5) or 546 nm (Rh).
For the FITC-liposome/ONs sample, the FITC-liposome concentration was kept constant (50 µM DOTAP, 0.1 µM FITC-DOPE) and the concentration of non-labeled ONs was varied. Excitation occurred at 492 nm, while the fluorescence was measured at 518 nm.

Figure 2 also shows that the fluorescence of the FITC-labeled liposomes was quenched upon complexation to non-labeled ONs. However, this quenching was less pronounced and independent of the +/- charge ratio.

3.3. Characterizing the association of ONs to cationic liposomes in buffer

Figure 3A shows the fluorescence fluctuation profile of free (i.e. non-complexed) Cy5-ONs in Hepes buffer. A diffusion coefficient of 0.82 ±0.09 x 10^{-10} m²/s was obtained when fitting the experimental correlation curve to a single component autocorrelation function (equation 1) [15] and agrees with values reported in literature [15;21]. The fluorescence fluctuation profile of the cationic FITC-liposomes in Hepes buffer (Figure 3B) shows clearly that highly intense peaks of FITC-fluorescence ("FITC-peaks") appear. As the concentration of liposomes in the sample is in the picomolar range (as estimated from the lipid concentration and the amount of lipids per liposome), the FITC-peaks must be due to the movement of individual liposomes, each liposome bearing several FITC labels, through the excitation volume. Although the FITC-peaks complicated the autocorrelation analysis, a diffusion coefficient of 3.5 ±0.5 x 10^{-12} m^2/s could be obtained. Using the Stokes-Einstein equation, a diameter of 140 nm was calculated from this diffusion coefficient, which agrees with the hydrodynamic diameter of the FITC-liposomes measured by DLS (140 nm ± 11, data not shown). The low fluorescence signal between the FITC-peaks in Figure 3B (which we term "baseline fluorescence") is due to the presence of subnanomolar concentrations of free FITC in the FITC-liposome samples. Indeed, autocorrelation analysis of the fluctuations of the baseline yielded a diffusion coefficient of fast diffusing molecules.

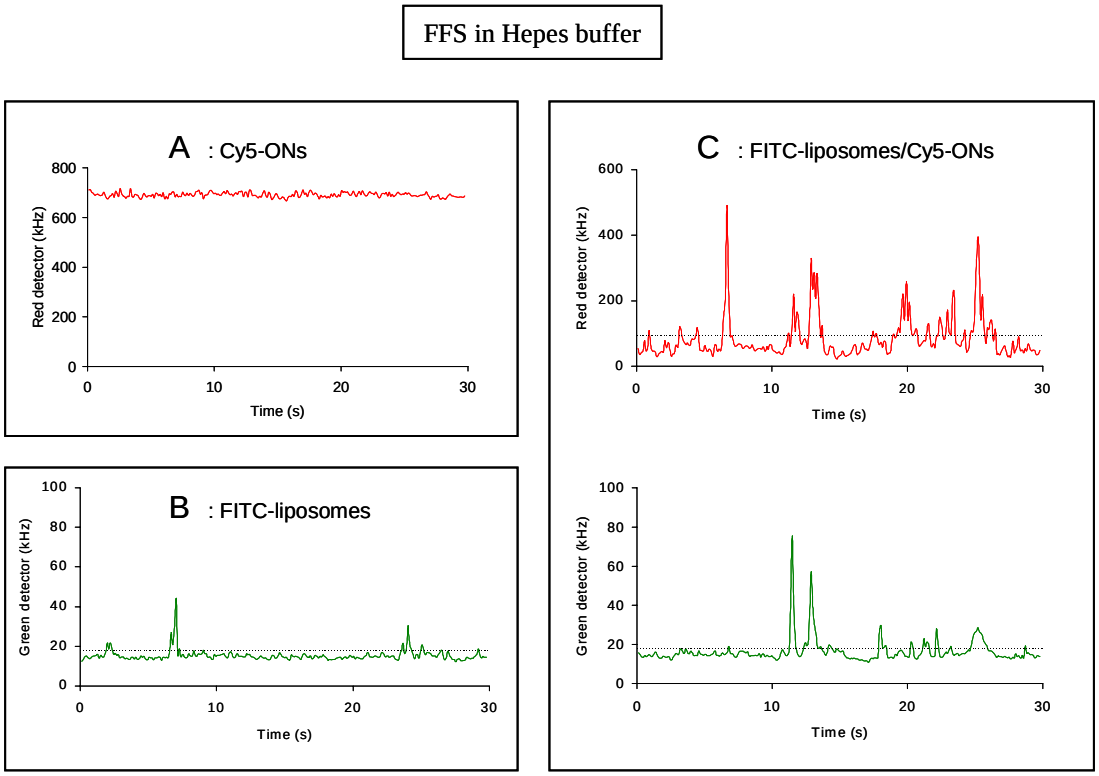

Figure 3. Fluorescence fluctuation profiles of Cy5-ONs (A), FITC-liposomes (B), and FITC-liposome/Cy5-ONs complexes (C). In C the fluorescence was simultaneously registered by the red (upper panel) and green (lower panel) detector. The +/- charge ratio of the FITC-liposome/Cy5-ONs complexes was 10. The final concentration of Cy5-ONs and FITC-liposomes equaled 0.2 µg/mL and 6 µM DOTAP respectively. All samples were prepared in Hepes buffer. The threshold fluorescence intensity value is indicated as a dotted line, discriminating the high fluorescence peaks from the baseline fluorescence.

Figure 3C shows that mixing Cy5-ONs and FITC-liposomes clearly influences the fluorescence fluctuation profile of both the Cy5-ONs and the FITC-liposomes. Hereby, both 488 nm and 647 nm laser lines were simultaneously used to excite the fluorescent labels. Compared to free Cy5-ONs (Figure 3A), the fluorescence in the red detection volume decreased, i.e. the Cy5-baseline fluorescence in Figure 3C (60 kHz) is much lower than the baseline fluorescence in Figure 3A (700 kHz). This is due to a lower concentration of free Cy5-ONs in the excitation volume and is a first indication that Cy5-ONs are associated to the FITC-liposomes. A second observation indicating complexation of Cy5-ONs were the highly intense peaks of Cy5-fluorescence ("Cy5-peaks" in the upper panel) which appeared simultaneously with highly intense peaks of FITC-fluorescence ("FITC-peaks" in the lower panel). This can be explained by the fact that many Cy5-ONs and FITC-liposomes move together, thus associated, through the excitation volume. The FITC-peaks of the complexes in

Figure 3C were higher in intensity when compared to the FITC-peaks observed for the FITC-liposomes (Figure 3B). This suggests that FITC-liposome/Cy5-ONs complexes consist out of more than one FITC-liposome. Additionally, the baseline fluorescence of the FITC-liposomes did not change upon complexation with the Cy5-ONs (compare Figure 3B with the lower panel of Figure 3C). This was also expected as the baseline fluorescence is due to free FITC, that most likely does not participate in the complexation. The distribution of the height of the Cy5-peaks and FITC-peaks in Figure 3C is probably related to the polydispersity of the lipoplexes with regard to the number of Cy5-ONs and FITC-liposomes per lipoplex, in combination with different degrees of mutual quenching between the labels. A closer look to Figure 3 reveals that after 7 seconds there is a Cy5-peak without simultaneous appearance of a FITC-peak, which we attribute to complete FITC-quenching in that lipoplex.

Figure 3 shows that FFS can detect the association of Cy5-ONs to the liposomes with the formation of liposome/ONs complexes that bear a large number of Cy5-ONs and consist out of more than one FITC-liposome. The latter was also supported from DLS experiments which revealed an increase in the size of the liposomes (from 150nm till 250nm) upon association with Cy5-ONs. Unfortunately, the FITC-peaks and Cy5-peaks in Figure 3C completely disturbed the autocorrelation analysis of the fluorescence fluctuations. Consequently, the association of the Cy5-ONs to the FITC-liposomes could not be studied from a change in diffusion time as no reproducible diffusion coefficient could be calculated.

3.4. Studying the dissociation of liposome/ONs complexes in buffer

In further experiments we evaluated whether FFS could monitor the dissociation of the FITC-liposome/Cy5-ONs complexes. As shown above (Figure 3) the decrease in baseline fluorescence of the Cy5-ONs and the simultaneous appearance of FITC-peaks and Cy5-peaks (FITC/Cy5-peaks) are hallmarks of liposome/ONs complex formation. Consequently, gradual dissociation of FITC-liposome/Cy5-ONs complexes is expected to result in a gradual increase of the baseline fluorescence of the Cy5-ONs and a progressive disappearance of the Cy5-peaks. To dissociate the lipoplexes we added increasing concentrations of NaCl to the lipoplexes and measured the baseline fluorescence of the (free) Cy5-ONs and the number of Cy5-peaks. To quantify the baseline and to identify high fluorescence peaks in the fluorescence fluctuation profiles, the software algorithm as reported by Van Craenenbroeck et al. was used [15;22].

Figure 4A shows that adding NaCl at a final concentration of 0.15M increased the Cy5-baseline fluorescence compared to a sample of FITC-liposome/Cy5-ONs complexes in Hepes buffer, indicating a partial dissociation of the Cy5-ONs from the complexes. Addition of more NaCl further increased the baseline fluorescence of the Cy5-ONs and decreased the height of the Cy5-peaks.

Figure 4B shows the percentage of dissociated Cy5-ONs after adding increasing amounts of NaCl. This percentage was obtained by comparing the baseline fluorescence of respectively free and complexed Cy5-ONs. A complete dissociation of the complexes by NaCl could not be obtained. Gel electrophoresis experiments showed similar results (data not shown). We observed that an anionic polymer (dextran sulfate) or a detergent (sodium dodecyl sulfate) was also not able to dissociate all Cy5-ONs from the complexes and Cy5-peaks remained.

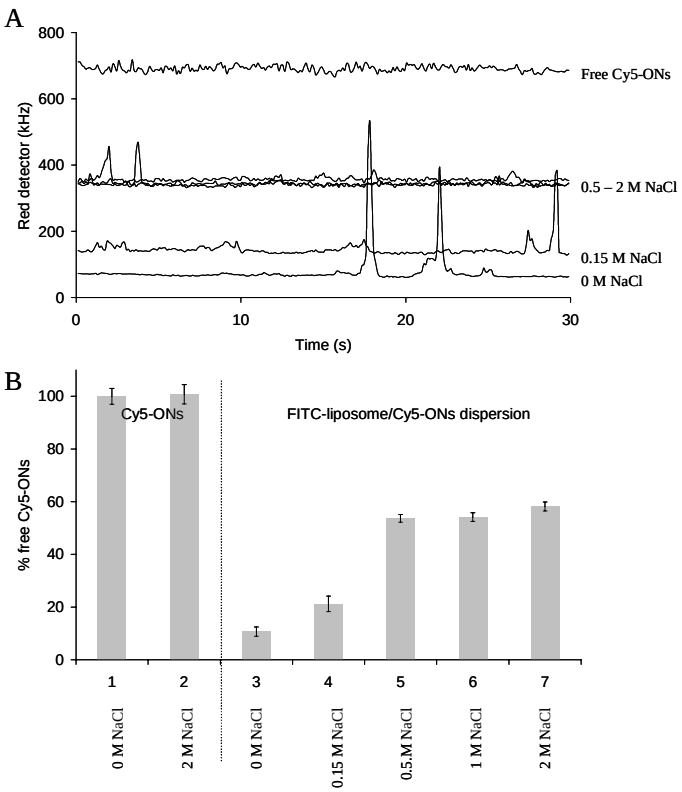

Figure 4. (A) Red fluorescence (Cy5) fluctuation profiles of free Cy5-ONs and of FITC-liposome/Cy5-ONs complexes (prepared in Hepes buffer) before and after adding increasing amounts of NaCl.
(B) Percentage of dissociated Cy5-ONs after adding increasing amounts of NaCl to the FITC-liposome/Cy5-ONs complexes. Shown are: free Cy5-ONs in Hepes buffer and in 2 M NaCl; FITC-liposome/Cy5-ONs complexes in Hepes buffer and in increasing amounts of NaCl (final NaCl concentrations 0.15 M, 0.50 M, 1.00 M and 2.00 M).

3.5. Monitoring the complexation of liposome/ONs complexes in cell lysates

A major goal of our work is to evaluate to what extent FFS is suitable to study lipoplexes in the cytoplasm of living cells. Therefore, we first examined how FFS experiments on respectively free Cy5-ONs and FITC-liposome/Cy5-ONs complexes incubated in cell lysate look like. The results of these experiments are summarized in Figure 5. Mixing of free Cy5-ONs with cell lysate resulted in a slight decrease of the baseline fluorescence (compare 650 kHz in Figure 5A with 700 kHz in Figure 3A) and in the appearance of a few Cy5-peaks. The Cy5-peaks are probably attributed to clustering of Cy5-ONs with cellular components, resulting in highly fluorescent molecular aggregates. Clearly, a major part of the Cy5-ONs remains free (as the baseline fluorescence hardly decreased) while only a small amount of the Cy5-ONs binds to components present in the cell lysate. This agrees with observations from gel electrophoresis experiments: lane 2 in Figure 6 shows that after incubation with cell lysate, nearly all Rh-ONs still migrate freely through the gel.

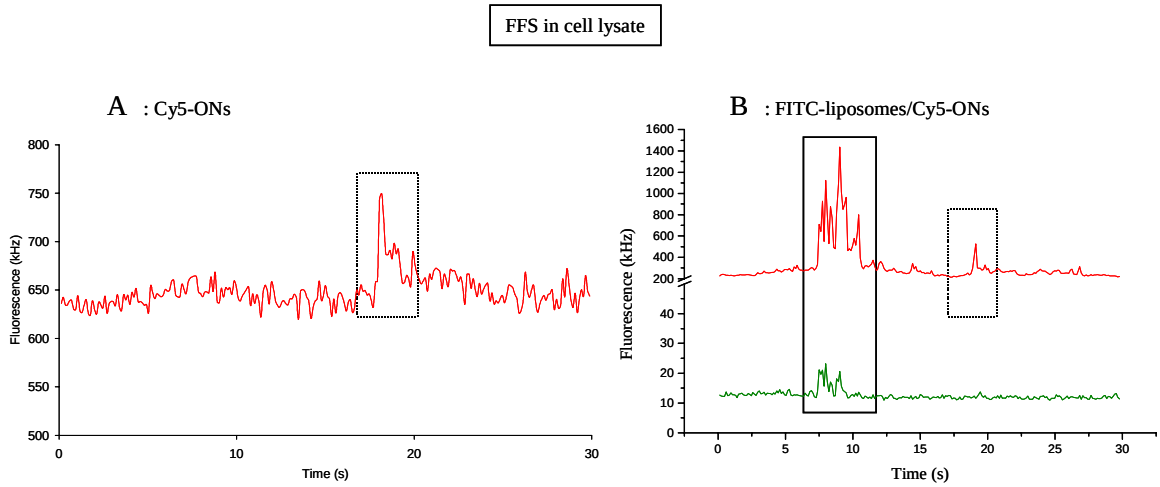

Figure 5. Fluorescence fluctuation profiles of Cy5-ONs (A) and FITC-liposome/Cy5-ONs complexes (B) in cell lysate. The green and red curves represent the fluorescence registered by the green and red detector upon simultaneous excitation with 488 nm and 647 nm. The FITC/Cy5-peak (full line frame) originates from aggregated FITC-liposome/Cy5-ONs complexes. The Cy5-peak in B (dashed line frame) is either attributed to a FITC-liposome/Cy5-ONs complex in which the FITC-fluorescence is quenched or to Cy5-ONs clustered with cellular components. The +/- charge ratio of the lipoplexes was 10. The final Cy5-ONs and FITC-liposome concentration equaled 0.2 µg/mL and 6 µM DOTAP, respectively.

Figure 5B shows FFS on FITC-liposome/Cy5-ONs complexes in cell lysate. Mixing lipoplexes with the cell lysate resulted in a nearly complete disappearance of the FITC-fluorescence. Also, both small as well as huge Cy5-peaks appeared. Only the huge Cy5-peaks

were accompanied by very weak FITC-peaks. The huge Cy5-peaks indicate the presence of very slowly diffusing, gigantic aggregates containing many Cy5-ONs and probably arrive from aggregated FITC-liposome/Cy5-ONs complexes. The small Cy5-peaks (not accompanied by a FITC-peak) can either be attributed to intact FITC-liposome/Cy5-ONs complexes with completely quenched FITC-fluorescence (similar to one peak in Figure 3C) or to Cy5-ONs clustered with cellular components (as demonstrated in Figure 5A). The red baseline fluorescence of the complexes in cell lysate is around 200 kHz (Figure 5B). This is higher than the red baseline fluorescence of the complexes in Hepes buffer (60 kHz, Figure 3C) and much lower than the value of free Cy5-ONs in Hepes buffer (700 kHz in Figure 3A). This indicates that only a small portion of Cy5-ONs dissociated from the complexes in cell lysate. This could also be confirmed by gel electrophoresis. Lane 4 in Figure 6 shows the result of gel electrophoresis on FITC-liposomes/Rh-ONs incubated in cell lysate. Only a small amount of freely migrating Rh-ONs can be detected, while the majority of the Cy5-ONs remains in the slots, either complexed to the original liposome carrier or aggregated with cellular components. From the small amount of released Cy5-ONs, a minor part might be associated with components present in the cell lysate (as concluded from the control experiment in Figure 5A and 6B in combination with lanes 1 and 2 in Figure 6). Therefore, one can conclude that the major part of the ONs remaining in the slots is still associated to the FITC-liposomes.

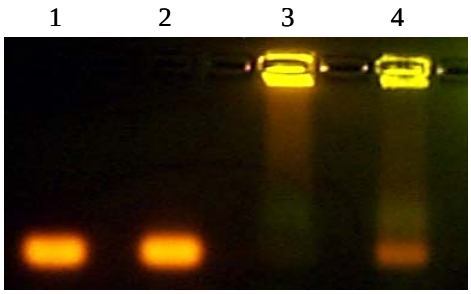

Figure 6. Gel after electrophoresis on Rh-ONs and FITC-liposome/Rh-ONs complexes (+/- charge ratio = 10). Lane 1 and 2 contain 0.3 µg free Rh-ONs in Hepes buffer respectively without (lane 1) and with (lane 2) addition of cell lysate. Lane 3 and 4 contain FITC-liposome/Rh-ONs complexes in Hepes buffer respectively without (lane 3) and with (lane 4) addition of cell lysate. (Note that Rh-ONs instead of Cy5-ONs were used in all gel electrophoresis experiments. The reason is that the UV-lamp used can visualize Rh-fluorescence but not Cy5-fluorescence).

3.6. Monitoring the complexation of liposome/ONs complexes in cells

As a control experiment dual color FFS measurements were first performed in the cytoplasm and nucleus of 'blanc' cells (i.e. cells which were not loaded with free Cy5-ONs or FITC-liposome/Cy5-ONs complexes). Generally, the fluorescence registered by the two detectors was very low while from time to time extremely small and negligible peaks appeared.

Microinjection of free Cy5-ONs in the cytoplasm resulted in nuclear accumulation of the Cy5-ONs within minutes (Figure 8C). This rapid nuclear accumulation has also been reported in literature [23-27]. Accordingly, the Cy5-fluorescence (as measured by FFS) was significantly higher in the nucleus than in the cytoplasm. In the nucleus, Cy5-peaks could not be observed by FFS, indicating that only free Cy5-ONs diffuse through the excitation volume. However, following autocorrelation analysis of the fluorescence fluctuations (using either 1-component (eq. 1) or 2-component (eq. 3) fits), a large amount of the Cy5-ONs seemed to be significantly retarded (data not shown). In the cytoplasm, however, Cy5-peaks were frequently observed, indicating interactions between Cy5-ONs and cellular components (Figure 7A) and in agreement with the FFS measurements on free Cy5-ONs in cell lysate (Figure 5A).

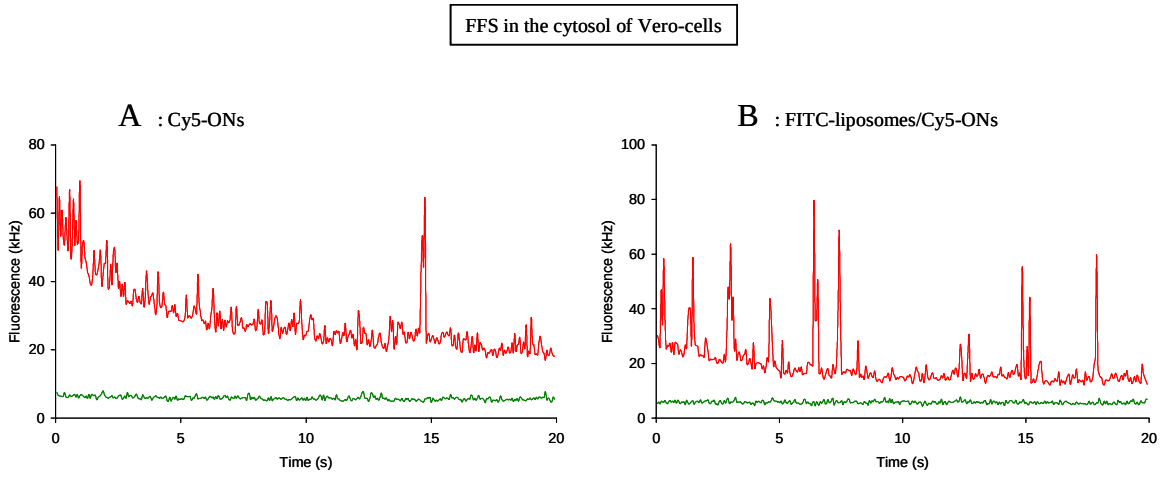

Figure 7. Fluorescence fluctuation profiles as measured by the green and red detector in the cytoplasm of a Vero-cell, after cytoplasmic injection of free Cy5-ONs (A) and a FITC-liposome/Cy5-ONs sample (B).

Microinjecting FITC-liposome/Cy5-ONs in the cytoplasm of Vero cells resulted within minutes in a higher Cy5-fluorescence (as measured by FFS) in the nucleus compared to the cytoplasm. This could be attributed to the small fraction of free Cy5-ONs in the lipoplex sample. However, we observed that the Cy5-fluorescence in the nucleus further gradually

increased with time (hours), suggesting that (at least part of) the Cy5-ONs were released from the complexes. The release of Cy5-Ons could be confirmed by CLSM imaging: Figures 8E and 8F show that the green fluorescence of the FITC-liposomes remains located in the cytoplasm, whereas the red fluorescence is also present in the nucleus. After microinjecting FITC-liposomes/Cy5-Ons complexes, Cy5-peaks could be regularly observed by FFS in the cytoplasm, however, they were never accompanied by simultaneous occurring FITC-peaks (Figure 7B). Again, these small Cy5-peaks can either be attributed to intact FITC-liposome/Cy5-Ons complexes with completely quenched FITC-fluorescence or to Cy5-Ons clustered with cellular components. Simultaneously occurring FITC/Cy5-peaks, attributed to aggregated lipoplexes and as seen in cell lysate (Figure 5B) were, however, not observed in the cytoplasm.

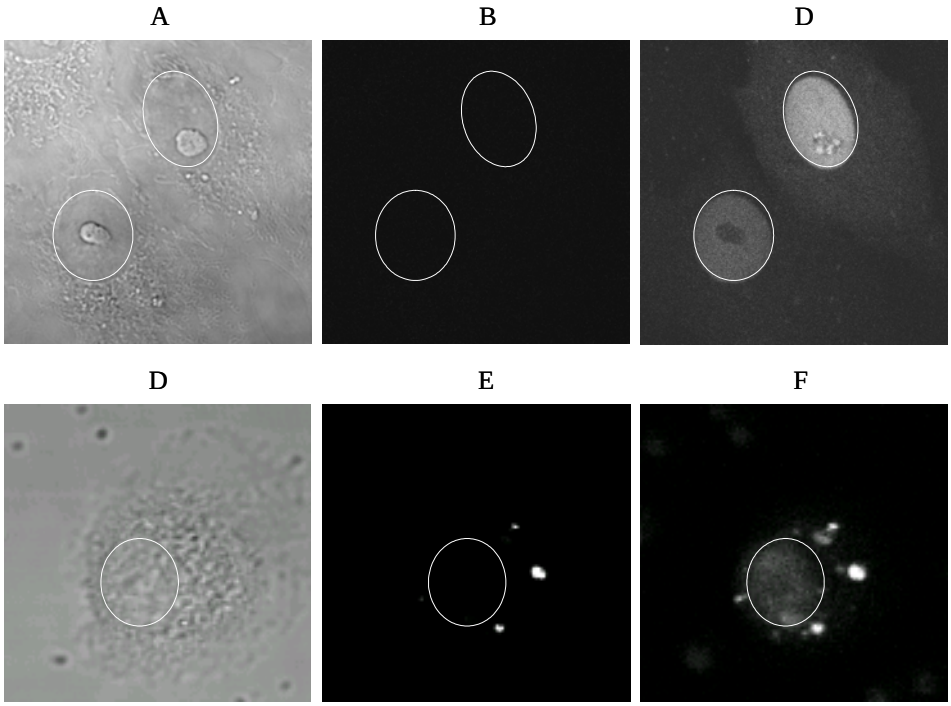

Figure 8. Transmission image (A) and green (B) and red (C) CLSM image of Vero-cells 10 minutes after cytoplasmic injection of a Cy5-ONs solution. Transmission image (D) and green (E) and red (F) CLSM image of a Vero-cell 30 minutes after cytoplasmic injection of a FITC-liposome/Cy5-ONs sample. A circle is drawn around the nucleus.

3.7. Why does FFS not detect simultaneous FITC/Cy5-peaks in the cytoplasm?

All experiments on the FITC-liposome/Cy5-Ons complexes injected in Vero cells so far indicate that a part of the Cy5-Ons is released as Cy5-Ons are detected in the nuclei. The other part seems to remain bound as Cy5-peaks frequently appear in the cytoplasm (Figure

7B). As the Cy5-peaks were not accompanied by simultaneous FITC-peaks we could have concluded that the Cy5-peaks would be due to a clustering of Cy5-Ons with cellular components and would not be due to Cy5-Ons still complexed to FITC-liposomes. However, the considerations below learn us that we cannot make this conclusion.

As the (large) FITC/Cy5-peaks (in cell lysate; Figure 5B) were attributed to aggregated lipoplexes, we first reasoned that simultaneous FITC/Cy5-peaks were not detected in the cytoplasm as the aggregates are too large to migrate through the cytoplasm crowded with cell organelles and thus cannot move through the excitation volume. To test this hypothesis we performed FFS measurements on respectively 'small' (90 nm) and 'large' (500 nm) dual labeled polystyrene beads. Microinjecting 90 nm beads in the cytoplasm of Vero cells resulted in the simultaneous appearance of FITC/Cy5- peaks (Figure 9), proving that these spheres are mobile in the cytoplasm. However, microinjected 500 nm beads seemed to be immobile in the cytoplasm as we did not observe simultaneous FITC/Cy5-peaks (which we did see for these beads in buffer; data not shown). Considering the hydrodynamic diameter of the lipoplexes to be around 250 nm (Figure 1), one can expect that the size of aggregated lipoplexes largely exceeds 500 nm. These observations suggest that simultaneous FITC/Cy5-peaks in the cytoplasm could not be observed by FFS as the aggregated (and possibly also non aggregated) lipoplexes were sterically entrapped.

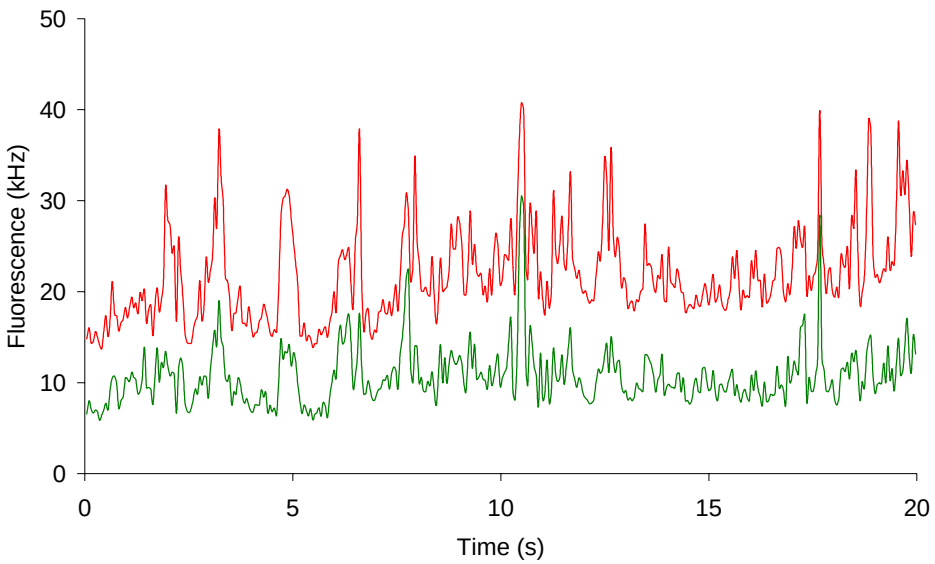

Figure 9. Fluorescence fluctuation profile as registered by the green and red detector in the cytoplasm of a Vero-cell, after cytoplasmic injection of dual labeled polystyrene spheres (90 nm diameter).

A second reason for the lack of simultaneous FITC/Cy5-peaks in the cytoplasm may be related to the quenching of the FITC-fluorescence in the FITC-liposome/Cy5-Ons complexes. Indeed, we observed that the extent of FITC-quenching is dependent on the solvent composition of the sample. E.g. we saw that the buffer in which the FITC-liposome/Cy5-Ons complexes were prepared had a major effect on the fluorescence fluctuation profiles: when using PBS (Dulbecco's phosphate buffered saline), instead of 20 mM Hepes buffer, simultaneous FITC/Cy5-peaks did also not appear and only Cy5-peaks were observed (compare Figure 10A with Figure 3C). The complete disappearance of the FITC fluorescence in PBS is probably due to excessive quenching of the FITC-molecules by the Cy5-molecules. This hypothesis was supported by the fact that partial release of the Cy5-Ons from the lipoplexes in PBS, upon increasing the NaCl concentration, did result in the appearance of simultaneous occurring FITC/Cy5-peaks (Figure 10B).

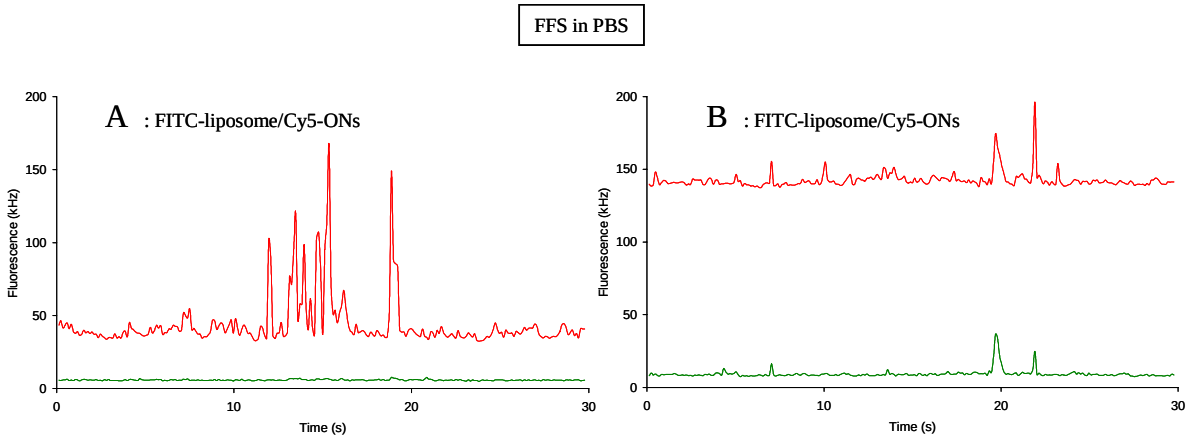

Figure 10. The fluorescence fluctuation profiles of a FITC-liposome/Cy5-ONs sample (charge ratio = 10; 0.2 µg/mL Cy5-ONs) in PBS before (A) and after (B) induced dissociation in 0.2M NaCl as *simultaneously* registered by the FFS green and red detector.

4. Conclusions

In a first setup, we studied the complexation behavior of Cy5-ONs to cationic FITC-liposomes in buffer. We observed that upon binding Cy5-ONs to FITC-liposomes significant fluorescence quenching (of both FITC and Cy5) occurs. This was attributed to (self)quenching of the labels in the complexes. We demonstrated that in Hepes buffer dual color FFS is able to monitor the binding of Cy5-ONs to the FITC-liposomes. Mixing Cy5-ONs with FITC-liposomes resulted in multimolecular complexes, which consist out of many Cy5-ONs and FITC-liposomes. These lipoplexes are highly fluorescent and, consequently, they are clearly detected. Also, upon mixing the Cy5-ONs with FITC-liposomes the 'baseline Cy5-fluorescence' of the fluorescence fluctuations as registered by the FFS instrument was drastically lowered. This decrease in baseline Cy5-fluorescence is caused by the decreased amount of free Cy5-ONs in the detection volume. Dissociation of the FITC-liposome/Cy5-ONs complexes, upon adding NaCl, could be clearly observed by FFS as the 'baseline Cy5-fluorescence' increased. The FFS results on the complexation behavior of the lipoplexes were confirmed by gel electrophoresis measurements.

FFS measurements on free Cy5-ONs in (diluted) cell lysate of Vero cells revealed that the major part of the Cy5-ONs remained free, however, a minor part of the Cy5-ONs seemed to cluster with cellular components. FFS measurements on FITC-liposome/Cy5-ONs complexes in (diluted) cell lysate indicated that most, however not all, of the Cy5-ONs remained complexed. We also observed that aggregation of FITC-liposome/Cy5-ONs complexes occurred.

FFS measurements on free Cy5-ONs injected in the cytoplasm of Vero cells revealed that (part) of the Cy5-ONs clustered with cellular components in the cytoplasm (in agreement with the observations in cell lysate) whereas a major part of the Cy5-ONs accumulated in the nucleus. Micro-injection of FITC-liposome/Cy5-ONs complexes revealed that part of the Cy5-ONs were clearly released from the lipoplexes as free Cy5-ONs were detected in the nucleus.

Finally, this study indicates that FFS shows potential to evaluate the biophysical properties of (sometimes rare) nanomaterials in complex biological media. As gel electrophoresis can tell us whether ONs are free or complexed, so does dual color FFS allow us to determine in the cytoplasm of a living cell whether the Cy5-ONs are migrating freely or

complexed, providing additional information to observations with CSLM. Also, experiments can be done on small sample volumes in the nanomolar concentration range: compare 50 µL of 0.2 µg/mL ONs for FFS-measurements with the 30 µL of a 20 µg/mL ONs solution needed for gel electrophoresis and the 1 mL of a 10 µg/mL ONs solution we used for the dynamic light scattering, zeta-potential and conventional fluorimeter experiments. However, to resolve in the cytoplasm whether the Cy5-ONs are still complexed to their carrier (showing simultaneous FITC/Cy5-peaks) or have dissociated and subsequently have underwent interactions with cellular components (showing only Cy5-peaks), the unforeseen quenching of FITC-fluorescence described in this chapter should be overcome. This is part of further research.

Reference List

1. Lewis,J.G., Lin,K.Y., Kothavale,A., Flanagan,W.M., Matteucci,M.D., DePrince,R.B., Mook,R.A., Hendren,R.W., and Wagner,R.W., A serum-resistant cytofectin for cellular delivery of antisense oligodeoxynucleotides and plasmid DNA, Proceedings of the National Academy of Sciences of the United States of America, 93 (1996) 3176-3181.

2. Meyer,O., Kirpotin,D., Hong,K.L., Sternberg,B., Park,J.W., Woodle,M.C., and Papahadjopoulos,D., Cationic liposomes coated with polyethylene glycol as carriers for oligonucleotides, Journal of Biological Chemistry, 273 (1998) 15621-15627.

3. De Oliveira,M.C., Boutet,V., Fattal,E., Boquet,D., Grognet,J.M., Couvreur,P., and Deverre,J.R., Improvement of in vivo stability of phosphodiester oligonucleotide using anionic liposomes in mice, Life Sciences, 67 (2000) 1625-1637.

4. Gokhale,P.C., Soldatenkov,V., Wang,F.H., Rahman,A., Dritschilo,A., and Kasid,U., Antisense raf oligodeoxyribonucleotide is protected by liposomal encapsulation and inhibits Raf-1 protein expression in vitro and in vivo: implication for gene therapy of radioresistant cancer, Gene Therapy, 4 (1997) 1289-1299.

5. Zelphati,O. and Szoka,F.C., Intracellular distribution and mechanism of delivery of oligonucleotides mediated by cationic lipids, Pharmaceutical Research, 13 (1996) 1367-1372.

6. Marcusson,E.G., Bhat,B., Manoharan,M., Bennett,C.F., and Dean,N.M., Phosphorothioate oligodeoxyribonucleotides dissociate from cationic lipids before entering the nucleus, Nucleic Acids Research, 26 (1998) 2016-2023.

7. Zelphati,O. and Szoka,F.C., Mechanism of oligonucleotide release from cationic liposomes, Proc. Natl. Acad. Sci. U. S A, 93 (1996) 11493-11498.

8. Szoka,F.C., Xu,Y.H., and Zelphati,O., How are nucleic acids released in cells from cationic lipid- nucleic acid complexes?, Advanced Drug Delivery Reviews, 24 (1997) 291.

9. Sanders,N.N., Van Rompaey,E., De Smedt,S.C., and Demeester,J., Structural alterations of gene complexes by cystic fibrosis sputum, American Journal of Respiratory and Critical Care Medicine, 164 (2001) 486-493.

10. Okuda,T., Niidome,T., and Aoyagi,H., Cytoplasmic soluble proteins induce DNA release from DNA-gene carrier complexes, Journal of Controlled Release, 98 (2004) 325-332.

11. Shi,F. and Hoekstra,D., Effective intracellular delivery of oligonucleotides in order to make sense of antisense, Journal of Controlled Release, 97 (2004) 189-209.

12. Torchilin,V.P., Levchenko,T.S., Rammohan,R., Volodina,N., Papahadjopoulos-Sternberg,B., and D'Souza,G.G.M., Cell transfection in vitro and in vivo with nontoxic TAT peptide-liposome-DNA complexes, Proceedings of the National Academy of Sciences of the United States of America, 100 (2003) 1972-1977.

13. Lucas,B., Van Rompaey,E., De Smedt,S.C., Demeester,J., and Van Oostveldt,P., Dual-color fluorescence fluctuation spectroscopy to study the complexation between poly-l-lysine and oligonucleotides, Macromolecules, 35 (2002) 8152-8160.

14. Lucas,B., Remaut,K., Braeckmans,K., Haustraete,J., De Smedt,S.C., and Demeester,J., Studying pegylated DNA-complexes by dual color Fluorescence Correlation spectroscopy., Macromolecules, 37 (2004) 3832-3840.

15. Van Rompaey,E., Sanders,N., De Smedt,S.C., Demeester,J., Van Craenenbroeck,E., and Engelborghs,Y., Complex formation between cationic polymethacrylates and oligonucleotides, Macromolecules, 33 (2000) 8280-8288.

16. Van Rompaey,E., Engelborghs,Y., Sanders,N., De Smedt,S.C., and Demeester,J., Interactions between oligonucleotides and cationic polymers investigated by fluorescence correlation spectroscopy, Pharmaceutical Research, 18 (2001) 928-936.

17. Van Rompaey,E., Chen,Y., Muller,J.D., Gratton,E., Van Craenenbroeck,E., Engelborghs,Y., De Smedt,S., and Demeester,J., Fluorescence fluctuation analysis for the study of interactions between oligonucleotides and polycationic polymers, Biological Chemistry, 382 (2001) 379-386.

18. Jurkiewicz,P., Okruszek,A., Hof,M., and Langner,M., Associating oligonucleotides with positively charged liposomes, Cellular & Molecular Biology Letters, 8 (2003) 77-84.

19. Merkle,D., Lees-Miller,S.P., and Cramb,D.T., Structure and dynamics of lipoplex formation examined using two-photon fluorescence cross-correlation spectroscopy., Biochemistry, 43 (2004) 7263-7272.

20. Zelphati,O. and Szoka,F.C., Mechanism of oligonucleotide release from cationic liposomes, Proc. Natl. Acad. Sci. U. S A, 93 (1996) 11493-11498.

21. Politz,J.C., Browne,E.S., Wolf,D.E., and Pederson,T., Intranuclear diffusion and hybridization state of oligonucleotides measured by fluorescence correlation spectroscopy in living cells, Proceedings of the National Academy of Sciences of the United States of America, 95 (1998) 6043-6048.

22. Van Craenenbroeck,E., Matthys,G., Beirlant,J., and Engelborghs,Y., A statistical analysis of fluorescence correlation data, Journal of Fluorescence, 9 (1999) 325-331.

23. Clarenc,J.P., Lebleu,B., and Leonetti,J.P., Characterization of the Nuclear-Binding Sites of Oligodeoxyribonucleotides and Their Analogs, Journal of Biological Chemistry, 268 (1993) 5600-5604.

24. Hartig,R., Shoeman,R.L., Janetzko,A., Grub,S., and Traub,P., Active nuclear import of single-stranded oligonucleotides and their complexes with non-karyophilic macromolecules, Biology of the Cell, 90 (1998) 407-426.

25. Lorenz,P., Baker,B.F., Bennett,C.F., and Spector,D.L., Phosphorothioate antisense oligonucleotides induce the formation of nuclear bodies, Molecular Biology of the Cell, 9 (1998) 1007-1023.

26. Tsuji,A., Koshimoto,H., Sato,Y., Hirano,M., Sei-Iida,Y., Kondo,S., and Ishibashi,K., Direct observation of specific messenger RNA in a single living cell under a fluorescence microscope, Biophysical Journal, 78 (2000) 3260-3274.

27. Leonetti,J.P., Mechti,N., Degols,G., Gagnor,C., and Lebleu,B., Intracellular-Distribution of Microinjected Antisense Oligonucleotides, Proceedings of the National Academy of Sciences of the United States of America, 88 (1991) 2702-2706.

Summary

In antisense therapy, single stranded oligonucleotides (ONs) are applied to inhibit the production of an unwanted protein in a living cell. At present, most antisense applications are in fundamental research, however, a growing interest remains in developing drugs based upon the antisense mechanism, mainly aimed at interfering with viral infections and cancer. The biological efficacy of administered antisense ONs is restrained by their inefficient cellular uptake and their sensitivity to degradation. Consequently, therapeutic ONs are strongly dependent on carriers to maintain their physicochemical properties in the extracellular matrix, to cross cellular membranes and to escape from the endosomes. Several laboratories have been encouraged to look for appropriate pharmaceutical carrier systems for ONs. One current strategy is screening a high number of pharmaceutical carriers for ONs delivery. While much effort is oriented towards the synthesis of new carriers, the optimization of the physicochemical and pharmaceutical features of the complexes is frequently neglected. We believe that rational design of improved vectors requires a better knowledge of the multistage process by which pharmaceutical vectors deliver ONs into cells. An important step, which has to occur once the complexes have arrived in the cytoplasm, is the release of the ONs from their carrier. To obtain further breakthroughs in understanding the complex matter of intracellular delivery of DNA complexes there is an urgent need for tools which allow studying the dissociation of DNA complexes in cells. In Chapter 1 we described how several advanced light microscopy techniques show potential for this purpose. To study the intracellular dissociation of two components (DNA and its carrier), the simultaneous observation of both components ensures a higher signal specificity. This can be obtained by labelling both components with spectrally different fluorophores (e.g. red and green) and detecting their emission light separately by two detectors simultaneously monitoring the same detection volume.

In confocal imaging, average intensities of fluorescence are directly measured as a function of space to monitor the distribution of the labeled components throughout the cells. The colocalization of the fluorescent markers may indicate that the DNA and its carrier are associated, a lack of colocalization may indicate that the DNA is released from its carrier.

However, due to the resolution limit of a light microscope it remains possible that the fluorescently labeled molecules are observed colocalized without being associated. Compared with the spatial analysis of the DNA and the carrier (as in dual color microscopy), the temporal analysis of the movement of the DNA and the carrier could be more robust to conclude whether the fluorescently labeled species are interacting. While dual color microscopy answers the question “are the DNA and the carrier located together”, dual color FFS may answer the question whether they really move together. With this idea in mind, we were interested to explore whether dual color FFS allows studying the dissociation of carrier/ONs complexes intracellularly. Especially because the experimental results in Chapter 2 illustrated the need for advanced microscopy techniques to understand why some carrier/ONs combinations show biological activity, whereas other combinations fail.

In the first part of Chapter 2, we studied the biological efficiency of ONs packed in several types of pharmaceutical carriers. We used a well-studied antisense assay in which the ability of the ONs to downregulate the expression of the intracellular adhesion molecule-1 (ICAM-1) is evaluated. A biological assay answers the question whether a certain pharmaceutical carrier successfully delivers ONs or not. However, it does not give an answer on the important question why one carrier is successful while another one fails. In the second part of Chapter 2, we tried to find out why some carrier/ONs combinations showed biological activity and why others did not. We were especially interested in knowing how cellular methods like flow cytometry and confocal laser scanning microscopy (CLSM) could provide us with additional information on the cellular delivery of the carrier/ONs combinations studied.

We showed that free PO-ONs and PS-ONs failed to decrease the ICAM-1 protein level. Using CLSM and flow cytometric measurements we showed that this was due to the inability of naked ONs to diffuse passively through the cellular membrane. Presumably because they are large, negatively charged hydrophilic molecules.

Although flow cytometric and CLSM experiments clearly showed cellular uptake for PS-ONs and PO-ONs complexed with Lipofectin, Lipofectin/PO-ONs did not show a decrease in the ICAM-1 protein level while Lipofectin/PS-ONs showed a biological effect. We therefore suggested that the absence of antisense activity of Lipofectin/PO-ONs complexes was not attributed to an inefficient entrance of the complexes in the cells but rather to enzymatic degradation of the PO-ONs. Due to the backbone modification, PS-ONs are more stable in cells than PO-ONs, which may explain why they showed biological activity.

Contrary to the liposome-based Lipofectin, the polymer graft-pDMAEMA efficiently increased the antisense activity of both types of ONs. Noticeably, graft-pDMAEMA/PS-ONs had a very efficient inhibition of the ICAM-1 expression. As expected, flow cytometric and (dual color) CLSM experiments showed indeed cellular uptake and intracellular dissociation of both graft-pDMAEMA/PS-ONs and graft-pDMAEMA/PO-ONs complexes.

The gel electrophoresis competition experiments revealed that graft-pDMAEMA formed more stable complexes with PS-ONs than with PO-ONs. However, as the graft-pDMAEMA/PS-ONs complexes were more biologically active than the graft-pDMAEMA/PO-ONs, it would be wrong to conclude from the gel electrophoresis experiments that the graft-pDMAEMA/PS-ONs complexes are too stable to dissociate intracellularly. Although in literature results from non-cellular experiments like gel electrophoresis are often used to predict the intracellular dissociation behavior of DNA complexes, our results clearly showed that measuring the dissociation behavior of DNA-complexes intracellularly is highly recommended.

Although flow cytometry and CLSM are useful to understand the cellular uptake and intracellular localization of ONs, our experiments showed that the outcome of CLSM and flow cytometry measurements could not explain why PO-ONs were active when complexed to graft-pDMAEMA while they were unactive when complexed to Lipofectin. Similarly, one could not explain from CLSM and flow cytometry why PS-ONs complexed to graft-pDMAEMA better decreased the ICAM-1 protein expression than PO-ONs complexed to graft-pDMAEMA. As PO-ONs become susceptible to degradation by cytoplasmic DNase as soon as they are released from their carrier, one could argue that a better understanding of the time and (intracellular) place at which dissociation of the complexes occurs is crucial to explain these observations. Because FFS can be applied on a cellular scale, we were interested to explore whether it would also allow to study the dissociation of crrier/ONs complexes intracellularly.

Therefore, in Chapter 3 the complexation behavior between oligonucleotides and the cationic polymer poly-L-Lysine (pLL) was first studied in buffer by both single and dual color FFS. In this Chapter we proved that dual color FFS is a straightforward method to detect the association and dissociation of pLL/ONs complexes. The FFS results on the dual labeled polymer/oligonucleotide complexes matched the observations seen in the single color FFS measurements. Although we have not observed controversies between the single color and dual color FFS results on pLL/ONs complexes, a clear disadvantage of dual color FFS is that

both interacting species have to be labeled, which enhances the risk of fluorophore induced artefacts. As explained above, a major advantage of dual color FFS over single color FFS in studying the complexation behavior of DNA complexes in cells is that it might yield a considerable improvement in signal specificity. In heterogeneous media like cells the DNA and the cationic polymers may interact not only with each other but also with many other different species.

By two-dimensional scatter plot analysis of the dual color FFS data, we obtained a more detailed view on the composition of the pLL/ONs complexes in the sample. Especially, dual color FFS proved that a substantial number of pLL/ONs complexes consisted out of numerous ONs bound to numerous pLL strands. Consequently, the appearance of highly intense fluorescence peaks simultaneously in both red and green detector proved that the carrier/ONs complexes did not dissociate. Whenever highly intense fluorescence peaks appeared in the fluctuations profiles, correlation and photon count histogram anlysis of the fluorescence fluctuation profile were no longer feasible. As a consequence one could not study the complexation of oligonucleotides based upon a change in their mobility as correlation analysis is necessary to obtain the diffusion coefficient from the fluctuations. Searching for the presence or absence of highly intense fluorescence peaks simultaneously in both fluorescence fluctuation profiles seemed to be the only way of analysis one could use to know whether oligonucleotides were respectively complexed to/or dissociated from their carriers.

In a next step, we wished to explore if dual color FFS was able to detect intact and dissociated polymer/ONs complexes in the cytoplasm of living cells and to what extent dual color FFS provided new information on the intracellular behavior of polymer/ONs complexes. In Chapter 4, we have shown that cationic polymers of high molar mass, like graft-pDMAEMA of 1700 kDa, also used in Chapter 2, could not enter the nucleus upon microinjection in the cytoplasm. When such (red-labeled) polymers were used as a carrier for (green-labeled) ONs, CLSM experiments were sufficiently suited to prove whether the polymer/oligonucleotide complexes were able to dissociate in the cytoplasm or not: upon dissociation the released green-labeled ONs entered the nucleus while the red-labeled polymer chains remained in the cytoplasm, consequently the red and green labels did not colocalize in the nucleus. However, in opposite to the high molar mass cationic polymers, cationic polymers of lower molar mass, like pLL of 30 kD used in this study, did enter the nucleus upon microinjection or transfection. Consequently, when such (red-labeled) polymers were

used as carriers for (green-labeled) ONs, the nuclei showed both green and red fluorescence, regardless of whether the polyplexes were dissociated or not. Clearly, CLSM experiments could not reveal whether the dual colored nuclei were due to intact Cy5-pLL/RhGr-ONs polyplexes or to dissociated Cy5-pLL and RhGr-ONs chains. Our results showed that dual color FFS, which monitors the movement of the fluorescent molecules, could solve this question. Upon cytoplasmic microinjection or upon transfection with Cy5-pLL/RhGr-ONs complexes, FFS was able to detect simultaneously red and green fluorescence peaks in the cytoplasm. In the nucleus, however, simultaneous peaks were never observed. From these results we could conclude that the Cy5-pLL and RhGr-ONs present in the nucleus after transfection were not associated.

As described in Chapter 5, pharmaceutical carriers bearing hydrophilic segments (such as polyethyleneglycol, pEG) represent an interesting type of pharmaceutical carriers, developed to stabilize and prolong the circulation lifetime of the drug/carrier particles, and to improve targeting strategies. These ‘pegylated carriers’ result in DNA-complexes consisting of a more or less hydrophobic core of partially neutralized polyion strands, surrounded by a shell of hydrophilic chains. In Chapter 5 we investigated whether dual color FFS also allowed evaluating the association/dissociation behavior of pegylated DNA-complexes in buffer. Two distinct types of pegylated polycations were investigated: a diblock copolymer and a multiblock copolymer, equal in chemical formula but of different molecular weight and degree of pegylation. Two distinct approaches were used to fluorescent label these copolymers: the fluorophore was either attached to the cationic segment or to the distal end of the pEG-strand of the copolymer.

For both diblock and multiblock pEG-pEI, the complexation with oligonucleotides resulted in the formation of pegylated DNA-complexes with a core-shell structure, as evidenced by zeta-potential measurements. However, differences in complexation behavior between the two types of pEG-pEI were observed. Gel electrophoresis demonstrated that the diblock pEG-pEI showed better complexation behavior for 25-mer Rh-ONs than for 20-mer Rh-ONs, whereas multiblock pEG-pEI was able to fully complex both types of Rh-ONs. In addition, conventional fluorimetry revealed that the fluorescence of Rh-labeled ONs was differently quenched upon complexation with diblock and multiblock pEG-pEI.

In cases where the fluorescent label (FITC) was attached to the free end of the pEG-segment of pEG-pEI, dual color FFS measurements on FITC-pEG-pEI/Cy5-ONs (for diblock as well as multiblock pEG-pEI) showed that both detectors simultaneously registered highly

intense fluorescence signals. This indicated that a group of oligonucleotides and polymer-chains migrated together through the detection volume and therefore proved that complexes were formed, which were composed out of many oligonucleotide and polymer strands. These observations proved the formation of multimolecular polyplexes, which was in agreement with the gel electrophoresis results and observations in literature. When the pEG-pEI polymers were fluorescent-labeled at their cationic pEI-segment, however, FFS did not detect multimolecular polyplexes. In the case of diblock pEG-pEI-Cy5, the absence of peaks of high fluorescence intensity was indeed due to the fact that no multimolecular polyplexes could be formed, as was shown by gel electrophoresis. However, gel electrophoresis showed that multiblock pEG-pEI-Cy5 did complex Rh-ONs. The absence of highly intense fluorescence peaks in FFS was due to the mutual quenching of both the Cy5- and Rh-labels that were in close proximity in the core of the core-shell complex. From these results, it could be concluded that dual color FFS alloweds studying the association and dissociation of pEG-pEI/ONs provided that the fluorescent label of the polymer was attached to the distal end of the pEG-chain.

Cationic liposomes represent a third type of pharmaceutical carriers. Most commercial transfection agents are liposome based. They have successfully been used as non-viral carriers for ONs, both in cell cultures and in animals. Giving that ONs have to be released from the lipoplexes in order to be biologically active, the intracellular dissociation of the lipoplexes is a crucial issue in the optimization of cationic liposomes for DNA-delivery. Therefore, we investigated in Chapter 6 whether dual color FFS allows evaluating the complexation behavior (being association and dissociation) of liposome/ONs complexes in respectively buffer, cell lysate and the cytoplasm of living cells.

In a first setup, we studied the complexation behavior of Cy5-ONs to cationic FITC-liposomes in buffer. We observed in conventional fluorimeter measurements that upon binding Cy5-ONs to FITC-liposomes significant fluorescence quenching (of both FITC and Cy5) occurs. This was attributed to (self)quenching of the labels in the complexes. We demonstrated that in Hepes buffer dual color FFS is able to monitor the binding of Cy5-ONs to the FITC-liposomes. Mixing Cy5-ONs with FITC-liposomes resulted in multimolecular complexes, which consist out of many Cy5-ONs and FITC-liposomes. These lipoplexes were highly fluorescent and, consequently, they were clearly detected. Also, upon mixing the Cy5-ONs with FITC-liposomes the 'baseline Cy5-fluorescence' of the fluorescence fluctuations as registered by the FFS instrument was drastically lowered. This decrease in baseline Cy5-

fluorescence was caused by the decreased amount of free Cy5-ONs in the detection volume. Dissociation of the FITC-liposome/Cy5-ONs complexes, upon adding NaCl, could be clearly observed by FFS as the 'baseline Cy5-fluorescence' increased. The FFS results on the complexation behavior of the lipoplexes were confirmed by gel electrophoresis measurements.

FFS measurements on free Cy5-ONs in (diluted) cell lysate of Vero cells revealed that the major part of the Cy5-ONs remained free, however, a minor part of the Cy5-ONs seemed to cluster with cellular components. FFS measurements on FITC-liposome/Cy5-ONs complexes in (diluted) cell lysate indicated that most, however not all, of the Cy5-ONs remained complexed. We also observed that aggregation of FITC-liposome/Cy5-ONs complexes occurred.

FFS measurements on free Cy5-ONs injected in the cytoplasm of Vero cells revealed that (part) of the Cy5-ONs clustered with cellular components in the cytoplasm (in agreement with the observations in cell lysate) whereas a major part of the Cy5-ONs accumulated in the nucleus. Micro-injection of FITC-liposome/Cy5-ONs complexes revealed that part of the Cy5-ONs were clearly released from the lipoplexes as free Cy5-ONs were detected in the nucleus.

However, to resolve in the cytoplasm whether the Cy5-ONs are still complexed to their carrier (showing simultaneous FITC/Cy5-peaks) or have dissociated and subsequently have underwent interactions with cellular components (showing only Cy5-peaks), the unforeseen quenching of FITC-fluorescence described in Chapter 6 should be overcome. This is part of further research.

Finally, this study indicates that FFS shows potential to evaluate the biophysical properties of (sometimes rare) nanomaterials in complex biological media. As gel electrophoresis can tell us whether ONs are free or complexed, so does dual color FFS allow us to determine in the cytoplasm of a living cell whether the Cy5-ONs are migrating freely or complexed, providing additional information to observations with CSLM. Furthermore, experiments can be done on small sample volumes in the nanomolar concentration range.

Samenvatting

Bij antisense therapie worden enkelstrengige oligonucleotiden (ON) toegediend om de productie van een ongewenste proteïne te verhinderen. Totnogtoe kaderen de meeste antisense toepassingen in het fundamenteel onderzoek. Nochtans blijft er grote belangstelling voor de ontwikkeling van geneesmiddelen gebaseerd op het antisense mechanisme, in het bijzonder met betrekking tot het bestrijden van virale infecties en kanker. De biologische doeltreffendheid van de toegediende ON wordt beknot door hun gevoeligheid voor afbraak en hun inefficiënte opname door de doelcellen. Bijgevolg zijn therapeutische ON erg afhankelijk van farmaceutische dragers om hun fysico-chemische eigenschappen in de extracellulaire matrix te bewaren, om de cellulaire membranen te overbruggen en om vrijgesteld te worden uit de endosomen. Verschillende laboratoria trachten geschikte farmaceutische dragers te ontwikkelen voor ON. De huidige strategie bestaat erin een zeer groot aantal mogelijke dragers te screenen. Terwijl veel aandacht besteed wordt aan de synthese van nieuwe mogelijke dragers, wordt de optimalisatie van de fysico-chemische en farmaceutische kenmerken van de ON-complexen vaak verwaarloosd. We zijn ervan overtuigd dat een rationeel design van verbeterde dragers een betere kennis vereist van de verschillende hindernissen die het ON-complex moet nemen. De vrijgave van de ON uit hun drager is een belangrijke stap, en die dient plaats te grijpen eens de complexen het cytoplasma bereikt hebben. Om verdere doorbraken te verzekeren in de complexe studie van de intracellulaire toediening van DNA-complexen, is er een dringende nood aan technieken die toelaten het dissociatiegedrag van DNA-complexen in de cellen te bestuderen. In hoofdstuk 1 hebben we beschreven hoe verschillende geavanceerde fluorescentiemicroscopietechnieken hiervoor in aanmerking komen. Om de intracellulaire dissociatie van 2 componenten (DNA en drager) te bestuderen, verzekert het gelijktijdig observeren van beide componenten een betere kijk op het gebeuren. Dat gelijktijdig observeren is mogelijk door een verschillende kleurstof (bv. rood en groen) te koppelen aan beide componenten en hun emissielicht afzonderlijk te registreren met 2 detectors die tegelijkertijd hetzelfde detectievolume bekijken.

Bij confocale beeldvorming worden gemiddelde fluorescentie-intensiteiten in functie van de ruimte gemeten om de distributie van de gelabelde componenten in de cel te achterhalen. Indien beide fluorescente kleurstoffen op dezelfde plaats worden waargenomen,

veronderstelt men dat DNA en drager geassocieerd zijn. Wanneer beide kleurstoffen niet op dezelfde plaats voorkomen, geeft dat aan dat het DNA vrijgesteld is van de farmaceutische drager. Door de resolutielimiet van een fluorescentiemicroscoop is het echter mogelijk dat de fluorescente moleculen samen gezien worden zonder dat ze geassocieerd zijn. Vergeleken met de ruimtelijke distributie van DNA en drager (zoals bij microscopie) is de analyse van het al dan niet samen bewegen van DNA en drager misschien een meer doeltreffende methode om vast te stellen of beide fluorescente soorten interageren. Terwijl tweekleurige microscopie een antwoord geeft op de vraag “Komen DNA en drager op dezelfde locatie voor?”, beantwoordt tweekleurige fluorescentie fluctuatie spectroscopie (FFS) de vraag of beide echt samen bewegen of niet. Op basis hiervan wilden we achterhalen of tweekleurige FFS toelaat om de dissociatie van drager/ON-complexen te bestuderen in cellen. In het bijzonder omdat de experimentele resultaten in hoofdstuk 2 illustreerden dat er nood is aan geavanceerde microscopietechnieken om te begrijpen waarom sommige drager/ON-combinaties biologische activiteit vertonen terwijl andere combinaties falen.

In het eerste deel van hoofdstuk 2 bestudeerden we het biologische effect van ON verpakt in verschillende types farmaceutische dragers. Daarvoor werd een welgekende antisense-test gebruikt waarbij werd nagegaan hoezeer de ON in staat zijn om de expressie van de intracellulaire adhesiemolecule-1 (ICAM-1) af te zwakken. Een biologische test beantwoordt de vraag of een bepaalde farmaceutische drager de ON succesvol in de cel aflevert of niet. De antisense-test geeft echter geen antwoord op de belangrijke vraag waarom een bepaalde drager wel succesvol is terwijl een andere faalt. In het tweede deel van hoofdstuk 2 probeerden we te achterhalen waarom sommige van de gebruikte drager/ON-combinaties wel biologische activiteit vertoonden en andere niet. We wilden meer bepaald weten hoe cellulaire methoden zoals flow cytometrie en Confocale Laser Scanning Microscopie (CLSM) bijkomende informatie kunnen verschaffen over de cellulaire toediening van de gebruikte drager/ON-combinaties.

We toonden aan dat vrije fosfodiëster oligonucleotiden (PO-ON) en fosfothioaat oligonucleotiden (PS-ON) het ICAM-1 expressieniveau niet deden afnemen. Aan de hand van CLSM en flow cytometriemetingen toonden we aan dat de verklaring daarvoor ligt in het feit dat de vrije ON niet doorheen het celmembraan kunnen dringen. Vermoedelijk is dat zo omdat de vrije ON grote, negatief geladen en hydrofiele moleculen zijn.

Zowel voor PS-ON als voor PO-ON gecomplexeerd met de commerciële liposoomdispersie ‘Lipofectin’ toonden flow cytometrie en CLSM-metingen een duidelijke cellulaire opname van de ON aan. Lipofectin/PO-ON waren niet in staat het ICAM-1

expressieniveau te laten afnemen terwijl Lipofectin/PS-ON wel biologisch effect vertoonden. We veronderstelden dat het gebrek aan antisense activiteit van Lipofectin/PO-ON niet veroorzaakt werd door een inefficiënte opname van de complexen door de cellen, maar eerder te wijten was aan enzymatische afbraak van de PO-ON. Door hun ruggengraatmodificatie zijn PS-ON immers stabieler in cellen dan PO-ON. Dat kan verklaren waarom zij in combinatie met Lipofectin wel biologisch actief waren.

In tegenstelling tot Lipofectin, verhoogde het polymeer graft-pDMAEMA de antisense activiteit van beide types ON. De combinatie graft-pDMAEMA/PS-ON in het bijzonder bleek zeer efficiënt om de ICAM-1 expressie te verhinderen. Zoals verwacht toonden flow cytometrie en (tweekleurige) CLSM-experimenten inderdaad cellulaire opname en intracellulaire dissociatie van zowel graft-pDMAEMA/PS-ON als graft-pDMAEMA/PO-ON-complexen.

Bij gelelektroforese toonden competitie-experimenten aan dat graft-pDMAEMA meer stabiele complexen vormde met PS-ON dan met PO-ON. Bovendien waren graft-pDMAEMA/PS-ON-complexen meer biologisch actief dan graft-pDMAEMA/PO-ON-complexen. Op basis van de gelelektroforese-experimenten zou men verkeerdelijk kunnen besluiten dat graft-pDMAEMA/PS-ON-complexen te stabiel zijn om intracellulair te dissociëren. Nochtans worden in de literatuur vaak voorspellingen gemaakt over het intracellulair dissociatiegedrag van DNA-complexen op basis van niet-cellulaire experimenten (zoals gelektroforese). Onze resultaten gaven echter duidelijk aan dat het aan te bevelen is om het dissociatiegedrag van DNA-complexen in de cellen zelf te bestuderen.

Hoewel flow cytometrie en CLSM een indicatie kunnen geven van cellulaire opname en intracellulaire localisatie van ON, gaven onze resultaten aan dat CLSM en flow cytometrie niet kunnen verklaren waarom PO-ON wel biologisch actief bleken in combinatie met graft-pDMAEMA terwijl ze inactief waren in combinatie met Lipofectin. CLSM en flow cytometrie verklaarden evenmin waarom PS-ON gecomplexeerd aan graft-pDMAEMA beter de ICAM-1-expressie inhibeerden dan PO-ON gecomplexeerd aan graft-pDMAEMA. Aangezien PO-ON ook in het cytoplasma gevoelig zijn voor afbraak door DNAse (van zodra zij vrijgesteld worden van hun farmaceutische drager), kan men veronderstellen dat een beter inzicht in het tijdstip waarop en de (intracellulaire) plaats waar dissociatie van de complexen optreedt, cruciaal is om die waarnemingen te verklaren. Vermits FFS toegepast kan worden op cellulair niveau, wilden we achterhalen of die techniek toelaat om de dissociatie van drager/ON-complexen intracellulair te bestuderen.

Daartoe werd in hoofdstuk 3 eerst het complexatiegedrag tussen oligonucleotiden en het cationisch polymeer poly-L-Lysine (pLL) in buffer bestudeerd door zowel eenkleurige als tweekleurige FFS. We bewezen dat tweekleurige FFS ondubbelzinnig zowel associatie als dissociatie van pLL/ON-complexen kan detecteren. De FFS-resultaten van tweekleurig gelabelde polymeer/oligonucleotide-complexen stemden overeen met de waarnemingen van eenkleurige FFS-metingen. Hoewel we geen tegenstrijdigheden hebben waargenomen tussen de resultaten van eenkleurige en tweekleurige FFS voor de pLL/ON-complexen, blijft een nadeel van de tweekleurige aanpak dat beide interagerende moleculen moeten worden voorzien van een fluorescent label. Dat verhoogt immers het risico op de introductie van artefacten. Het voornaamste voordeel van tweekleurige FFS ten opzichte van eenkleurige FFS bij het bestuderen van het complexatiegedrag van DNA-complexen in cellen is wel dat tweekleurige FFS in staat is om het gedrag van beide interagerende componenten gelijktijdig te evalueren. In heterogene media zoals in cellen hoeven DNA en cationisch polymeer niet enkel te interageren met elkaar maar kunnen ze dat ook met vele andere componenten.

Via een tweedimensionele scatteranalyse van de tweekleurige FFS-data verkregen we een meer gedetailleerd beeld van de samenstelling van pLL/ON-complexen. Tweekleurige FFS bewees dat een aanzienlijk aantal van de pLL/ON-complexen bestond uit verschillende ON gebonden aan verschillende pLL-strengen. Bijgevolg bewees het gelijktijdig opduiken van sterk intens fluorescente pieken in de groene en de rode detector dat de drager/ON-complexen niet gedissocieerd waren. Wanneer sterk intens fluorescente pieken optreden in de fluorescentiefluctuatieprofielen blijken zowel correlatie-analyse als ‘photon count histogram’-analyse van het fluorescentiefluctuatieprofiel niet langer mogelijk. Vermits correlatie-analyse vereist is om een diffusiecoëfficient uit de fluorescentiefluctuaties te berekenen, kan de complexatie van de oligonucleotiden niet bestudeerd worden aan de hand van wijzigingen in hun mobiliteit. Evalueren of sterk intens fluorescente pieken gelijktijdig in beide fluorescentiefluctuatieprofielen optreden, is bijgevolg de enige manier om te analyseren of de oligonucleotiden en hun dragers gecomplexeerd of gedissocieerd zijn.

Vervolgens wilden we onderzoeken of tweekleurige FFS in staat is om intacte en gedissocieerde polymeer/ON-complexen te detecteren in het cytoplasma van levende cellen en in hoeverre tweekleurige FFS nieuwe inzichten verschaft over het intracellulair gedrag van polymeer/ON-complexen. In hoofdstuk 4 toonden we aan dat cationische polymeren met hoog molecuulgewicht, zoals graft-pDMAEMA van 1700 kDa uit hoofdstuk 2, niet in staat zijn om de celkern te bereiken na micro-injectie in het cytoplasma. Wanneer dergelijke (rood-gelabelde) polymeren fungeerden als drager voor (groen-gekleurde) ON, volstonden CLSM-

experimenten om vast te stellen of de polymeer/oligonucleotide-complexen gedissocieerd waren in het cytoplasma of niet: bij dissociatie migreerden de vrijgestelde groen-gelabelde ON naar de celkern terwijl de rood-gelabelde polymeerketens in het cytoplasma achterbleven. Bijgevolg kwamen rood en groen niet samen voor in de celkern.

Cationische polymeren met een laag molecuulgewicht, zoals pLL van 30 kDa uit hoofdstuk 3, waren echter wel in staat om naar de celkern te migreren na micro-injectie in het cytoplasma of na transfectie. Wanneer dergelijke rood-gelabelde polymeren (bv. Cy5-pLL) als farmaceutische drager gebruikt werden voor groen-gelabelde ON (RhGr-ON), vertoonden de celkernen gelijktijdig groene en rode fluorescentie. Het is duidelijk dat via CLSM-experimenten niet achterhaald kon worden of de tweekleurige celkernen veroorzaakt werden door intacte Cy5-pLL/RhGr-ON-polyplexen of door gedissocieerde Cy5-pLL-ketens en RhGr-ON. Onze resultaten toonden aan dat tweekleurige FFS hierover wel uitsluitsel kan geven omdat die techniek het al dan niet samen bewegen van de fluorescente moleculen detecteert. Na cytoplasmatische micro-injectie of transfectie met Cy5-pLL/RhGr-ON-complexen was FFS in staat om gelijktijdig optredende groene en rode fluorescente pieken te detecteren in het cytoplasma. In de kern werden echter nooit gelijktijdige pieken geobserveerd. Daaruit konden we besluiten dat de Cy5-pLL en RhGr-ON die in de kern voorkomen na transfectie inderdaad niet meer geassocieerd waren.

Zoals beschreven in hoofdstuk 5, vormen polymeren die hydrofiele segmenten (zoals polyethyleenglycol, pEG) bevatten een interessant type van farmaceutische dragers. Zij werden ontwikkeld om de gevormde geneesmiddel/drager-complexen te stabiliseren, hun circulatietijd in het lichaam te verlengen en doelgerichte strategieën te verbeteren. Deze ‘gepegyleerde’ dragers vormen DNA-complexen die bestaan uit een min of meer hydrofobe kern van gedeeltelijk geneutraliseerde polyionstrengen die omgeven wordt door een mantel van hydrofiele ketens. In hoofdstuk 5 werd onderzocht of tweekleurige FFS ook in staat is het associatie/dissociatiegedrag van gepegyleerde drager/ON-complexen te bestuderen in buffer. Twee verschillende types van gepegyleerde polycationen werden onderzocht: een diblok-copolymeer en een meervoudig blok-copolymeer, beide gelijk in scheikundige samenstelling maar verschillend in molecuulgewicht en graad van pegylatie. Twee verschillende strategieën werden toegepast om deze copolymeren fluorescent te labelen: het fluorescent label werd ofwel gebonden aan het cationisch segment, ofwel aan het uiteinde van de pEG-keten van het copolymeer.

Zowel voor het diblok als voor het meervoudig pEGpEI leidde de complexatie met oligonucleotiden tot de vorming van gepegyleerde DNA-complexen met een kern-

mantelstructuur (zoals werd bewezen met zeta-potentiaalmetingen). Nochtans werden verschillen in complexatiegedrag tussen de twee types pEGpEI waargenomen. Gelelektroforese toonde aan dat diblok pEGpEI een betere complexatie vertoonde met 25-meer Rh-ON dan met 20-meer Rh-ON, terwijl meervoudig pEGpEI in staat was om beide types Rh-ON volledig te complexeren. Conventionele fluorimetrie toonde verder aan dat de fluorescentie van de Rh-gelabelde ON bij complexatie verschillend gequenched werd door diblok en meervoudig pEGpEI.

Wanneer het uiteinde van de pEG-keten van pEGpEI fluorescent gelabeld was (met FITC) bewezen tweekleurige FFS-metingen op FITC-pEGpEI/Cy5-ON (zowel voor diblok als voor meervoudig pEGpEI) dat beide detectoren gelijktijdig sterk intense fluorescente pieken registreerden. Dat gaf aan dat een groep ON en polymeerstrengen samen door het detectievolume migreerden, wat aldus bewees dat de complexen waren opgebouwd uit verschillende ON gebonden aan verschillende polymeerstrengen. De waarnemingen bewezen de vorming van multimoleculaire complexen en bevestigden zo gelelektroforeseresultaten en literatuurgegevens. Wanneer echter het cationisch deel van de pEGpEI-polymeren fluorescent gelabeld werd, was FFS niet in staat om multimoleculaire complexen te detecteren. Bij diblok pEGpEI-Cy5 was het gebrek aan sterk intense fluorescente pieken inderdaad het gevolg van het feit dat geen multimoleculaire complexen gevormd werden, hetgeen met gelelektroforese gestaafd kon worden. Gelelektroforese toonde echter aan dat meervoudig pEGpEI-Cy5 wel in staat was de Rh-ON te complexeren. Het gebrek aan sterk intense fluorescente pieken in de FFS-metingen was het gevolg van wederzijdse quenching tussen de Cy5- en de Rh-labels, die in de kern van het kern/mantelcomplex in elkaars nabijheid zitten. Daaruit konden we besluiten dat tweekleurige FFS in staat is om het associatie/dissociatiegedrag van pEGpEI/ON-complexen te bestuderen op voorwaarde dat het fluorescente label van het polymeer bevestigd was aan het uiteinde van de pEG-keten.

Cationische liposomen vertegenwoordigen een derde type van farmaceutische dragers. Bijna alle in de handel verkrijgbare transfectiemiddelen zijn gebaseerd op liposoomformuleringen. Dat type dragers is reeds succesvol aangewend als niet-virale drager voor ON, zowel in celkweek als in dieren. Aangezien de ON dienen vrijgesteld te worden uit de lipoplexen om biologisch actief te zijn, is de intracellulaire dissociatie van de liposoom/ON-complexen een cruciale stap in het optimalisatieproces van cationische liposomen voor ON-toediening. Op grond daarvan werd in hoofdstuk 6 nagegaan of tweekleurige FFS toelaat om het complexatiegedrag van liposoom/ON-complexen te bestuderen in buffer, in cellysaat en in levende cellen.

Vooreerst werd het complexatiegedrag van Cy5-ON aan cationische FITC-liposomen in buffer bestudeerd. Conventionele fluorescentiemetingen toonden dat bij binding van Cy5-ON aan FITC-liposomen een significante quenching van de fluorescentie optrad bij zowel FITC als Cy5. Die werd toegeschreven aan (zelf)quenching van de labels in de complexen. In buffer was tweekleurige FFS in staat om de binding van Cy5-ON aan FITC-liposomen te volgen. Het mengen van Cy5-ON met FITC-liposomen leidde tot multimoleculaire complexen die bestonden uit verschillende Cy5-ON en FITC-liposomen. Die FITC-liposoom/Cy5-ON-complexen waren sterk fluorescent en werden daarom duidelijk gedetecteerd. Bovendien daalde de 'basisruis Cy5-fluorescentie' van de fluorescentiefluctuaties bij complexatie van Cy5-ON aan FITC-liposomen. Die daling in basisruis Cy5-fluorescentie werd veroorzaakt door een lagere hoeveelheid vrije Cy5-ON in het detectievolume. Door toevoeging van NaCl werden de FITC-liposoom/Cy5-ON-complexen gedissocieerd. Door tweekleurige FFS kon dit duidelijk gevolgd worden door een stijging in de basisruis Cy5-fluorescentie. De FFS-resultaten stemden overeen met de gelelektroforese-resultaten.

FFS-metingen op vrije Cy5-ON in (verdund) cellysaat van Vero-cellen onthulden dat het merendeel van de Cy5-ON vrij in oplossing bleef. Een klein deel van de Cy5-ON bleek echter te clusteren met cellulaire componenten, met de vorming van sterk fluorescente partikels tot gevolg. FFS-metingen op FITC-liposoom/Cy5-ON-complexen in (verdund) cellysaat gaven aan dat het merendeel van de Cy5-ON gecomplexeerd bleef. Aggregatie van de FITC-liposoom/Cy5-ON-complexen werd eveneens waargenomen.

FFS-metingen op vrije Cy5-ON geïnjecteerd in het cytoplasma van Vero-cellen gaf aan dat een deel van de Cy5-ON clusterde met cellulaire componenten in het cytoplasma (wat overeenstemde met de FFS-resultaten van vrije ON in cellysaat), terwijl de meerderheid van de Cy5-ON in de celkern accumuleerde. Micro-injectie van FITC-liposoom/Cy5-ON-complexen onthulde dat een deel van de Cy5-ON vrijgesteld werd uit de lipoplexen vermits vrije Cy5-ON gedetecteerd werden in de celkern. Om te achterhalen of de Cy5-ON in het cytoplasma nog gecomplexeerd zijn aan hun originele farmaceutische drager (waarbij gelijktijdig FITC/Cy5-pieken optreden) of reeds gedissocieerd zijn en vervolgens geclusterd zijn op cellulaire componenten (waarbij enkel Cy5-pieken optreden), dient het onvoorziene quenchingfenomeen van FITC-fluorescentie vermeden te worden. Dat maakt deel uit van verder onderzoek.

Als algemeen besluit kan gesteld worden dat FFS een krachtige techniek is om biofysische kenmerken van (soms zeldzaam) nanomateriaal in complexe biologische media te

bestuderen. Zoals gelelektroforese aangeeft of ON vrij of gecomplexeerd zijn, kan tweekleurige FFS in het cytoplasma van een levende cel onderzoeken of de Cy5-ON vrij migreren of gecomplexeerd zijn. Bovendien kunnen in vitro-experimenten opgezet worden in kleine volumina met nanomolaire concentraties aan fluorescent materiaal.

CURRICULUM VITAE

Personalia

Bart Lucas

Geboren te Zottegem op 3 Februari 1977

Woonachtig te Rooigemlaan 133, 9000 Gent

Studies

Middelbaar onderwijs

1995: diploma van het secundair onderwijs aan het Onze Lieve Vrouw van Deinsbeke College te Zottegem

Universitaire opleiding

1997: de academische graad van kandidaat-bio-ingenieur, behaald met onderscheiding (Universiteit Gent)

2000: de academische graad van bio-ingenieur in de scheikunde, behaald met onderscheiding (Universiteit Gent)

2003: doctoraatsopleiding Farmaceutische Wetenschappen (Universiteit Gent)

Loopbaan

2000-2004: Doctoraatsstudent, IWT-mandaat (01/10/2000-30/09/2004)
Laboratorium Algemene Biochemie/Fysische Farmacie
Faculteit Farmaceutische Wetenschappen
Universiteit Gent
promotoren: Prof. dr. apr. J. Demeester en Prof. dr. apr. S. De Smedt

2004-.....: Assistent Laboratorium Algemene Biochemie/Fysische Farmacie aan de Faculteit Farmaceutische Wetenschappen (Universiteit Gent)
promotoren: Prof. dr. apr. J. Demeester en Prof. dr. apr. S. De Smedt

Lijst van publicities (in internationale tijdschriften met referee system)

2002

‘Dual color fluorescence fluctuation spectroscopy to study the complexation between poly-L-lysine and oligonucleotides’
Lucas B., Van Rompaey E., Van Oostveldt P., De Smedt S.C., Demeester J.
Macromolecules, 2002, 35 (21), 8152-8160.

2004

‘On the biological activity of anti-ICAM-1 oligonucleotides complexed to non-viral carriers.’
Lucas B., Van Rompaey E., Remaut K., Sanders N.N., De Smedt S.C., Demeester J.
Journal of Controlled Release, 2004, 96 (1), 207-219.

‘Studying pegylated DNA-complexes by dual color fluorescence fluctuation spectroscopy.’
Lucas B., Remaut K., Braeckmans K., Haustraete J., De Smedt S.C., Demeester J.
Macromolecules, 2004, 37 (10), 3832-3840.

2005

‘Studying biophysical barriers to DNA delivery by advanced light microscopy’
De Smedt S.C., Remaut K., Lucas B., Braeckmans K., Sanders N.N., Demeester J.
Advanced Drug Delivery Reviews, 2005, 57 (1),191-210.

‘FRET-FCS as a tool to evaluate the stability of oligonucleotide drugs after intracellular delivery’
Remaut K., Lucas B., Braeckmans K., Sanders N.N., De Smedt S.C., Demeester J.
Journal of Controlled Release, 2005, 103 (1), 259-271.

‘Towards a better understanding of the dissociation behavior of liposome-oligonucleotide complexes in the cytosol of cells
Lucas B., Remaut K., Sanders N.N., Braeckmans K., De Smedt S.C. Demeester J.
Journal of Controlled Release, 2005, 103 (2), 435-450.

‘Studying the intracellular dissociation of polymer-oligonucleotide complexes by dual color FFS and CLSM
Lucas B., Remaut K., Sanders N.N, Braeckmans K., De Smedt S.C. Demeester J.
Biochemistry, considered for publication with major revision

Studieverblijven in het buitenland

Advanced FEBS Course: ‘Microspectroscopy: Monitoring Molecular Interactions and Reactions in Living Cells’
Wageningen, Nederland (29 September 2002 -5 Oktober 2002)

Verblijf aan de Universiteit Tubingen (Duitsland) onder leiding van Dr. Roland Brock (Institute for Cell Biology Tübingen) (16 – 21 december 2002)

Short term EMBO fellowship aan het EMBL in Heidelberg (Duitsland) onder leiding van dr. Rainer Pepperkok (Cell Biology/Cell Biophysics Programm) (23 Februari 2004 - 12 Maart 2004)

Congressen, symposia en lezingen waarop een actieve bijdrage geleverd werd

Dual color fluorescence fluctuation spectroscopy to study the association and dissociation of cationic polymer/nucleic acid complexes (poster)
5th International Carl Zeiss Workshop on FCS and related Methods
25-27 April 2001, Jena, Duitsland

Dual color fluorescence fluctuation spectroscopy to study the association and dissociation of cationic polymer/nucleic acid complexes (poster)

Biofarmacie dag

18 Mei 2001, Amsterdam, Nederland

Dual color fluorescence fluctuation spectroscopy to study the association and dissociation of cationic polymer/nucleic acid complexes (poster)

7th Conference on Methods and Applications of Fluorescence: Spectroscopy, Imaging and Probes

16-19 September 2001, Amsterdam, Nederland

Dual color fluorescence fluctuation spectroscopy to study the association and dissociation of cationic polymer/nucleic acid complexes (poster)

9th Meeting of the European Society of Gene Therapy

2-4 November 2001, Antalya, Turkije

Dual color fluorescence fluctuation spectroscopy to monitor the dissociation of oligonucleotides from their pharmaceutical carrier (poster)

7th European Symposium on Controlled Drug Delivery

3-5 April 2002, Noordwijk aan Zee, Nederland

Dual color fluorescence fluctuation spectroscopy to monitor the dissociation of oligonucleotides from their pharmaceutical carrier (poster)

Biofarmacie dag

13 December 2002, Leuven, België

Studies on the Intracellular Release of Genetic Drugs from Pharmaceutical Carriers (poster)

Winter Symposium & 11th International Symposium on Recent Advances in Drug Delivery Systems

3-6 Maart 2003, Salt Lake City, Utah, USA

Studies on the intracellular release of genetic drugs from pharmaceutical carriers (poster)
Biofarmacie dag
23 Mei 2003, Utrecht, Nederland

Studies on the intracellular release of genetic drugs from pharmaceutical carriers (lezing)
European Summerschool on Nanocapsules with functionalised surfaces and walls
18-25 Juli 2003, International University Bremen (Duitsland)

Dual color fluorescence fluctuation spectroscopy to study the behaviour of DNA-nanoparticles in living cells (lezing)
Festive Seminar of the Belgian Particle, Colloid & Interface Society in honour of Prof. J. Vanderdeelen
26 Oktober 2004, Gent

Congressen, symposia en lezingen zonder actieve bijdrage

GA58 postgraduate course in biophysics: 'Biological applications of modern fluorescence techniques'
18-20 September 2000, Leuven, België

Cursus 'Optische en Digitale Microscopie' georganiseerd door Analis
3-4 Oktober 2001, Groot-Bijgaarden, België